Formation Navigation and Relative Localisation of Multi-Robot Systems

Dissertation

zur

Erlangung des Doktorgrades (Dr. rer. nat.)

der

Mathematisch -Naturwissenschaftlichen Fakultät

der

Rheinischen Friedrich-Wilhelms-Universität zu Bonn

vorgelegt von

Frank E. Schneider

aus

Köln

Bonn 2012

Angefertigt mit Genehmigung der Mathematisch-Naturwissenschaftlichen
Fakultät der Rheinischen Friedrich-Wilhelms-Universität zu Bonn

1. Referent: Prof. Dr. Armin. B. Cremers
2. Referent: Prof. Dr. Joachim Hertzberg
Tag der Promotion: 12.April 2013
Erscheinungsjahr: 2013

To my family

Acknowledgments
First, I wish to thank my advisor Prof. Dr. Armin B. Cremers for his guidance, encouragement, and enduring patience. Also I would like to thank Prof. Dr. Joachim Hertzberg for his willingness to be the co-referent. In addition, I would like to express my gratitude to Dr. Dirk Schulz who made many valuable suggestions, which helped to improve this work a lot. Finally, I would like to thank especially Dennis Wildermuth for the joyful working atmosphere over the years and for providing the framework necessary to evaluate my ideas.

Abstract

When proceeding from single to multiple robots, cooperative action is one of the most relevant topics. The domain of robotic security systems contains typical applications for a multi-robot system (MRS). Possible scenarios are safety and security issues on airports, harbours, large industry plants or museums. Additionally, the field of environmental supervision is an up-coming issue. Inherent to these applications is the need for an organised and coordinated navigation of the robots, and a vital prerequisite for any coordinated movements is a good localisation.

This dissertation will present novel approaches to the problems of formation navigation and relative localisation with multiple ground-based mobile robots. It also looks into the question what kind of metric is applicable for multi-robot navigation problems. Thereby, the focus of this work will be on aspects of

1. coordinated navigation and movement

A new potential-field-based approach to formation navigation is presented. In contradiction to classical potential-field-based formation approaches, the proposed method also uses the orientation between neighbours in the formation. Consequently, each robot has a designated position within the formation. Therefore, the new method is called directed potential field approach.

Extensive experiments prove that the method is capable of generating all kinds of formation shapes, even in the presence of dense obstacles. All tests have been conducted with simulated and real robots and successfully guided the robot formation through environments with varying obstacle configurations. In comparison, the non-directed potential field approach turns out to be unstable regarding the positions of the robots within formations. The robots strive to switch their positions, e.g. when passing through narrow passages. Under such conditions the directed approach shows a preferable behaviour, called “breathing”. The formation shrinks or inflates depending on the obstacle situation while trying to maintain its shape and keep the robots at their desired positions inside the formation.

For a more particular comparison of formation algorithms it is important to have measures that allow a meaningful evaluation of the experimental data. For this purpose a new formation metric is developed. If there are many obstacles, the formation error must be scaled down to be comparable to an empty environment where the error would be small. Assuming that the environment is unknown and possibly non-static, only actual sensor information can be used for these calculations. We developed a special weighting factor, which is inverse proportional to the “density” of obstacles and which turns out to model the influence of the environment adequately.

2. relative localisation

A new method for relative localisation between the members of a robot group is introduced. This relative localisation approach uses mutual sensor observations to localise the robots with respect to other objects – without having an environment model. Techniques like the Extended Kalman Filter (EKF) have proven to be powerful tools in the field of single robot applications. This work presents extensions to these algorithms with respect to the use in MRS. These aspects are investigated and combined under the topic of improving and stabilising the performance of the localisation and navigation process. Most of the common localisation approaches use maps and/or landmarks with the intention of generating a globally consistent world-coordinate system for the robot group. The aim of the here presented relative localisation approach, on the other hand, is to maintain only relative positioning between the robots.

The presented method enables a group of mobile robots to start at an unknown location in an unknown environment and then to incrementally estimate their own positions and the relative locations of the other robots using only sensor information. The result is a robust, fast and precise approach, which does not need any preconditions or special assumptions about the environment. To validate the approach extensive tests with both, real and simulated, robots have been conducted. For a more specific evaluation, the Mean Localisation Error (MLE) is introduced. The conducted experiments include a comparison between the proposed Extended Kalman Filter and a standard SLAM-based approach. The developed method robustly delivered an accuracy better than 2 cm and performed at least as well as the SLAM approach. The algorithm coped with scattered groups of robots while moving on arbitrarily shaped paths.

In summary, this thesis presents novel approaches to the field of coordinated navigation in multi-robot systems. The results facilitate cooperative movements of robot groups as well as relative localisation among the group members. In addition, a solid foundation for a non-environment related metric for formation navigation is introduced.

Zusammenfassung

Kooperative Zusammenarbeit ist eins der wichtigsten Arbeitsfelder beim Übergang von Einzel- zu Mehrrobotersystemen. Das Gebiet automatisierter Sicherheitssysteme enthält typische Anwendungen für Mehrrobotersysteme (MRS). Mögliche Umgebungen, in denen Sicherheitsfragen von Belang sind, sind beispielsweise Häfen, Flughäfen, große Industrieanlagen oder Museen. Auch die Kontrolle und Überwachung von Umweltaspekten stellt ein Aufgabenfeld von wachsender Bedeutung dar. Allen diesen Aufgabengebieten gemeinsam sind Anforderungen in Bezug auf organisierte und koordinierte Positionierung und Fortbewegung der Roboter, sowie – als unbedingte Voraussetzung dafür – eine geeignete Lokalisierung.

Diese Dissertation zeigt neue Lösungsansätze und Methoden für die Problemgebiete Formationsfahren und relative Lokalisierung in Gruppen unbemannter Landfahrzeuge (UGV). Außerdem wird die Frage betrachtet, welche Metriken zur Bewertung von Navigationsverfahren für MRS geeignet sind. Der Fokus der Arbeit liegt dabei auf

1. koordinierter Navigation und Fortbewegung

Im Rahmen der Dissertation wird ein neuer Potenzialfeldansatz zur Navigation von Roboterformationen entwickelt. Im Gegensatz zu klassischen Potenzialfeld-basierten Ansätzen für das Fahren in Formationen betrachtet diese neue Methode nicht nur Abstände, sondern auch die Ausrichtung der Roboter innerhalb der Zielformation und wird daher als gerichteter Potenzialfeldansatz bezeichnet. Hier hat jeder Roboter eine genau bestimmte Zielposition und -ausrichtung innerhalb der jeweils aktuellen Formation der Gruppe.

Ausführliche Experimente belegen, dass die Methode beliebige Arten von Formationen sogar in Umgebungen mit großer Hindernisdichte aufrechterhält. Diese Tests wurden sowohl in der Simulation als auch mit realen Robotersystemen durchgeführt. Die klassische ungerichtete Methode zeigt im Vergleich Probleme beim Einhalten von Positionen innerhalb der Formation. Unter bestimmten Bedingungen, zum Beispiel beim Durchfahren von schmalen Gängen, kommt es immer wieder zu ungewünschten Positionswechseln innerhalb der Gruppe. Demgegenüber zeigt der neue gerichtete Algorithmus ein in den meisten Fällen zu bevorzugendes Verhalten: Selbst beim Durchfahren von Engstellen oder bei hoher Hindernisdichte kommt es lediglich zu vorübergehenden räumlichen Stauchungen oder Ausdehnungen der Formation, die relativen Positionen der Roboter zueinander bleiben jedoch erhalten.

Um die Ergebnisse quantifizierbar zu machen und einen aussagekräftigen Vergleich der unterschiedlichen Formationsalgorithmen zu ermöglichen, wurde eine neue Metrik für Roboterformationen entwickelt. Mit Hilfe dieser Metrik wurden die aufgezeichneten Experimentaldaten anschließend ausgewertet. Abweichungen von den angestrebten Positionen innerhalb der Formation werden dabei unterschiedlich bewertet, abhängig davon wie viele Hindernisse in der Umgebung vorhanden und wie weit diese entfernt sind. Unter der Annahme einer a priori unbekannten und möglicherweis auch nicht-statischen Umgebung, können zur Berechnung dieser Metrik ausschließlich lokale

Sensorinformationen verwendet werden. Daher wurde ein spezieller Gewichtungsfaktor entwickelt, der invers-proportional zur Hindernisdichte in der Umgebung ist und der damit einen geeigneten Vergleich der Formationsfahrten in unterschiedlichen Umgebungen ermöglicht.

2. relativer Lokalisierung

Im zweiten Teil der Dissertation wird eine neue Methode zur sogenannten relativen Lokalisierung innerhalb einer Robotergruppe eingeführt. Dieser Lokalisierungsansatz verwendet ausschließlich lokale Sensorinformationen für eine gegenseitige Lokalisierung der Roboter und verzichtet dabei auf ein Umgebungsmodell. Techniken wie der Extended Kalman Filter (EKF), die bei der Lokalisierung einzelner Roboter zum Einsatz kommen, werden für den Einsatz in Mehrrobotersystemen angepasst und erweitert. Ein wichtiger Aspekt der Arbeit ist die gleichzeitige Verbesserung der Ergebnisse sowohl des Lokalisierungs- als auch des Navigationsprozesses.

Die meisten der verbreiteten Lokalisierungsmethoden verwenden Karten und/oder Landmarken mit dem Ziel einer konsistenten globalen Positionierung, d.h. mit Bezug auf ein festes Weltkoordinatensystem. Die hier vorgestellte relative Lokalisierung hingegen bezieht sich auf die relativen Positionen der Roboter untereinander, also Abstand und Richtung zwischen allen Robotern. Die Implementierung des Algorithmus erlaubt es einer Gruppe von Robotern, an unbekannten Positionen in einer unbekannten Umgebung zu starten und dann inkrementell die jeweils eigene sowie die relativen Positionen der übrigen Roboter zu schätzen. Dabei kommen nur die lokalen Sensorinformationen der einzelnen Roboter zum Einsatz. In umfangreichen Tests, sowohl in der Simulation als auch mit realen Robotersystemen, wurden Robustheit und Genauigkeit des Verfahrens validiert.

Für eine präzisere quantitative Bewertung wurde der sogenannte Mean Localisation Error (MLE) als spezielle Metrik in relativen Lokalisierungssystemen entwickelt. Mit dessen Hilfe konnte ein Vergleich zwischen dem neuen relativen EKF-basierten Verfahren und einem globalen Standard-SLAM-Algorithmus durchgeführt werden. Die erzielte Genauigkeit von durchgängig weniger als 2 cm lag dabei mindestens im gleichen Gütebereich wie beim SLAM-Verfahren. Das vorgestellte relative Lokalisierungsverfahren funktioniert zuverlässig mit beliebig aufgeteilten Robotergruppen in einer Vielzahl von möglichen Umgebungskonfigurationen.

Zusammenfassend präsentiert diese Arbeit neue Methoden und Algorithmen für das Gebiet koordinierter Navigation in Mehrrobotersystemen. Die Ergebnisse beleuchten insbesondere Aspekte des koordinierten Fahrens in Robotergruppen und der relativen Lokalisierung innerhalb von Mehrrobotersystemen. Darüber hinaus wurde eine solide Grundlage zur umgebungsunabhängigen Bewertung von Formationsfahrten eingeführt.

Table of contents

Index of figures

Index of tables

1 Introduction

The research in the field of robotics has reached a state where first realistic real world applications are possible (e.g. Rhino Museum Tour-guide, Jijo-2, Helpmate, Care-o-bot, etc.). This progress in fundamental methods and functionality allows exploring more complex extensions of robotics like the emerging field of multi-robot systems (MRS).

One of the most relevant questions, when proceeding from one to multiple robots, is co-operative action. Typical applications for a MRS are for example reconnaissance and surveillance, which has its use in the area of security systems. Possible scenarios are also safety and security issues on airports, harbours, large industry plants, or museums. In addition, the field of environmental supervision by air or sea is an up-coming issue.

Two important research topics in this field of MRS are:

I. Co-ordination of navigation and movement

The co-ordinated navigation or movement of a group of robots is one of the essential topics in the field of mobile MRS. When operating in close proximity, limited space or in a collaborative task that requires some sort of related acting, the movements of the robots have to be co-ordinated efficiently. Typical examples are formations of robots or their convoying. The main challenges are to set-up and maintain a desired formation even in the presence of obstacles while moving. In real world applications, this navigation co-ordination requires a computationally fast solution so that travel speed can be maintained.

II. Localisation

Since almost any navigation is based on some sort of geometrical reference most of the actions performed with mobile robots require some kind of localisation. While localisation itself is an on-going research topic, it is also a vital component in the co-ordination of navigation and movement. This holds especially when dealing with MRS. In addition to the possibility to use the environment as reference, a MRS can make use of the opportunity to localise each robot with respect to the other team members. The desired solution should take the special characteristics of co-operative navigation into account.

A typical example for a formation process in nature is that of migratory birds (see fig. 1-1). The birds maintain a directed formation to increase aerodynamic efficiency and to reduce energy consumption. In addition, they use the distance and angle to the next neighbour to locate themselves in relation to the swarm and to their magnetoception.

Figure 1-1. A typical crane "V" formation.

The topics identified in the previous paragraphs have been separately studied, mostly for single robots and in a relatively small community. The combination of even some of the issues in conjunction with multiple robot systems is rather hard to find in the literature.

Formation navigation in its beginnings has been studied mostly on a theoretical basis due to the lack of enough computing power for comprehensive simulations. The research concentrated on rather idealised geometrical problems [158] and specialisations like the piano moving problem [149]. In the later years, singular publications on studies with real robots have been published [5]. Most of this research concentrated on questions concerning communication or had the focus on behaviour-based realisation of navigation activities [25, 56]. While some aspects for formation navigation could be expected to be used in real world applications, it is still sparsely present in the literature (see fig. 1-2). In recent years, the control community shows a rising interest in the topic, reflected by an increasing number of publications.

In general, the situation looks different in the area of localisation. There has been a tremendous amount of publications on localisation for mobile robots. Most of them focus on "Simultaneous Localization and Mapping" (SLAM) based methods. All sorts of filters (e.g. Kalman, Particle, or EM filter [55, 77]) have been applied to the problem of improving the position estimate of the robot by somehow mapping the sensor information onto a model of the environment. A large quantity of the studies, however, has its focus on single robots. In addition, most of the methods rely solely on an

environment that provides enough features to support the process. Only a rather small fraction of publications is referring to multi-robot localisation while focusing on SLAM based methods. Environment detached approaches can be found very rarely (fig. 1-3).

Field: Publication Year	Record Count	% of 28	Bar Chart
1991	1	3.5714 %	
1995	1	3.5714 %	
2003	3	10.7143 %	
2005	6	21.4286 %	
2006	6	21.4286 %	
2008	3	10.7143 %	
2009	4	14.2857 %	
2010	4	14.2857 %	
Field: Publication Year	Record Count	% of 28	Bar Chart

Figure 1-2. Search query with "Scorpus" and "ISI Web" Title=(formation AND navigation) AND Topic=(robot* OR unmanned); fromFeb 2011.

Field: Publication Year	Record Count	% of 9	Bar Chart
1988	1	11.1111 %	
1998	1	11.1111 %	
2004	2	22.2222 %	
2005	1	11.1111 %	
2006	1	11.1111 %	
2007	3	33.3333 %	
Field: Publication Year	Record Count	% of 9	Bar Chart

Figure 1-3. Search query with "Scorpus" and "ISI Web" Title=(relative AND localisation) AND Topic=(robot* OR unmanned); fromFeb 2011.

This dissertation will present novel approaches to the problems of formation navigation and relative localisation with multiple ground based mobile robots. It also examines the question what kind of metric is applicable for those multi-robot navigation problems.

To achieve these objectives, co-ordinated navigation in formations will be used to stabilise and improve the localisation process. Therefore, the dissertation will focus on the aspects of

1. Co-ordinated navigation and movement

A new potential field based approach to formation navigation is presented. Intensive experiments will show that the method is capable of coping with considerable numbers of robots without significant performance decay. Important boundary conditions are performance, flexibility, and the ability to be easily distributed even with heterogeneous groups of robots. The research will also look into the question of appropriate metrics for MRS and include tests with real robot groups of up to four members. For the field of co-ordinated navigation the research will concentrate on a potential field method. A new extension is presented that shows a better performance with particular respect to the desired shapes of the formations.

2. Relative localisation

A method for relative localisation between the members of a robot group is introduced. The research includes the comparison between the proposed Extended Kalman Filter and a standard SLAM based approach. The experiments will show that the selected method is robust and does not need a central component. The results include intensive testing with multiple real robots.

The research in the areas of localisation and tracking will focus on probabilistic methods for MRS. Techniques like the Extended Kalman Filter have proven to be powerful tools in the field of single robot applications. The work will present extensions to these algorithms with respect to the use in MRS. These aspects will be investigated and combined under the topic of improving and stabilising the performance of the localisation and navigation process. The suitability of the methods and their combination will be shown by experiments with both simulated and real robots.

The remainder of this thesis is organized as follows: In the following chapter, the problem of setting up and maintaining a formation of robots is considered. An approach for directed formation navigation based on potential fields is presented. After this, Chapter 3 sets the focus on evaluation methods and describes a possible metric for navigations aspects in multi robot systems. In Chapter 4 the problem of position estimation in MRS is addressed. An EKF based solution that considers navigation issues is developed. Chapter 5 finally concludes and summarises the presented work.

2 Formation Navigation

The idea of multiple robots working together in order to accomplish a task efficiently has become increasingly popular in the last several years. Many situations can be found in which the sub-problem of generating some task-specific formation and maintaining it during a movement must be solved. In this context, the term formation can be defined - according to the Merriam-Webster dictionary - as an orderly arrangement of a group of persons or things in some prescribed manner, often for a particular purpose. Moving in formation, respectively, means traveling and manoeuvring together in a disciplined, synchronized, predetermined manner. In the present case, a formation of a MRS is a group of robots arranged to a geometric figure.

Applications differ in the strictness of the formation constraints needed. While, for instance, a transport mission requires very tight constraints on the robot pattern to share the workload equally among all robots, other applications like reconnaissance and surveillance for environmental monitoring need the robots to be spread more or less uniformly over a specified area. Some tasks like convoying or demining build a formation but allow a distortion or partition of the pattern, for example, while passing obstacles. In this chapter, a novel approach for potential field based formation navigation with a directional force is introduced. The new directed force method enables the formation to make use of the orientation between neighbours within the formation.

2.1 Related Work

Research in the area of Multi Robot Formation Navigation goes back to the very beginnings of multi robot systems themselves. First systematic research was done in the "Cellular Robotics" project. In [12, 99] a Cellular Robotic System (CRS) is characterized as an arbitrary number of robots in a one- or two-dimensional grid. The robots are able to sense neighbouring cells and communicate with other robots via a signboard mechanism. Protocols are presented for creating different patterns, for example, alternating robots, and spaces in a one-dimensional grid, covering the top row of a two-dimensional grid by robots, or covering the boundary of a two-dimensional grid. Egecioglu and Zimmermann [48] pose the "Random Pairing" problem, and seek a set of rules by which for any given number a CRS will converge to a pattern such that there is a group of two robots with that number of vacant spaces between them (see also [13]). A comparable approach is adopted by Genovese et al. [64], who describe the simulation of a system of pollutant seeking mobile robots. The simulation uses a potential field mechanism to attract robots to the pollutant and to repulse robots from each other. The combined effect of these two forces yields a gradient pattern that "points" toward the source of the pollutant. Several improvements have been added to the idea of CRS, for example in [165] Ueyama et al. use genetic algorithms to configure special structures, and in [176] group formations are generated by distributed control schemes.

Related to CRS is the newer approach of robot swarms [47], which is inspired by the collective behaviour of some social insects, the so-called swarm intelligence. A considerable amount of attention has focused on swarm-related problems during the last decade. Among the extensive work, a number of authors directly address the topic of building different kinds of formations within robot swarms [135, 32, 78]. However, in the majority of cases, the more swarm-typical goal of defining a region over which the individual members evenly spread is considered [75, 164]. In [164], e.g., Turgut et al. describe a self-organized flocking behaviour and give some metrics to evaluate the flocking quality. In [7] the authors use artificial potential fields to organize the robot swarm into a formation, controlling only the overall swarm geometry and the individual member spacing. Michael et al. present a generic control framework for swarming applications and describe their experimental testbed for evaluation of the results [108]. Note that we focused the discussion of the vast number of works on formation navigation in robotic swarms to the ones we think are most closely related to our work.

The original concept of the Cellular Robotic Systems (CRS) was followed by research that was concerned with the set-up of geometric formations. Most of the papers are focused on the circle formation. Several approaches about establishing and maintaining of a formation pattern can be found in the literature, which mostly do not address the problem of avoiding obstacles. Examples include papers by Wang [170], who uses neighbour tracking and a mathematical model of the leader-follower co-ordination strategy, and Suzuki et al. [154, 157, 2].

Suzuki concentrated on the formation problem of a distributed "circle forming" algorithm that guarantees the robots will actually end up in a circle. For this problem the best known solution is the distributed algorithm in [154], which guarantees that the robots will end up in a shape of constant diameter (for example, a Reuleaux triangle can be the result). It is assumed that the i^{th} mobile robot knows the distances D_i and d_i to its farthest and nearest neighbours, respectively; the algorithm attempts to match the ratios $D_i = d_i$ to a prescribed constant. No method of detecting the termination of the process is given.

Cao [167] noted that the algorithm of Suzuki could be slightly modified: rather than each robot seeking to achieve a predefined ratio $D_i = d_i$, each robot could seek to achieve a predefined angle (close to 90 degrees) subtended by its farthest neighbour and its closest neighbour to the right. This uses very similar sensing capabilities but guarantees the desired circular shape.

In [2] Suzuki presented a theoretical approach where a large set of robots, represented as points in the plane, congregated at a single position. Moving synchronously in discrete time steps, robots iteratively observed neighbours within some visibility range, and followed simple rules to update their position.

In [155] Suzuki achieved the pattern formation by communicating the global positions of all others to each robot. In this study, an algorithm is developed for each pattern. The proposed method can uniformly distribute robots creating different simple pattern

formations (circles, polygons, line, filled circle, and filled polygon). Each robot oriented itself to, e.g. the furthest and nearest robot. It can also split a group of robots into an arbitrary number of nearly equally sized groups. Even though the simulation results obtained by this decentralized algorithm are inspiring, the global broadcasting communication required to share information among the whole group makes it less scalable. In [158] Suzuki and Yamashita recapitulate most of the results of their work on formation generation.

Suzuki's work has been picked up by many scientists for example by Chen [30, 31] who extends the method of Suzuki to incorporate collision avoidance when the robots are moving. In [31] formation generation by distributed control for maintaining robot formations is demonstrated. Large groups of robots are shown to cooperatively move in various geometric formations. This research also addresses the analysis of group dynamics and stability, and again does not provide obstacle avoidance. The work has a similar set-up to the one presented by Suzuki, but here also group motion was considered, for example a matrix formation performing a right turn. Investigations have been done in simulation using more theoretical approaches to enable a formal performance analysis.

Yamaguchi [174] addresses the shape generation problem using systems of linear equations; starting at some initial location, each robot changes its (x; y) position according to a linear function of its neighbours' positions and some fixed constant. Simulations of the method show that a group of initially collinear robots will converge into the shape of an arc. Yamaguchi also investigated how robots can use only local communication to generate a global grouping behaviour [175]. It can be observed that the circle-forming problem, while quite simple to state, reveals several pitfalls in formulating distributed geometric tasks. Also information lower bounds, e.g., for robots to be able to realize that they have achieved the prescribed formation, are largely unexplored in the literature. In [176] Yamaguchi examined the influence of central and distributed control schemes on formation generation.

One of the first researches on leader-follower control strategies for formations was Wang [170]. A strategy for robot formations was developed where individual robots maintain a given specific position relative to a leader or neighbour. Sensory requirements for these robots are reduced since they only need to know about a few other robots. The analysis was focussed on feedback control for formation maintenance and stability of the resulting system. It did not include integrative strategies for obstacle avoidance and navigation. Later on Wang continued his work on formation control in the field of aerial robotics and spacecraft [171].

Probably stimulated by his earlier work a team around Ron Arkin and Tucker Balch started their research on formation navigation with a behaviour-based approach to robot formation keeping. Reactive behaviours, implemented as so-called motor schemas, correspond to the different influences, which have an effect on the movements of the robots: move-to-goal, avoid-obstacle, avoid-robot, and maintain-formation.

In [4] Arkin and Balch identified three principles of formation control:

- unit-centre-referenced
  where the robot references itself to the centroid of all robots,
- leader-referenced
  where the robot uses the position of a predetermined leader,
- neighbour referenced
  where the robot's nearest/predetermined neighbour is used as a reference point.

In their approach, each robot determines other robots' positions by dead reckoning, GPS, or by direct perception, and its own coordinates in the global co-ordinate system are broadcasted to all robots. So global knowledge is assumed where each robot knows the position of all others. A behaviour-based, decentralized control architecture is used, where each individual platform makes sure that it is placed appropriately with respect to its neighbours. Additionally the advantages and disadvantages of the different formations in dynamic environments as well as the usefulness of various approaches under certain environmental constraints are discussed. A set of metrics for formation evaluation is also briefly sketched.

In [3] experiments were done with both simulated and real robots. The high reliance upon a centralized worldview and the need to transmit coordinates between robots might have a negative impact on performance, as the paper states. The work does not demonstrate neighbour-referenced formations with real robots using only local information. It also does not address the issue of formation generation dealing with line-of-sight constraints.

In [5] Arkin and Balch extended this approached by an additional motor schema which is based on a potential field method and which can be used to define uniform and structured “geometric” formations. Separate motor schemas compute a vector for moving to the proper formation position, avoiding static obstacles, avoiding other robots, and maintaining the current formation. The simulated robots had a set of predetermined attachment sites defined, spread uniformly around the robot body. Possible attachment site geometries include shapes resembling “X”, “|”, “--“ or “+”, where the robot is the centre of the shape and the attachment sites are the ends of the line segments (see figure 2-1). Other robots can only connect their own attachment sites to those of the other robots. The robots search for the first available position in the formation. The choice of one position with respect to another depends on the robot’s overall behaviour generated by the superposition of the potential functions, called by the author’s social potentials. Each robot builds a list of potential attachment sites and generates an attraction vector for the closest, allowing the group to “snap” into a shape, as robots were “pulled” toward each other's sites. While a group of robots is moving in a formation, they avoid obstacles by splitting around it and re-joining after passing. The approach is validated in simulation. However, due to the symmetrical nature of the attachment site approach there is no predefined spot for each robot. Several configurations with the same attachment sites are possible, while only a specific one

may be desired. Therefore, a guarantee for a desired formation cannot be given, see for example, figure 2-2 for a formation changing after a temporary division.

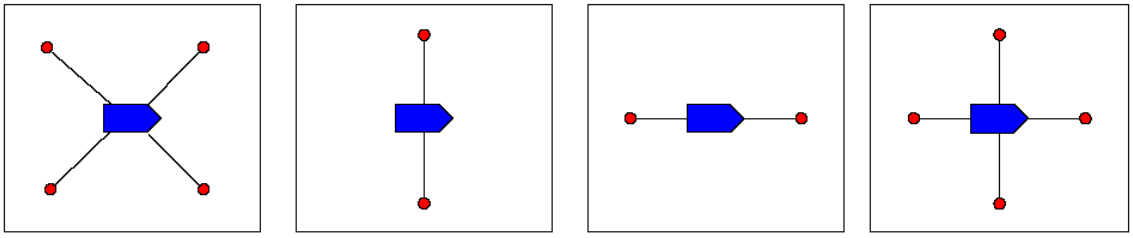

Figure 2-1. From the point of view of each robot in the group, every other robot has several local attachment sites (red dots) to which other robots may be attracted.

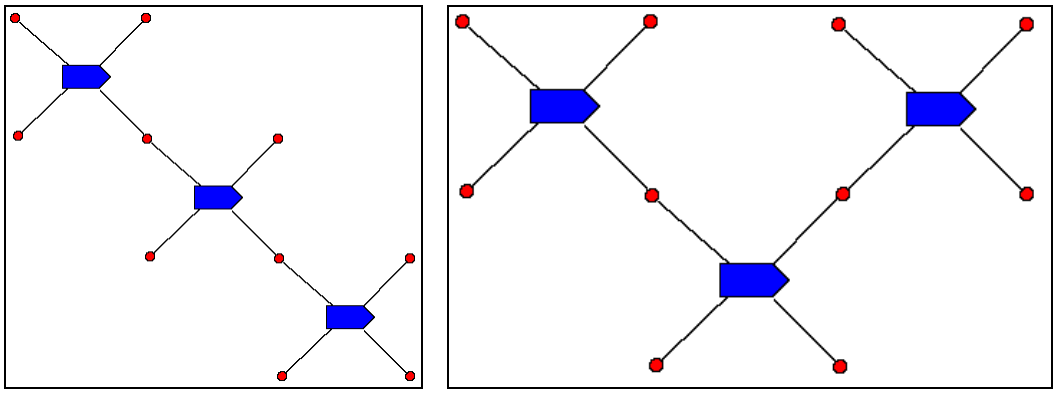

Figure 2-2. Example of a formation changing after a temporary division.

Balch's behaviour-based model accepts temporary distortions in a formation in order to avoid obstacles. It also has some kind of relative goal positions for the robots, and makes use of a virtual potential field to move the robots to the desired formation. Additionally, Balch wants the robots to be randomly distributed over the possible formation positions. Further, he can only design special uniformly structured formations because the possible relative positions are the same for each robot. The concept of the motor schema-based architecture was picked up and enhanced by others, see for example [24].

Lynne Parker was also one of the research pioneers regarding the navigation in multi-robot systems (MRS). In [25, 26] a cooperative leader-following strategy for a team of robots is introduced. The robots are able to maintain a specific formation while simultaneously moving in a linear pattern and avoiding dynamic obstacles. In addition, the robots use local sensor information and explicit broadcast communication among themselves. Two levels of behaviours were implemented for tasks: team-level and robot-level behaviours. Transitions are made when necessary among specific behaviours in these two levels. For example, when a member of the team faces an obstacle, the whole team waits together with that member for the obstacle to go away for a certain amount of time. If this time is exceeded, that member circumnavigates the obstacle and the team returns to its main task of moving in a formation.

In [121] Parker proposes a reactive, distributed, strongly coordinated MRS, composed from homogeneous, behaviour-based robotic agents to deal with ”Cooperative Multi-robot Observation of Multiple Moving Targets” (COMMT). The system is realized through the behaviour based ALLIANCE architecture, combined with techniques based on potential fields and a target seeking system. Parker also discusses the proper balancing between local and global knowledge while moving in a formation [120]. Global information about goals and obstacles should influence the robots' local behaviour when avoiding obstacles.

In [56, 57] Maja Mataric has presented a distributed approach to formation navigation that uses behavioural modules to control formation. Local information is used to establish and maintain formations among robots. Each robot has a unique ID and a designated friend robot, which it can see through a “friend sensor”. A conductor robot that can be seen by all followers maintains the overall heading of the formation. There is also minimal communication between robots: heartbeat signals (robots broadcast their IDs), swerve signals (changing direction), and formation messages. Each robot can learn the number of robots in formation and the type of formation using broadcasted messages. For each formation, each robot has a pre-assigned ordering, which determines the angle it should keep between its front direction and the direction of its friend. This angle is calculated locally. Each follower must keep its leader centred in the field of view of its camera. Therefore, each robot has a colour-coded cylinder on its encasing so that the other robots can recognize it. The camera is fixed at an angle according to the formation. Consequently, formations are rigid, i.e., the formation cannot change shape when dealing with obstacles. In addition, a laser range finder is used to infer the distance between robots. This provides much more accurate distance measurements than just using vision. Position assignment in the formation is done based on the ID number of the robot. As the formation dynamically emerges, different robots can be assigned the leader role. Also switching a formation is possible but may require repositioning depending on the formation to switch to. Additionally, if the robots in the group are initially in a random position, the time required to initialise the formation shape may not be optimal. The possible formations are limited to chain-shaped ones that do not make a backward curve.

In [38, 51] Kumar suggests a hybrid distributed approach that is based on multiple controllers which can be seen as behaviours selected according to a finite state machine. These states define control laws that consider nearby robots and the obstacles in proximity. The approach is vision-based using omni-directional cameras, and each robot is identified by colour. Because the formation, its leader, and the allowed switches between formations must be predetermined, the approach achieves poor results if the environments are unknown or if it is not possible to initialise the position of the robots in a good configuration for the desired formation. A control graph describes the relationships between the leader and its followers. By maintaining certain control heuristics, the follower can maintain its position in the formation with respect to the leader. The choice of the formation strategy is based on the ability of each individual robot to change formation to avoid obstacles. In most of the experiments, the control

graph is static and defined a priori. In a few cases the control graph is allowed to vary but within rigid limits.

Another approach by Kumar controls each robot using only local information, by either referencing itself to one neighbouring robot or maintaining a certain distance and angle to it, or to two neighbours and maintaining two fixed distances to those. Thus, the required information is the position and orientation of one robot close by and within line of sight. An experiment with physical robots (though only two) is reported, where the follower robot keeps a pre-set heading and distance to the leading robot. The control method was adopted in [1] as part of the leader-follower behaviour. In an experiment with two physical robots the follower (using a colour camera and colour-blob tracking) kept a fixed heading and distance to the leader.

In [11] Kumar proposes a centralized trajectory computation scheme that uses kinetic energy shaping. Instead of using a constant kinetic energy metric, they employ a function smoothly changing the kinetic energy metric. The method generates smooth trajectories for a set of mobile robots. The proximity between the robots can be controlled via a parameter. However, the method does not consider obstacle avoidance and is not scalable.

In [151] Song and Kumar present a potential field approach where the robot group has to get into a certain formation at a specified goal point. It is not clear if the formation can move as a whole. Only static obstacles are assumed. It is important to note that a single robot cannot have a specified location in the formation. In [52] Kumar et al. very well summarise the results of this later work.

Current approaches in the field of robot formation control mainly address one of the following approaches: *behaviour-based methods*, *virtual structure methods*, *leader-follower approaches*, *potential fields* and new *control theory methods*.

Like in the already mentioned early work of Tucker and Balch, in general, behaviour-based approaches start by designing simple behaviours or motion primitives for each individual robot, e.g., formation keeping, trajectory tracking, goal seeking, and obstacle avoidance. Then, more complex motion patterns can be generated by using a weighted sum of the relative importance of these primitives. Examples of recently published work can be found, e.g., in [59, 177], where hybrid approaches based on the leader-follower scheme and low-level behaviour-based controllers are presented, or in [15], which combines behaviour-based methods with a virtual structure formation approach. The main drawback of behaviour-based methods is that the mathematical analysis of this approach is difficult and, consequently, the stability of the formation and its convergence to a desired configuration cannot be guaranteed.

In the virtual structures approach, originally described in [98], robots are considered as particles, inserted into a rigid, so-called virtual structure, which represents the whole formation. The control law for each single robot is derived by defining the dynamics of the complete virtual structure and, then, translating its motion into the desired motion of each vehicle. As mentioned above, in [15] the virtual structure approach uses a low-

level behaviour-based control. Urcola et al. control formation movement applying a virtual structure composed of spring-damper elements, allowing the formation to comply with the environment shape [168].

The main advantages of the virtual structure approach are that it is easy to describe the coordinated behaviour of the group and that the formation can be maintained well during manoeuvres. However, since the formation has to maintain the same virtual structure all the times, the possible applications are limited, because for any necessary distortions the formation shape has to be reconfigured.

Among the already cited early work in the formation navigation domain, many researchers used leader-follower strategies. With the leader-following strategy, generally, some robots are considered as leaders, while others act as followers. Recent examples of leader-follower based approaches can be found in [68, 162]. Additionally, in [123], for instance, leader-following is combined with artificial potential fields, and in [61] leader-follower deformable formations are achieved using the Voronoi Fast Marching (VFM) method.

The primary advantage of leader-follower methods is that this approach, in principle, can be reduced to a tracking problem. Consequently, convergence and stability of the formation can be shown through standard control-theoretic techniques. Popular control techniques for the leader-follower strategy include dynamic feedback linearization [59], backstepping [43, 28] and sliding mode control [136, 60, 150].

However, important disadvantages of most leader-follower approaches are that the chain structure leads to a poor disturbance rejection and the leader's motion is independent of the followers, i.e. there exists no explicit feedback from the followers back to the leader. Overall, the formation does not tolerate leader faults. Additionally, in many leader-following algorithms, a trajectory is designed only with regard to the leader and then each individual is forced to follow. This approach generally does not work well for a system having heterogeneous robots with different dynamic constraints at each single vehicle.

A somewhat related approach to formation building and maintaining is to model the relationship between the members of the robot group as a system of virtual springs and dampers [104, 168]. Due to the inherent chain structure of the robot's relations, this approach also suffers from one of the typical leader-follower problems: large oscillations and poor disturbance rejection.

Another way to solve the formation control problem is to formulate it as an optimization problem. In theory, this approach provides provable stability of the method as well as the optimal control of the formation, under the premise of good robot and environmental models. An early approach based on planning and optimal control, addressing the problem of obstacle avoidance, can be found in [42]. Due to the increasing availability of computational power on the robots,, in the recent years a considerable amount of work focused on optimal control approaches to formation navigation [79, 44, 124].

As an alternative, Receding Horizon Control (RHC), also known as Model Predictive Control (MPC), is sometimes considered as a solution to formation navigation tasks [138, 37, 50]. RHC describes a well-known, but computationally expensive control strategy in which the current control action is computed by solving a finite horizon optimal control problem online. Regarding formation problems, receding horizon approaches are occasionally used in the context of leader-follower schemes [138, 37].

However, the major problem with these control strategies is that the control problems soon get computationally complex as the number of robots in the formation increases. Therefore, most of the authors deal with only very few homogenous robots.

Another important group of approaches, which in general is computationally less demanding, is based on artificial potential fields (APF) or vector fields. In this method, various virtual forces are assigned to individual robots, obstacles and to the desired formation shape and, then, these forces are combined and used to steer the robots. The following sections will address potential field approaches in detail. There have also been a number of singular publications on the topic of formation navigation, see for example [6, 80, 97].

2.2 Potential Field Approach

The artificial potential field (APF) method proposed by Khatib [83] is one of the most widely used techniques for mobile robot local collision avoidance. It is well adapted for real-time motion control when the environment is perceived only through the robot's own sensors. Its principle is simple: the robot is usually subject to two kinds of forces:

1. Repulsive forces
   Repulsive forces are generated by obstacles or other robots.
2. Attractive forces
   Attractive forces are generated by goals or certain positions.

The repulsive forces can easily be generated from sensor readings, especially by sonar or laser sensors, but also from IR-sensors or vision modules. The attractive forces are in most cases simply goal points. See figure 2-3 for a basic example. Since the forces are represented through vectors, the math is well understood. Another fact is that the basic APF needs very little computing power. Today the APF is often used in the area of real-time collision avoidance and path planning for manipulators.

Some extensions to the basic method were proposed. For example, in Krogh [89] the potential is a function of speed to better control the motion. Krogh enhanced the concept by taking into consideration the robot’s velocity in the vicinity of obstacles. In [63] Ge and Cui adopted this idea and added the velocity of obstacles and even of the target point to the definition of the potential function. In Poty [122] this approach is further improved by employing fractional potentials, thereby achieving smooth variations of the potential depending on the distance to obstacles. Some authors use the mathematically

related method of vector fields instead of APF to model the different factors which influence a robot's trajectory, e.g. in [94, 73].

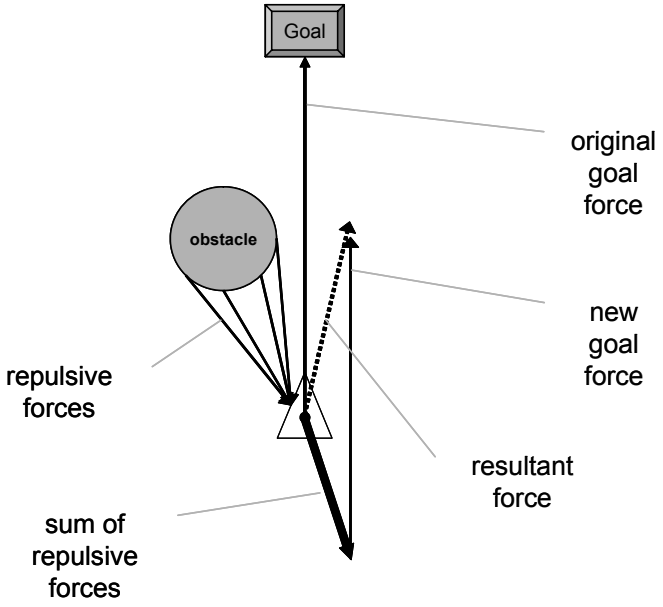

Figure 2-3. Example of the artificial potential field.

Alternative approaches were also proposed, but without the direct link that the APF provides between perception and control. Thorpe [160] has applied the potential field method to off-line path planning. Krogh and Thorpe [90] suggested a combined method for global and local path planning which uses Krogh's generalized potential field [89] approach. Other examples are Borenstein and Koren [16] and Manz [106] who use a local model derived from the certainty grid [112] consisting of a one-dimensional polar histogram representing local obstacle density. The direction of motion is selected according to the obstacle distribution. APF made its way into the standard techniques for certain navigation aspects [16, 130] and motion planning [17, 18].

The major disadvantage of the APF method is the existence of local minima that occur whenever the attractive and repulsive forces cancel each other out [86]. One approach to cope with this problem is to build a local model of the environment to determine possible "escape" sub-goals or to define "vortex fields" [41], or to make random motions [8]. In addition, the use of harmonic potential fields [96] is a solution, but computationally expensive. Kim et al. [84] use APF with so-called angle distribution to cope with local minima. As a special sub-topic their work also addresses the GNRON problem [62], meaning the case that the potential of the goal is over-whelmed by the potential of an obstacle. Vadakkepat [169] tries to combine techniques from evolutionary computation and the APF approach in order to optimize potential field functions and to avoid local minima. In formation-related work regarding potential fields one can find, e.g., bell-shaped potential functions modelling obstacles [72] or bifurcating potential fields [14] in order to eliminate or at least to narrow down the

problem of local minima. In [129] Rezaee and Abdollahi get rid of minima using special rotational potential fields, but as a trade-off their approach is limited to circle formations.

Some authors try to tackle the problem of local minima and analyze the resulting performance and stability of their algorithms analytically. But, as the models based on artificial potential functions are, in general, discontinuous, such an analysis usually involves differential inclusions and non-smooth analysis, which often leads to very bulky computations [151][159]. Saez-Pons et al. [134], in contrast, present a stability analysis based on geometric concepts, which allows avoiding heavy computations while at the same time providing qualitative proofs of attainability of the desired formations.

Another significant problem that is inherent to potential field methods and independent of the particular implementation is the tendency of the robot to oscillate in narrow passages.

A narrow corridor for example is defined as a passage in which the robot experiences repulsive forces simultaneously from opposite sides. Under steady state conditions, the repulsive forces from both sides balance the robot on an equilibrium line, which is usually on or close to the centre of the corridor. If, however, the robot strays slightly to either side of the centre-line, it experiences a strong virtual repulsive force from the near wall, while the repulsive force from the far wall decreases. As a result, the robot will turn to the far wall, overshoot the equilibrium line, and consequently experience a strong repulsive force in the opposite direction. This effect may result in oscillatory and unstable motion.

2.2.1 Artificial Potential Fields for Formation Navigation

The concept of using a potential field method for controlling a formation is based on the idea that not only obstacles and goals can exert forces onto a robot [17]. The basic design is that each robot in a formation can exert repulsive and attractive forces to other robots. These virtual forces can be used to keep the robots in the desired formation.

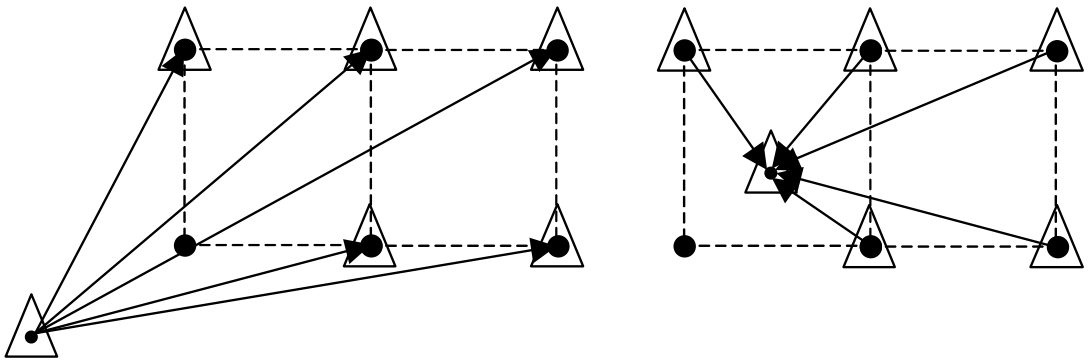

Figure 2-4. Robot outside (left) and inside (right) the formation.

The example in figure 2-4 shows a robot that is outside the formation. The attractive forces of the other robots will “pull” it back into the formation. On the other hand, the attractive force of the robot itself will cause the formation to move towards its position. If a robot has moved too close to the formation, the repulsive forces of the other robots will “push” it away. In both cases, the forces will move the robot and the formation into the desired constellation. Figure 2-5 and figure 2-6 show the attractive and the repulsive formation forces for a square formation of four robots, respectively.

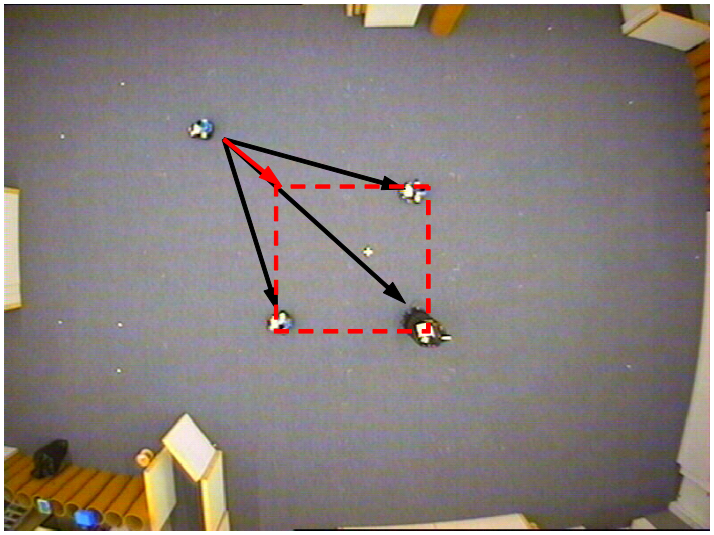

Figure 2-5. Attractive position forces (square formation).

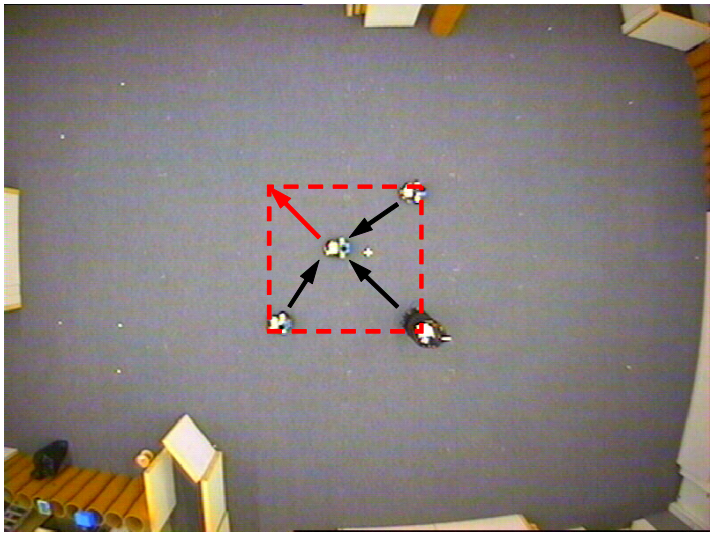

Figure 2-6. Repulsive position forces (square formation).

If strict formation constraints are not required and deforming of the formation in the presence of obstacles is allowed, two opposite influences on the resulting paths for each robot can be identified: avoiding obstacles and maintaining the formation. Obviously,

these two demands contradict in many environments, e.g. at doorways or in narrow corridors. Without distortion of the formation, a detour might be necessary. In extreme cases, this might be close to the piano moving problem [149]. In order to model this situation a potential field approach as described in [86] is used and each robot is assigned to a specific position inside the formation.

As an extension to the related method presented in [174] not only a shape-forming force is used to generate the formation, but also additional types of forces are modelled and combined to achieve more functionality and flexibility. Some other APF-based approaches to different formation aspects can be found in literature. Many of them are related to large-scale robot groups [87] or robot swarms [85, 7] and, therefore, consider the problem mainly from a theoretical point of view, often presenting only simulation results, e.g., in [34].

2.2.2 Mathematical Background

2.2.2.1 Basic Formation Forces

Let $p_i \in \mathbb{R}^2$, $i = 1,\ldots,n$ be the intended positions of n robots in the formation in an arbitrary Cartesian co-ordinate system T_F. And let $x_i \in \mathbb{R}^2$, $i = 1,\ldots,n$ be the actual positions of the robots in some world co-ordinate system T_W. To determine the potential field, which arranges the robot group in the desired formation, the most straightforward approach is to define

$$\hat{p}_{j,k} = x_j + \left(x_k - x_j\right)\left(\frac{\left\|p_k - p_j\right\|}{\left\|x_k - x_j\right\|}\right) \tag{1}$$

for each two different robots j and k. With this definition, only the required distance between two robots j and k in the target formation is taken into account for generating formation forces. Let be

$$U^k_{form,j}\left(w\right) = \frac{1}{2}\xi\left\|w - \hat{p}_{j,k}\right\|^2, \tag{2}$$

with $U^k_{form,j} : \mathbb{R}^2 \to \mathbb{R}$, $j = 1,\ldots,k-1,k+1,\ldots,n$, and ξ a constant scaling factor, then the formation potential $U^k_{form} : \mathbb{R}^2 \to \mathbb{R}$ for each robot k can be defined as

$$U^k_{form}\left(w\right) = \sum_{\substack{j=1 \\ j\neq k}}^{n} U_{form,j}\left(w\right). \tag{3}$$

Accordingly, the force $F^k_{form} : \mathbb{R}^2 \to \mathbb{R}^2$ that applies to a robot k at position *w is*

$$F^k_{form}(w) = -\nabla U^k_{form}(w), \tag{4}$$

which can be calculated as follows:

$$F^k_{form}(x,y) = \begin{pmatrix} -\frac{\partial}{\partial x}\sum_{\substack{j=1 \\ j\neq k}}^{n} U^k_{form,j}(x,y) \\ -\frac{\partial}{\partial y}\sum_{\substack{j=1 \\ j\neq k}}^{n} U^k_{form,j}(x,y) \end{pmatrix}^T$$

$$= \begin{pmatrix} -\sum_{\substack{j=1 \\ j\neq k}}^{n} \frac{\partial}{\partial x}\frac{1}{2}\xi \left\| (x,y) - \hat{p}_{j,k} \right\|^2 \\ -\sum_{\substack{j=1 \\ j\neq k}}^{n} \frac{\partial}{\partial y}\frac{1}{2}\xi \left\| (x,y) - \hat{p}_{j,k} \right\|^2 \end{pmatrix}^T$$

$$= \begin{pmatrix} -\sum_{\substack{j=1 \\ j\neq k}}^{n} \frac{\partial}{\partial x}\frac{1}{2}\xi \left[\left(x - \hat{x}_{j,k}\right)^2 + \left(y - \hat{y}_{j,k}\right)^2 \right] \\ -\sum_{\substack{j=1 \\ j\neq k}}^{n} \frac{\partial}{\partial y}\frac{1}{2}\xi \left[\left(x - \hat{x}_{j,k}\right)^2 + \left(y - \hat{y}_{j,k}\right)^2 \right] \end{pmatrix}^T$$

That finally leads to

$$F^k_{form}(x,y) = \xi \left(\sum_{\substack{j=1 \\ j\neq k}}^{n} \left(\hat{x}_{j,k} - x\right), \sum_{\substack{j=1 \\ j\neq k}}^{n} \left(\hat{y}_{j,k} - y\right) \right), \tag{5}$$

where $\left(\hat{x}_{j,k}, \hat{y}_{j,k}\right) := \hat{p}_{j,k} \in \mathbb{R}^2$ as defined in (1).

As already stated above, because of the definition of $\hat{p}_{j,k}$, no orientation information is used within this force calculation, meaning that the robots will not have specific poses in the formation. The resulting formation forces depend on the distance of the robots in the target formation and are undirected attractive or repulsive forces between the robots.

This results in the fact that a formation, e.g., of two robots, can take any combination (see figure 2-7). Also all formation pairs shown in figure 2-8 are equivalent.

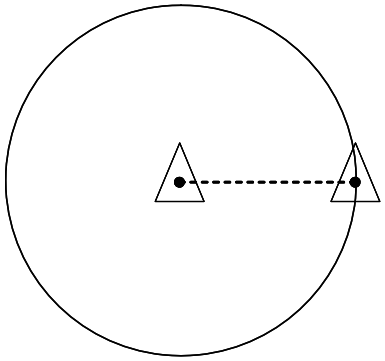

Figure 2-7. Possible positions in a non-directed two robot formation.

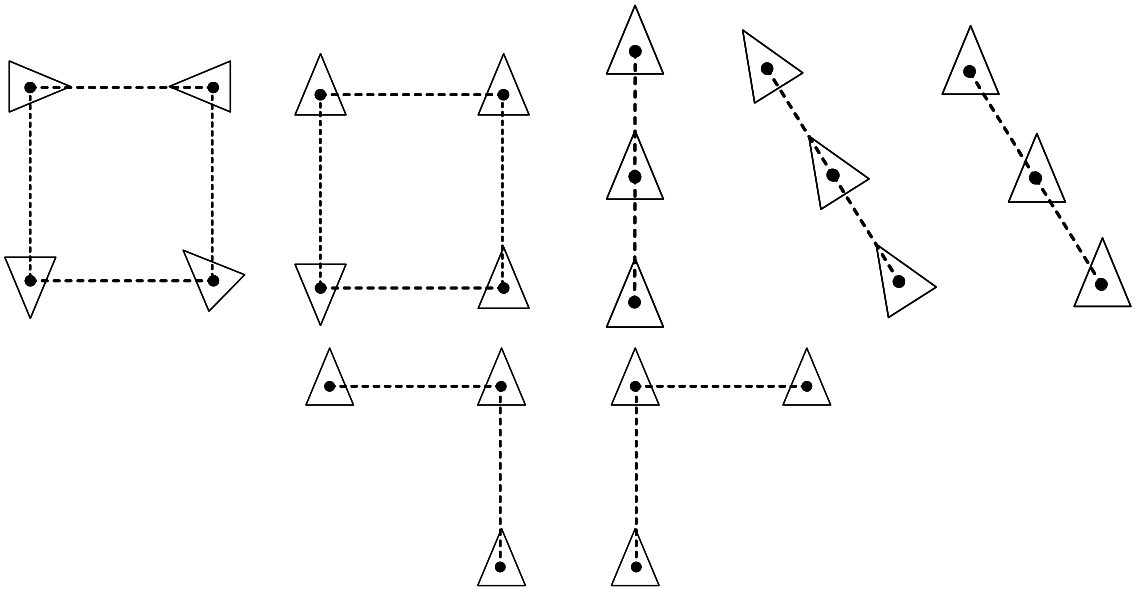

Figure 2-8. Equivalent formation pairs in non-directed formations.

2.2.2.2 Directed Formation Forces

In addition to the method described in the last section, directional information can be used to define the formation forces (see figure 2-9). Independent of the configuration of T_F in the world co-ordinate system T_W each robot k expects any other robot at a certain position seen from its own "point of view". Under the assumption that robot j already has reached its desired goal position, the expected goal position $\hat{p}_{j,k}$ of robot k seen from robot j is

$$\hat{p}_{j,k} = x_j + \begin{pmatrix} \cos(\omega) & -\sin(\omega) \\ \sin(\omega) & \cos(\omega) \end{pmatrix} (p_k - p_j) \quad . \tag{6}$$

Thereby, the angle ω can be defined in different ways. If the robots were "free floating" i.e., with the ability to move in any driving direction without turning, ω can be defined as

$$\omega = \phi_{actual,j} - \phi_{form,j}, \tag{7}$$

where $\phi_{actual,j} \in [0;2\pi)$ is the actual orientation of robot j and $\phi_{form,j}$ denotes its orientation in the goal formation. This approach can also be used if the goal is only to build up a formation, not to maintain it while moving.

Since even most omni-directional robots (like the B21 from IRobot) can only move forward or backward along their view axis, normally ω is defined differently: in the current implementation of the method it is

$$\omega = \phi_{goal,j} - \phi_{form,j}, \tag{8}$$

with $\phi_{form,j}$, like in (7) above, robot j's orientation in the goal formation, but with $\phi_{goal,j}$ the direction towards the goal point as seen from robot j. As can be seen in the experimental section, this leads to very stable results.

Like in the last section, $\hat{p}_{j,k}$ from formula (6) can then be used with (2) in order to define the formation potential U^k_{form} for each robot k. Using (4), the resulting formation forces can be generated.

Now, simply worded, for every robot the attractive or repulsive force to (re-)establish the desired formation is calculated with respect to the positions and the orientations of the other robots.

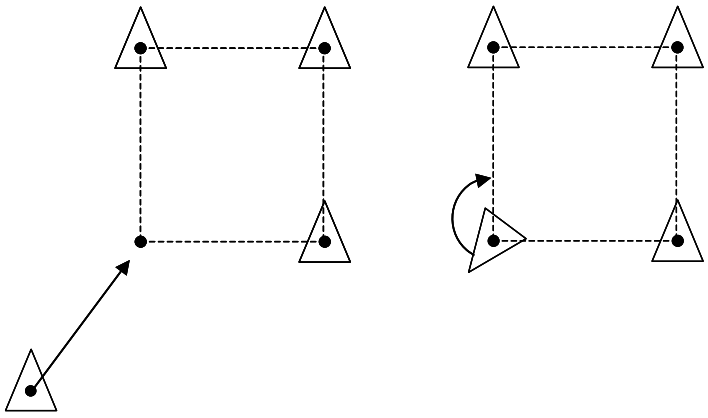

Figure 2-9. Position force (left) and orientation force (right).

The following section will constitute the application of the formulae on a group of four robots that should build a square formation.

2.2.2.3 Applied Example of the Directed Formation Forces

In contradiction to the un-directed formation forces, the proposed approach not only uses the distances between the robots but also the orientations. This makes the method intricate to visualise. The following figures show the applied method for a square formation without goal and obstacle forces. The left illustration of figure 2-10 shows the desired square formation for a group of four robots. Figure 2-10b shows the present positions and orientations of the four considered robots.

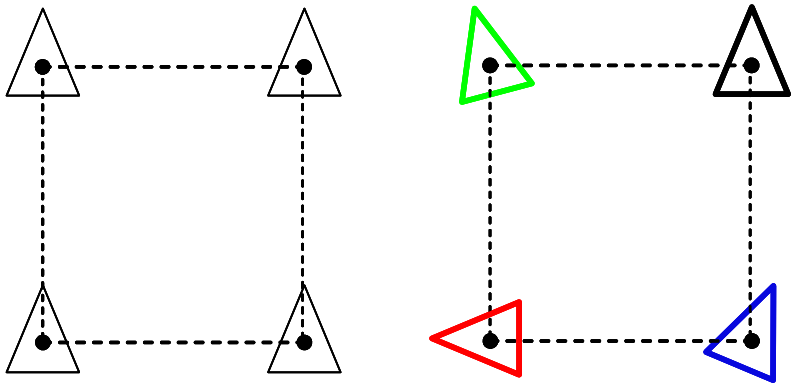

Figure 2-10. Desired shape (left) and actual shape (right) of a square formation.

The following four figures show the separate formation view of each robot. The views are colour coded by the colour of the considered robot. In figure 2-11a the formation is shown as it is expected by the black robot in the upper right corner. Figure 2-11b shows the formation as it is expected by the blue robot in the lower right position. Since the blue robot has a heading different from the black one, it expects the other robots in positions that are rotated by the same heading.

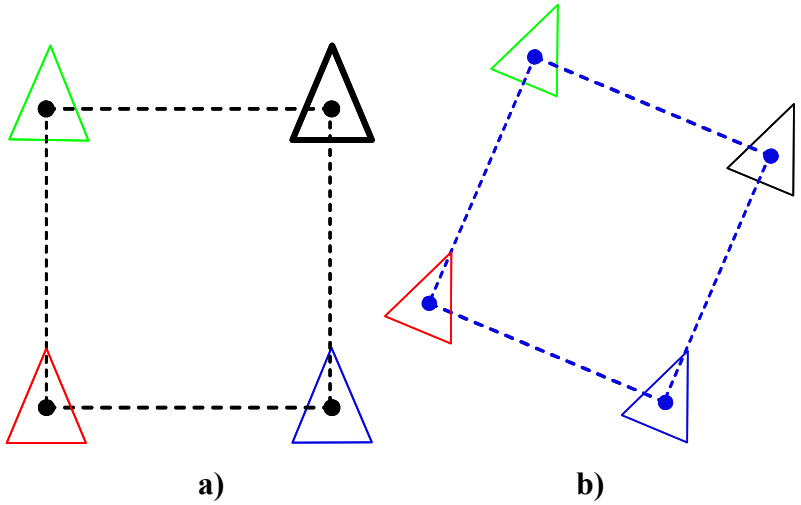

Figure 2-11. Expected formation from black robot's view (left) and from blue robot's view (right).

The same holds for the red robot in figure 2-12a, which expects the formation to be rotated about 90 degrees relative to the black robot, and the green robot in figure 2-12b.

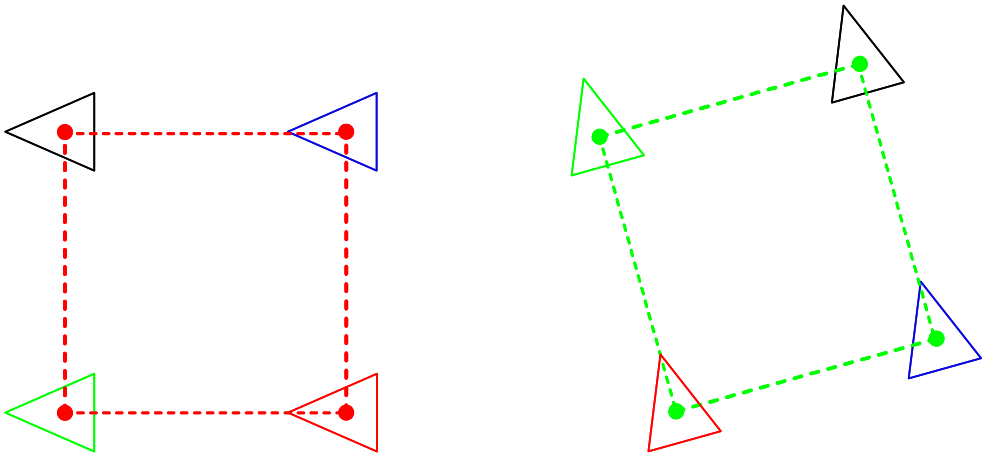

Figure 2-12. Expected formation from red robot's view (left) and from green robot's view (right).

Now each robot compares its "personal" view or expectation of where the other robots should be (figure 2-11 and figure 2-12) to the real positions of the group members (figure 2-10b). This is done for each of the group members separately. The results are three vectors for each robot, which describe the difference between the actual and the desired formation positions of the other formation members. Using this information, each robot calculates its own new position and orientation that comes closest to re-establish the desired formation.

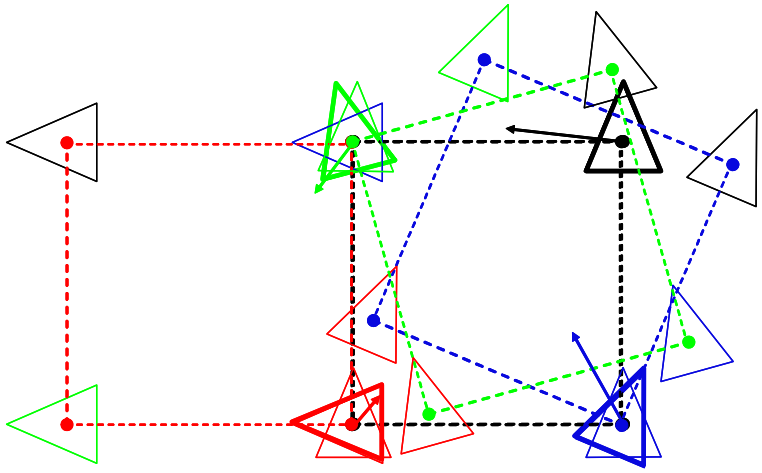

Figure 2-13. Overall sum of expected positions and resultant forces (arrows).

In figure 2-13 the sum of the different robot views is printed. Additionally, the resulting new position vector for each robot is drawn (arrows). This view, which on the first look might be confusing, shows that the method is intuitive. The red robot has only to move

a very short distance. This correlates with its position in all four "robot views". The green robot has a slightly larger magnitude or length in its formation vector. This results from the formation view of the red robot. The formation forces of the black and blue robot are both strongly influenced by the view of the red and green robot.

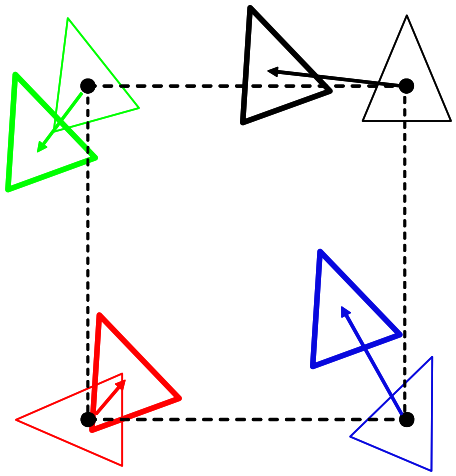

Figure 2-14. Old robot positions (light triangles) and new robot positions (bold triangles).

The view in figure 2-14 shows the robots in the new positions, which re-established the formation.

2.2.2.4 Obstacle and Goal Forces

In addition to the formation forces, a repulsive force caused by obstacles (or by other robots) and, in this version of the implementation, a goal force that attracts the formation to a certain point must be taken into account.

Let $H \subset \mathbb{R}^2$ be the set of all obstacles, so for all points $x \in \mathbb{R}^2 - H$ outside of the obstacles the repulsive potential is $U_{rep} : \mathbb{R}^2 \to \mathbb{R}$ with

$$U_{rep}(w) = \begin{cases} \frac{1}{2}\eta\left(\frac{1}{\delta(w)} - \frac{1}{\delta_0}\right)^2 & \text{, if } \delta(w) \le \delta_0 \\ 0 & \text{, if } \delta(w) > \delta_0. \end{cases} \tag{9}$$

where $\delta(w) := \min_{w' \in H} \|w - w'\|$ is the minimal distance to all obstacles and δ_0 the maximum influence of the obstacles. Correspondingly, for the repulsive force $F_{rep} : \mathbb{R}^2 \to \mathbb{R}^2$, that affects robot k of a group on position w, there applies $F_{rep}(w) = -\nabla U_{rep}(w)$ which is

$$F_{rep}(w) = \begin{cases} \left(-\frac{\partial}{\partial x} U_{rep}(w), -\frac{\partial}{\partial y} U_{rep}(w) \right), & \delta(w) \le \delta_0 \\ 0 & , \delta(w) > \delta_0 \end{cases} \\ = \begin{cases} \eta \left(\frac{1}{\delta(w)} - \frac{1}{\delta_0} \right) \frac{1}{\delta^2(w)} \nabla \delta(w), & \delta(w) \le \delta_0 \\ 0 & , \delta(w) > \delta_0 \end{cases} \tag{10}$$

To reduce the computing costs in the current implementation, a simplified approach in order to calculate the repulsive forces is used. Let o_i the vector of a single laser beam that hits an obstacle in a distance smaller as d_{max} then force F_{rep} is calculated by

$$F_{rep} = \kappa \sum_{i=1}^{n_{total}} \left[\left(\frac{d_{max} - \|o_i\|}{d_{max}} \right)^3 o_i \right], \tag{11}$$

where κ is a scaling factor and n_{total} is the number of laser beams taken into account.

The method for generating the repulsive forces is a modified approach similar to the one proposed by Borenstein and Koren [86]. The laser sensor readings are directly transformed into the corresponding repulsive forces. These forces are scaled depending on the distance and, finally, summed up.

The approach for calculating the goal force is similar to the one for the formation force. Let $z := (x_z, y_z) \in \mathbb{R}^2$ be the desired goal position. Then the corresponding potential field is defined as $U_{att} : \mathbb{R}^2 \to \mathbb{R}$,

$$U_{att}(w) = \frac{1}{2} \zeta \|w - z\|^2, \tag{12}$$

with a positive scaling constant $\zeta \in \mathbb{R}$. For the resulting attracting force $F_{att} : \mathbb{R}^2 \to \mathbb{R}^2$, which affects a robot at position *w*, there holds

$$F_{att}(w) = -\nabla U_{att}(w), \tag{13}$$

leading to

$$F_{att}(x,y) = \left(-\frac{\partial}{\partial x} U_{att}(x,y), -\frac{\partial}{\partial y} U_{att}(x,y) \right) \\ = \zeta (x_z - x, y_z - y) \tag{14}$$

Thus, the overall resulting force $F_k(w): \mathbb{R}^2 \to \mathbb{R}^2$ which affects a robot k at position w is

$$F_k(w) = F^k_{form}(w) + F_{rep}(w) + F_{att}(w). \quad (15)$$

The following pictures demonstrate two typical obstacle situations for a multi-robot formation. In figure 2-15 the formation is affected by an obstacle that is close to the desired path. As soon as the sensors detect the obstacle, the resulting repulsive forces will push the robots that "see" the obstacle aside. Since all robots try to keep up the formation even robots that did not detect the obstacle will be pushed away.

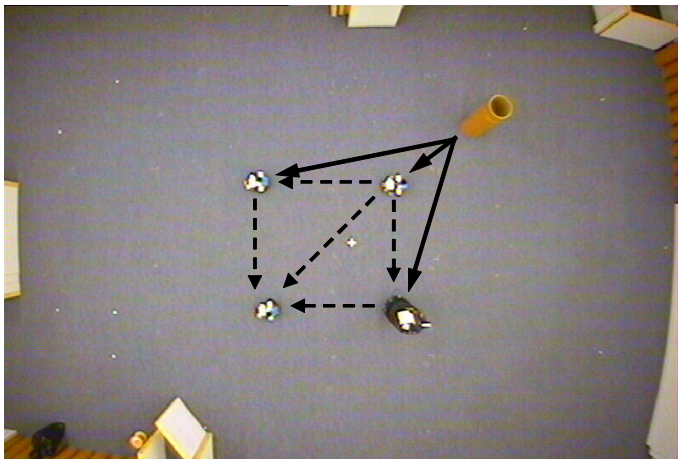

Figure 2-15. Obstacle "pushing away" the whole formation.

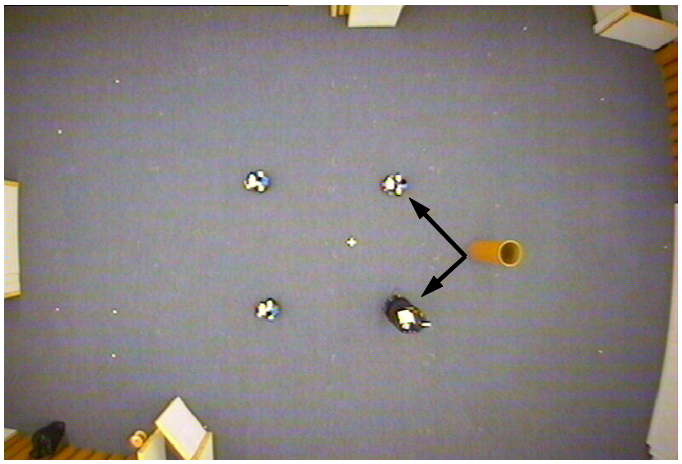

Figure 2-16. Obstacle dividing the formation.

If the formation is widely spread and the obstacle small enough the formation might split up (see figure 2-16). In this case, the formation will expand while passing the obstacle and contract again after passing the obstacle.

Basic considerations on this potential field approach to formation generation and navigation and, especially, its mathematical foundations have been published in earlier work [140, 142]. Thereby, [142] presents a first comparison of the conventional non-directed and the novel directed potential field method.

2.3 Experiments for Formation Navigation

The following section will describe experiments that were carried out to test the fundamental framework of the approach. The experiments show the general behaviour of the developed method when:

1. Generating formations
2. Moving as a formation
3. Moving as a formation in the presence of obstacles

In these experiments, the directed approach is compared against the non-directed approach in various configurations.

2.3.1 Comparison of Directed and Non-Directed Potential Field Approaches

To validate that the presented methods can be transferred into a real world environment, experiments with a real multi-robot system as well as with the simulator have been performed. The simulation environment completely models a group of physical robots, including dynamics, odometry error, and laser sensor readings. The test environment in the laboratory consists of a 15 x 17 meter hall with two B21 and two MagellanPro Robots by RWI. Several settings have been evaluated to demonstrate the usability of the presented methods and the differences between the two approaches. Three of these settings will be described in the forthcoming sections: generation of formations, moving in formation and obstacle avoidance.

2.3.1.1 Generating Formations

One of the basic abilities in formation navigation is to set-up a number of robots in a desired geometric shape aka generating a formation. This procedure does not mean that the involved robots will move as a formation but try to establish the specified formation and then stop. This differs from the scenario where robots set-up the formation while already moving to a certain goal point.

Figure 2-17 depicts a basic situation with three robots and no goal force present. From their starting positions (upper left), the robots shall proceed into a triangle formation (upper right). The lower left illustration shows the result for the non-directed approach. Since only distances are taken into account for building the formation and the middle robot starts a bit left of the two others, the resulting formation is mirrored compared to the required one. The lower right picture gives the result for the directed force approach: the three robots converge exactly into the required target formation because each robot's actual orientation is considered for the generation of the formation forces.

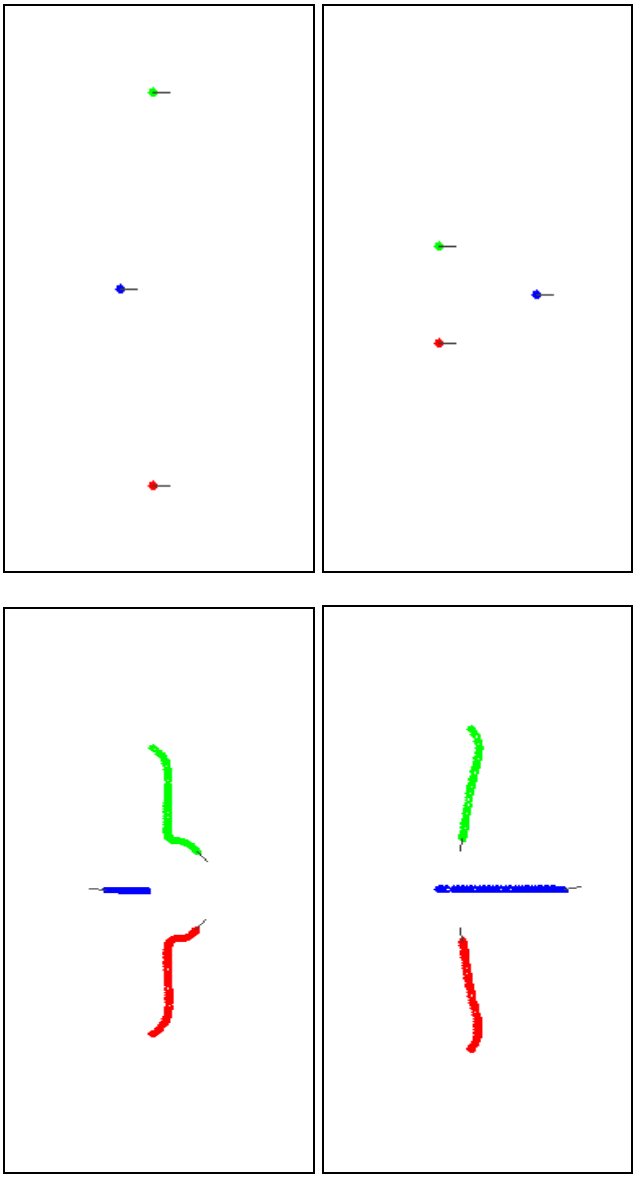

Figure 2-17. Formation generation example. Starting points (top left) and target formation (top right) for three robots, results for non-directed (lower left) and directed force method (lower right).

To test that the generation of a formation is also possible in cluttered environments like public places, an experiment with a high obstacle density was conducted. The following pictures in figure 2-18 show the set-up of a square formation with the directed force method in a cluttered setting. The four robots start in a line formation and proceed into the desired square formation (upper left to lower right). Since in this experiment obstacles are present, the robots cannot move in straight lines.

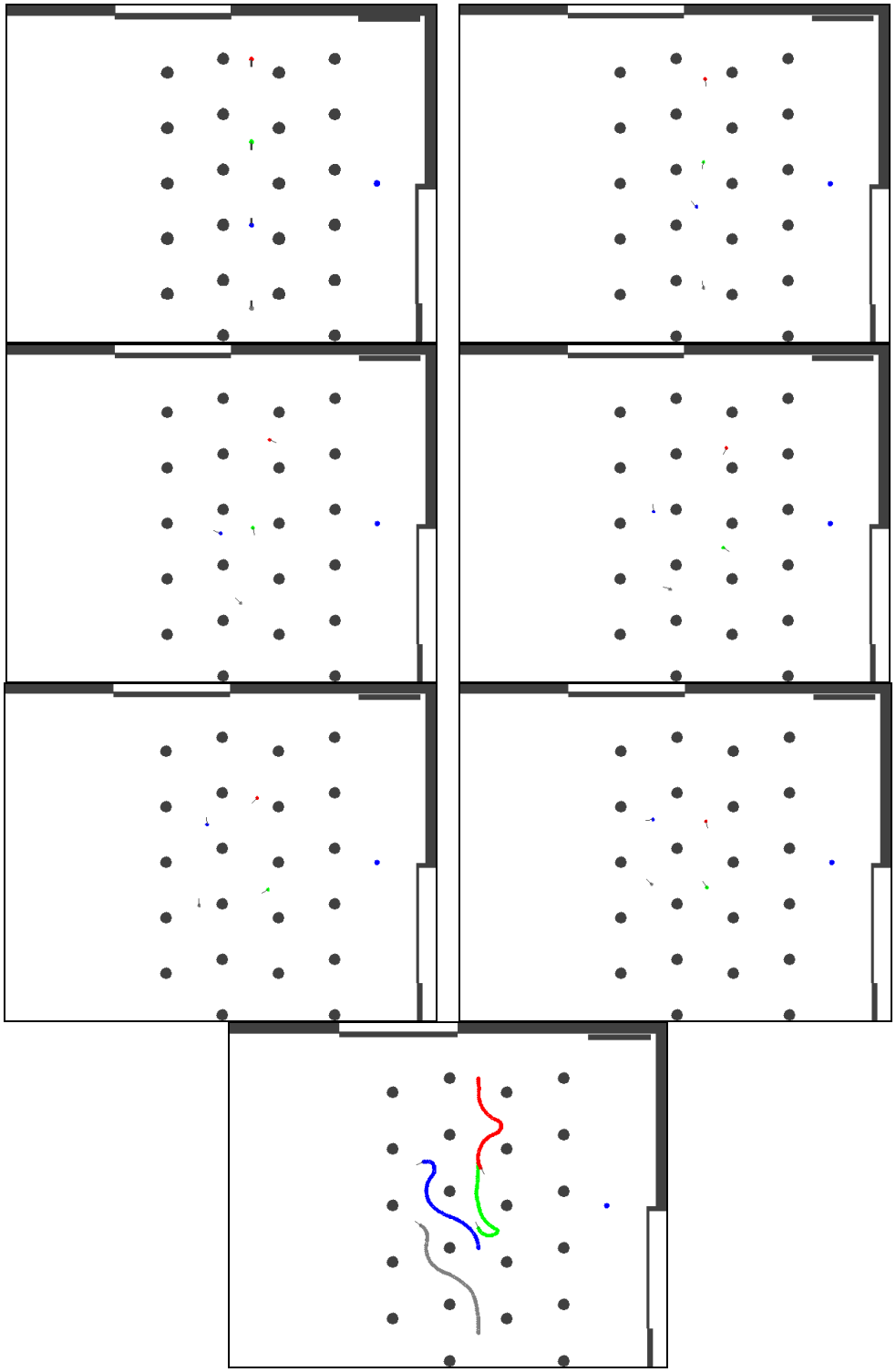

Figure 2-18. Formation generation with high obstacle density. Four robots (top left) move into a square formation (bottom right). In the last picture the driven tracks of the robots are drawn for clarification.

In this scenario, the robots do not only use the formation forces but also the build-in collision avoidance. The repulsive forces generated through the obstacles are directly extracted from the laser sensor readings as described in section 2.2.2.4. This direct combination of formation and obstacle forces allows a very quick and smooth path generation. In the final picture of figure 2-18 (lowest picture), the driven tracks of the four robots are drawn for clarification.

A similar but more unsymmetrical real world experiment is shown in figure 2-19. Four robots (two B21 and two MagellanPro) take a square formation through a passage. The important detail in this scene is the fact that an obstacle is between the robot before and after the set-up of the formation.

In the first pictures (from upper left to lower right), the formation starts to expand. This results from the fact that three robots are on the right side of the passage and the upper left robot is far more out of position. When the black B21 is pushed and pulled through the passage due to the formation forces, the group expansion slows down. This example also demonstrates that the balance between the formation forces and the obstacle forces is important and must be chosen depending on the desired behaviour. However, the experiment also shows that the method is capable of handling quite heterogeneous robots, since the B21 has a completely different driving system compared to the MagellanPro.

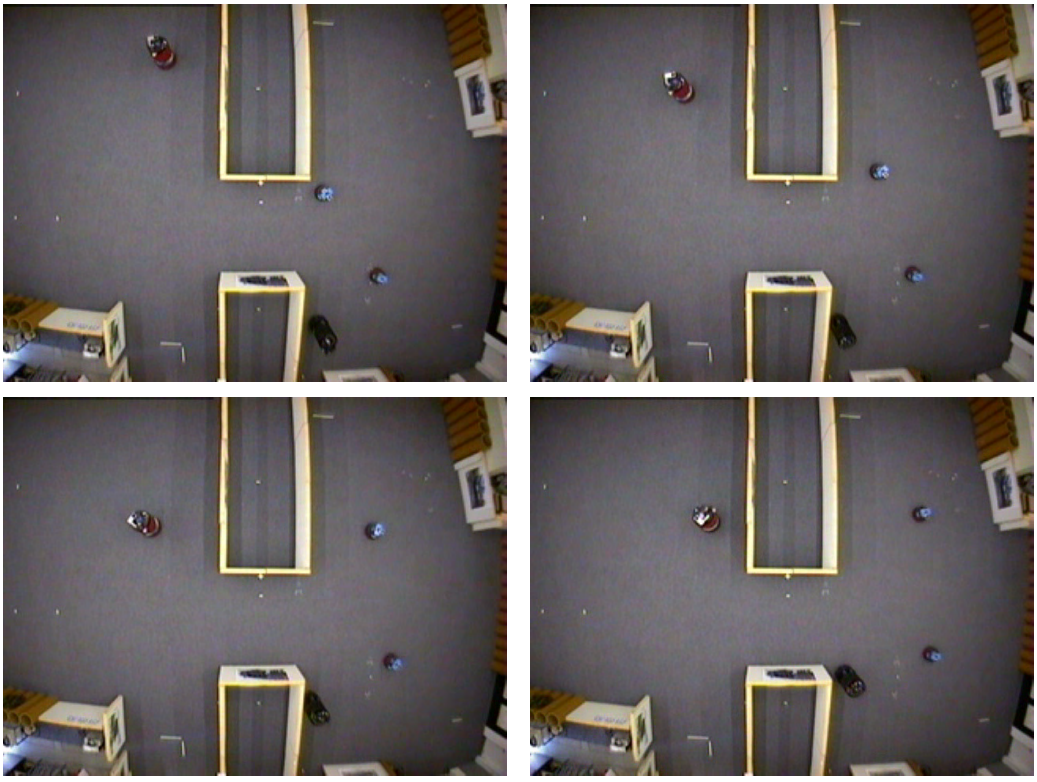

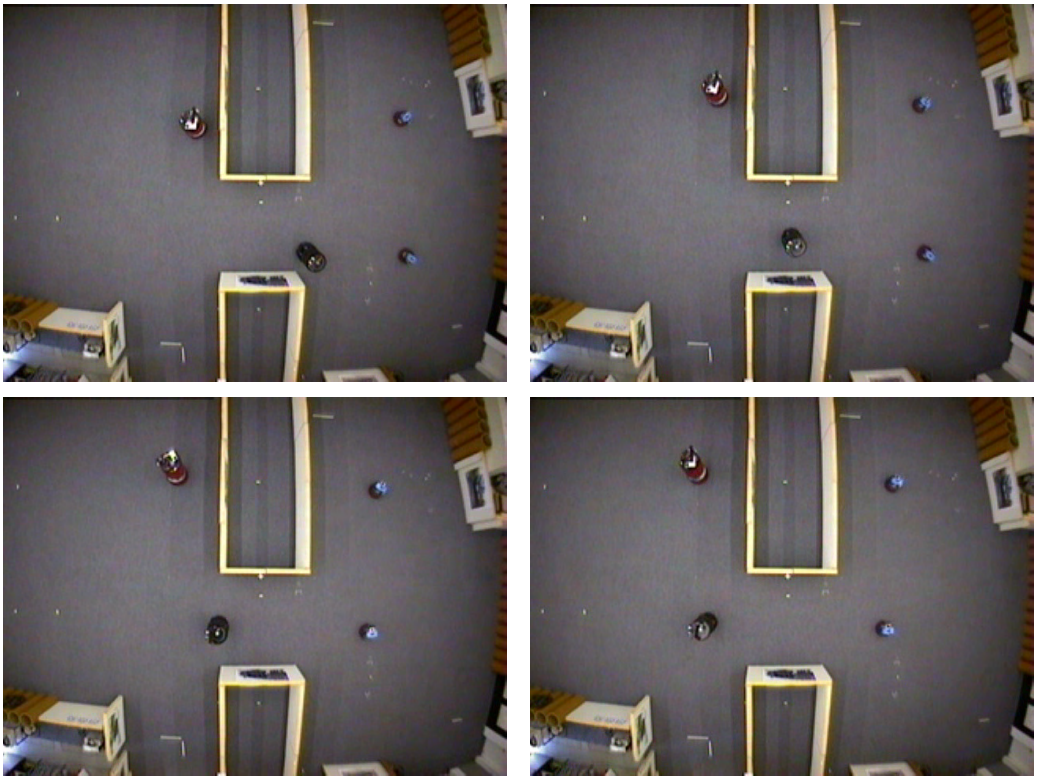

Figure 2-19. Formation generation with a large obstacle inside the formation. Four robots (top left) move into a square formation (bottom right).

2.3.1.2 Movement in Formation

The next logical step is to drive the robots while being in a formation and maintain the formation when manoeuvring. The following experiments show the basic capabilities of the two methods for moving in formation in absence of obstacles. Nevertheless, the robots will use collision avoidance to omit clashes.

The first series of illustrations (figure 2-20) gives a descriptive example. The target formation consists of three robots in a straight line, all looking towards the first goal point near the bottom left corner of both figures. In both, left and right experiment, the formation then moves towards this goal, and just before reaching it, a new target point near the bottom right corner of the figure is given. This is repeated three times in order to let the formation move counter-clockwise on a square path.

The left part of figure 2-20 shows the result for the non-directed method. Because direction is not used in the computation, the line formation does not turn while moving on the square path. The right part shows the result for the directed force approach. As stated in the mathematical background in section 2.2.2 the direction to the goal point influences the calculation of the formation forces. Consequently, the robots always try to keep the initial formation, i.e. all in a line pointing towards the target point. Of course, this leads to some local disturbance when the goal point changes, which can be

seen at each corner of the square path. The front robot has to reach its front position again, the robot at the rear position also has to change place, and the robot in the middle only turns around. The schematic outline of the scenario is shown in figure 2-21.

Clearly, it is application dependent whether one of these two behaviours is preferable. If there is some kind of leader-follower relationship among the robots of a group, it might be a requirement that the leader stays at the same position relative to the driving direction. On the other hand, for robot transport missions or with regular formations (e.g. circles) the individual positions of each robot might be of less importance.

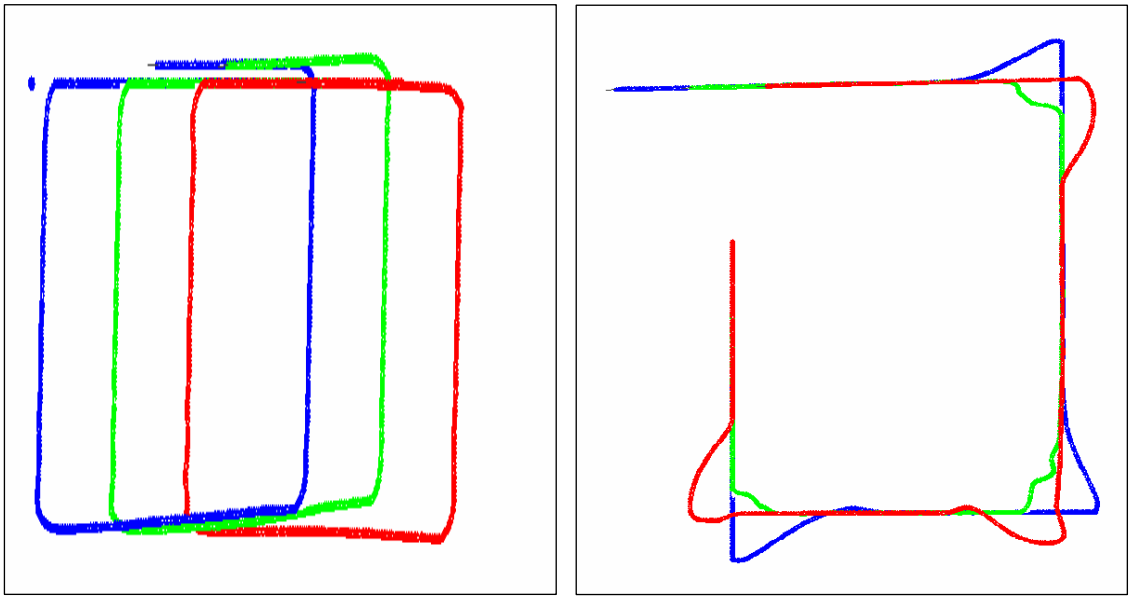

Figure 2-20. Three robots in a line formation moving around a square path. Non-directed method: orientation of the formation does not change (left). Directed force approach: line formation turns around 90 degrees for each new goal point (right).

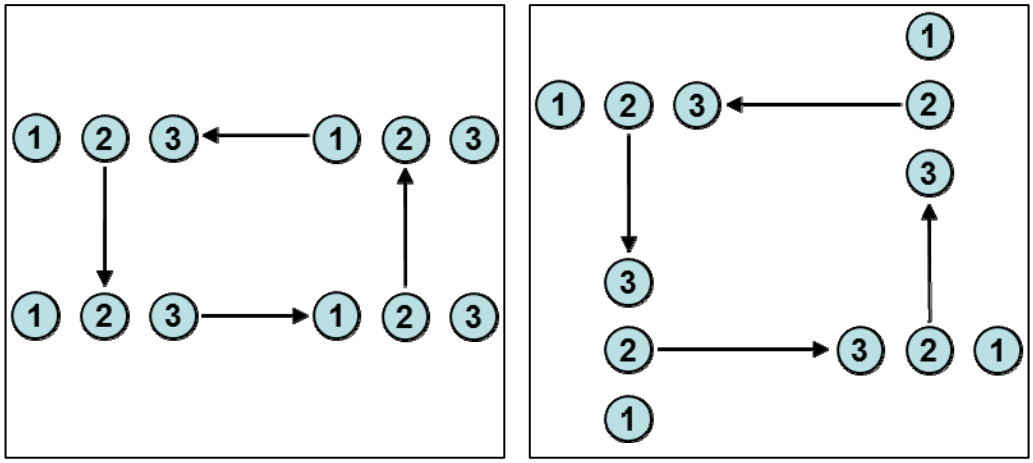

Figure 2-21. Schematic drawing of the formation movement from figure 2-20.

The following two series demonstrate the behaviour of the two methods in a more complex manoeuvre. The formation has to drive a figure that looks like an eight or an uppercase “B”. Again, there are no obstacles, but collision avoidance is used.

The first set of six pictures (figure 2-22) shows the behaviour of three robots in a triangle formation using the non-directed method. While the robots keep up the triangle shape, it is obvious that they change their position within the formation at every turning point. This leads to the situation that the shape is maintained, but the orientation of the triangle changes. In the upper left picture and before the first turn the red robot is on top of the formation and triangle. After the first turn, the red robot is still on top of the triangle, but – since the robot formation did not maintain its direction – the blue robot now is on top of the formation. These position changes continue at every turn until the formation finally arrives “backwards” at the goal position.

The next set of pictures (figure 2-23) shows the same formation setting with the directed method. The first picture (upper left) already illustrates the major difference to the former setting. To keep the formation in shape some of the robots have to detour when turning in larger angles. This behaviour ensures that at every time in a manoeuvre each robot is as close as possible to its formation position. In the presented scenario the red robot for example keeps in place in every of the six turns and arrives as the leading robot just as it started. Large formation might face a somewhat scurry behaviour, but in the non-directed method the robots would “chaotically” snap into some position.

The advantage of using a directed force-based method is that even large or complex formations can easily be defined and maintained in terms of strict positions within the formation. In sensing (e.g.: de-mining) or transporting missions (e.g.: heavy loads), the robots must maintain their assigned position inside the formation. The special formation problem of marching would not be possible with the non-directed method because changing a position inside the formation is not desired.

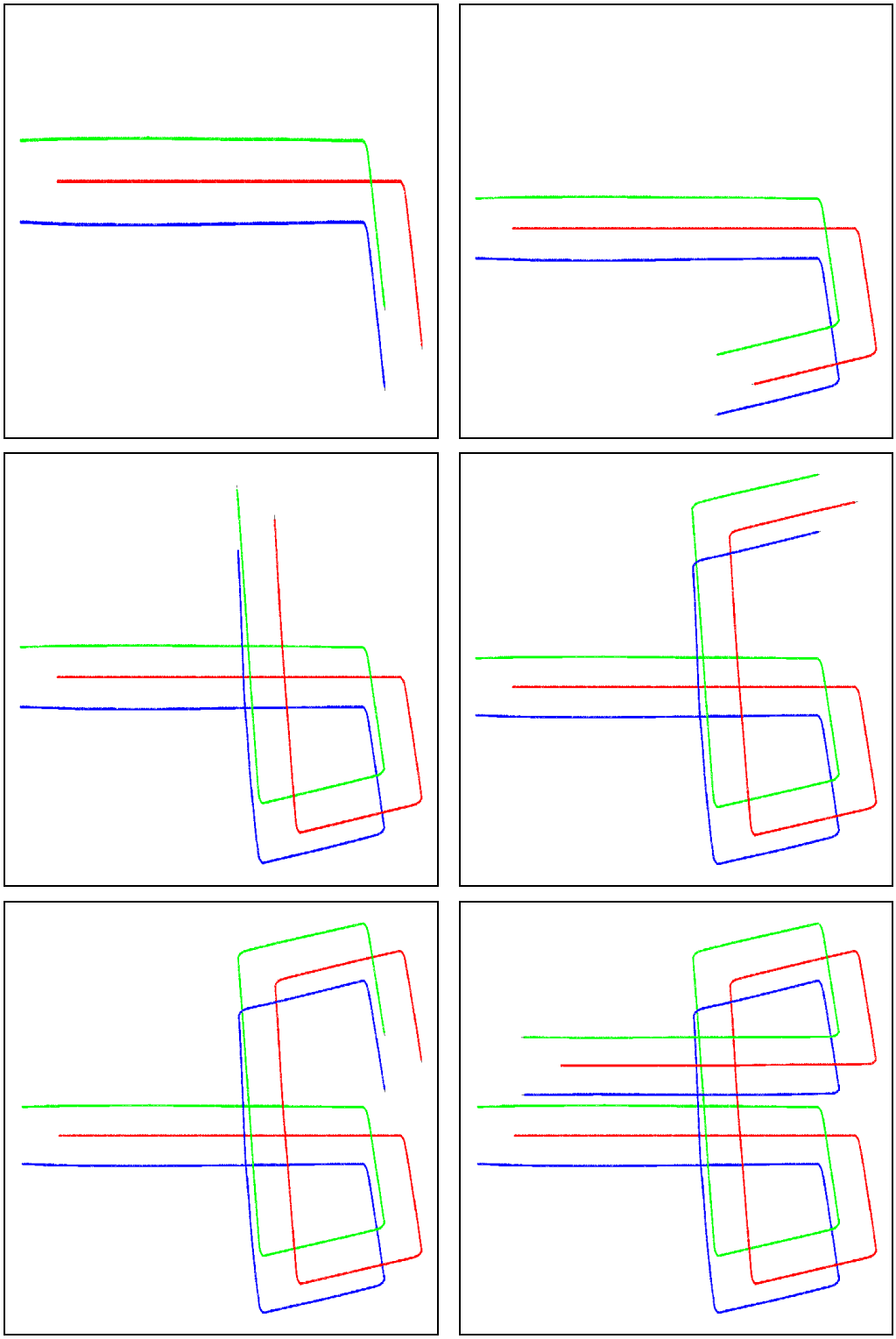

Figure 2-22. Three robots in a triangle formation with the non-directed method moving on a "B"-like course (top left to bottom right).

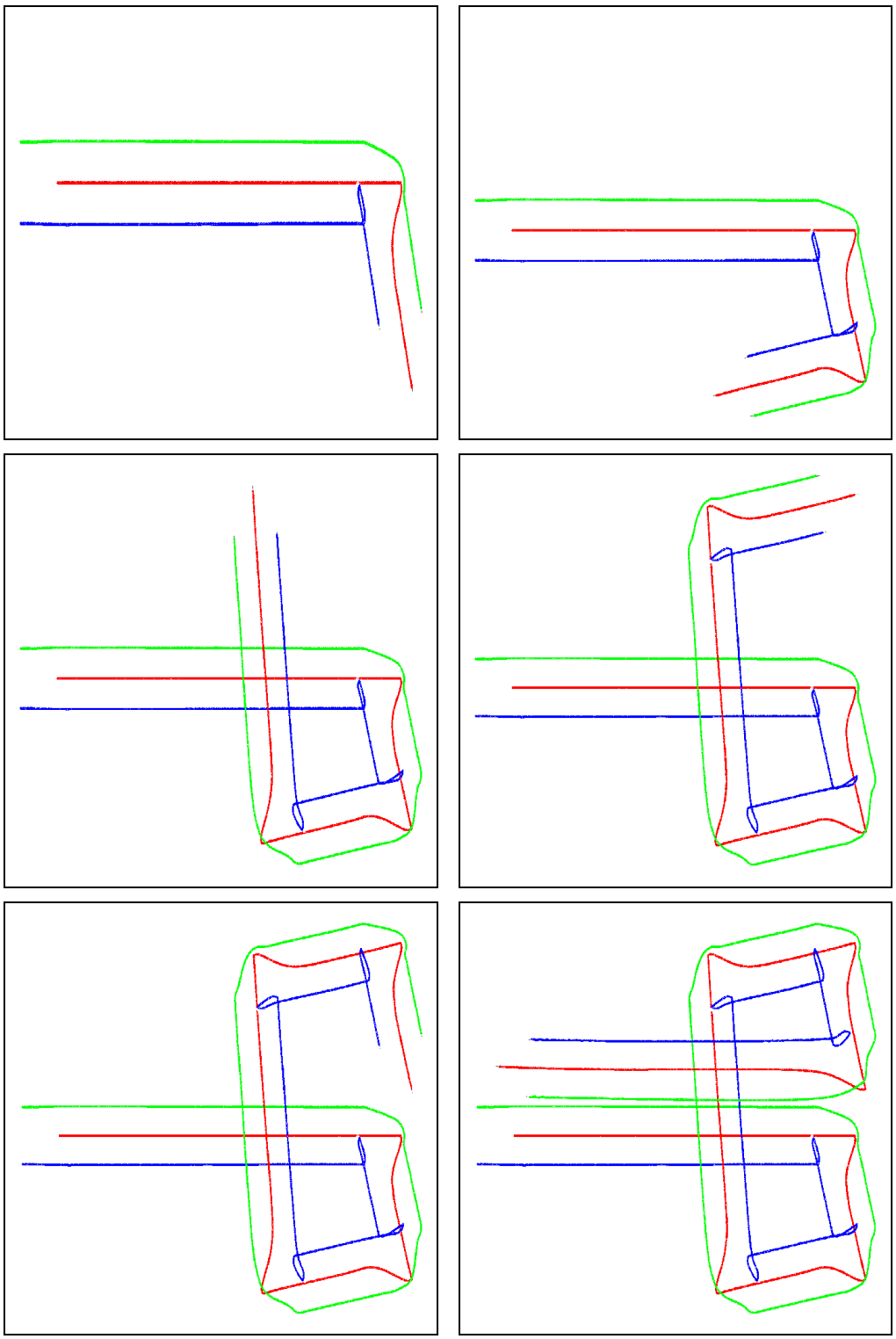

Figure 2-23. Three robots in a triangle formation with the directed method moving on a "B"-like course (top left to bottom right).

The series of fundamental experiments, finally, addresses the combination of formation movement and obstacles. The first scenario in figure 2-24 shows a situation with two obstacles that the robot formation has to pass on its way towards the goal point. This time an irregular triangle formation is used, and the goal point at the right remains the same throughout the experimental run.

Use of the directed force approach (upper) leads to the expected results: the two cylindrical obstacles produce some local deviation in the robot formation, which is corrected by the formation forces shortly after passing the obstacles. In most of the cases, the non-directed method produces more or less the same result. However, sometimes the forces exerted by one of the obstacles lead to a complete change of the resulting formation.

In the lower part of figure 2-24, an example for this behaviour can be seen. The obstacle forces produced by the lower obstacle let the bottommost robot evade to the upper direction. Since at the same time the other obstacle forces the topmost robot to the opposite direction, suddenly another configuration of the formation is more appropriate, at least in terms of distances between the robots. Because any formation with the same inter-robot distances is considered as correct, now the formerly bottommost robot "snaps" to the top position. As can be seen from the illustration, after some time the resulting formation again converges into a consistent triangle formation.

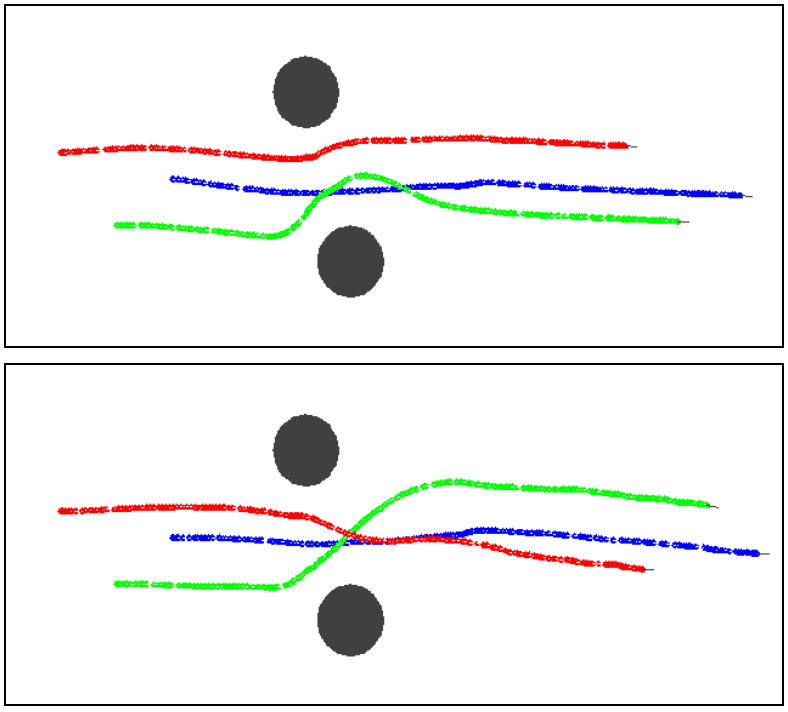

Figure 2-24. Movement in the presence of obstacles. With the directed force method the robots always return to their formation position (top). In the non-directed case the formation might get rearranged: sometimes two robots switch their positions (bottom).

The two examples in figure 2-25 show a triangle formation driving through an obstacle field. These plots of recorded real world data show that already minor differences or disturbances can lead to quite different paths. In both scenarios, the same robot started in the same position from the same starting point. Nevertheless, even with that imponderability the directed formation approach maintained the formation. Using the non-directed approach, the blue and the red robot in the left scenario the green and the red robot or in the right scenario might have switched positions.

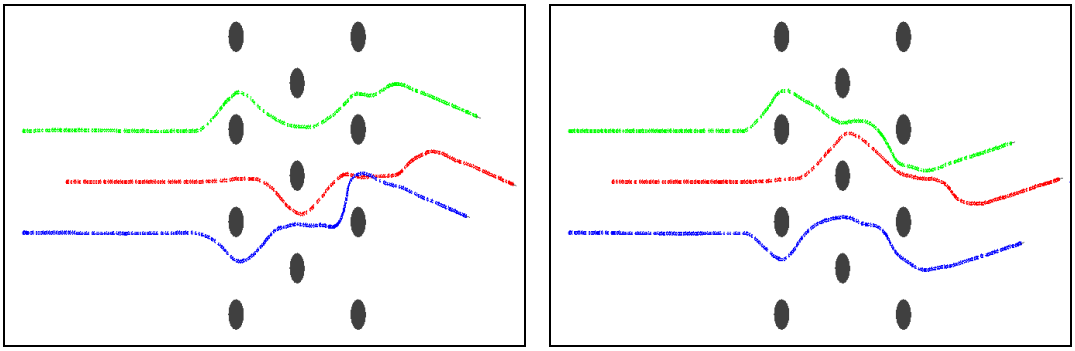

Figure 2-25. Two examples for the directed method in a more cramped scenario.

The inter-robot forces are easy to see in the first scene when the green robot circumnavigates the last obstacle. Although the red robot has already passed all obstacles, it has an additional knoll in its lane, compensating the formation forces due to the increasing inter-robot distance to the green robot. The same happened just as the blue robot arrives at the last obstacle again resulting in a knoll in its driving lane.

Figure 2-26 shows a similar behaviour with a four robot square formation using the directed approach. Again, even in a symmetric environment and a symmetric formation the slight fluctuations in the sensor readings or the drive systems result in different lanes at the last obstacle. Even in those situations, the potential field approach shows its strength to handle navigation tasks for heterogeneous robot groups without any special treatment. The only detriment might be the slight “oscillation”.

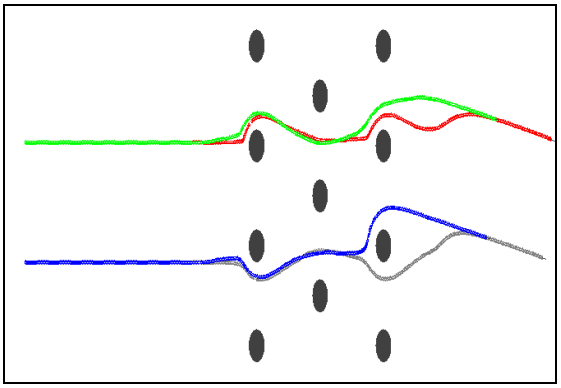

Figure 2-26. An example of four robots in a square formation crossing an obstacle field.

In the scenario depicted in figure 2-27 the six robots start in a line, build a formation while moving and pass several obstacles. This experiment includes most of the issues mentioned before. First, it shows that the method is capable of setting-up a formation while moving. Second, it demonstrates that even complex shapes and formations can be maintained while manoeuvring in the presence of obstacles. The third and important fact is that the formation is able to deform when passing the narrow passage between the obstacles and inflate again.

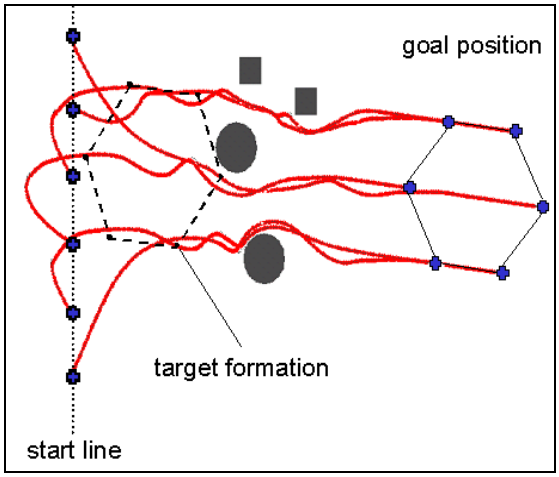

Figure 2-27. A complex formation setting-up and maintaining shape even in a patchy environment.

This leads to the last experiment it this section, the deformation of a formation when passing a constriction. This situation occurs when the formation is larger in its circumference than the available space to manoeuvre (e.g. doorways, hallways, or narrow passages). As shown in the previous scenarios the directed formation approach allows the shape to be deformed without switching the robot positions inside the formation. If the method would not allow deformation, the formation might not be able to navigate in crowded places or office environments for example. This would also transfer formation navigation to the piano-moving problem [149].

However, the presented potential field based approach allows the formation not only to deform, it also inherently includes the ability to expand or shrink without distorting the shape. The following figure 2-28 shows a triangle formation passing a narrow section. When the wider part of the formation comes to the narrowing, it simply squeezes together. After the formation has left the passage, the formation inflates back into its desired size.

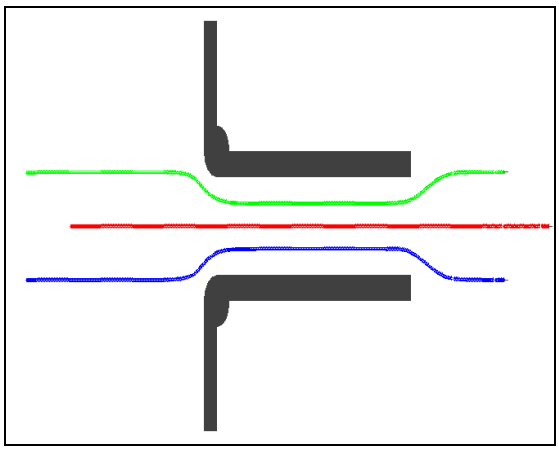

Figure 2-28. Behaviour of a directed triangle formation moving through a narrow passage.

The series of pictures in figure 2-29 demonstrates that behaviour more clearly. Again, a triangle formation has to pass a passage that is smaller than the formation. A strong goal force pulls the formation to the right side of the experimental hall. When the robot on top of the formation is approximately in the middle of the passage, the two robots of the wider formation part face the narrowing. The goal force and the formation forces exerted by the leading robot pull the two other robots into the passage. The formation shrinks, but maintains the distance between the two following robots and the first robot. Due to the orientation forces in the directed approach the shape of the overall formation is maintained. After the passage, the formation immediately disperses into the original shape. The two robots are pushed back into their formation positions by the position forces. Note that parts of the experimental validation presented in this section are based on earlier work published in [143].

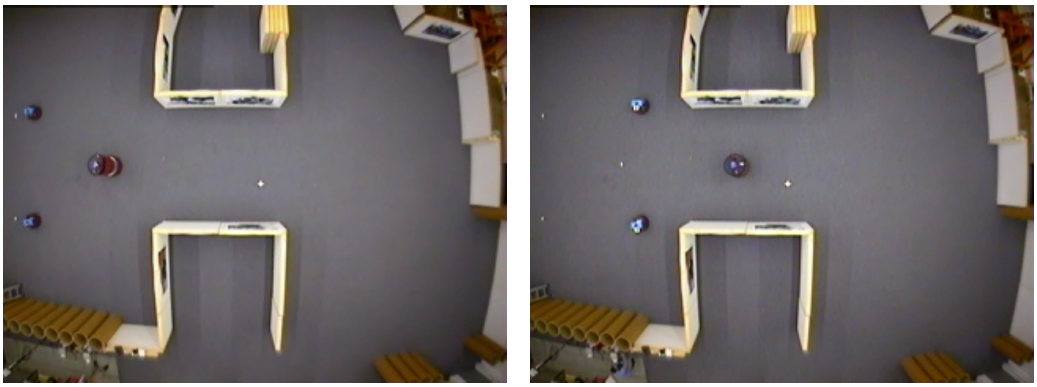

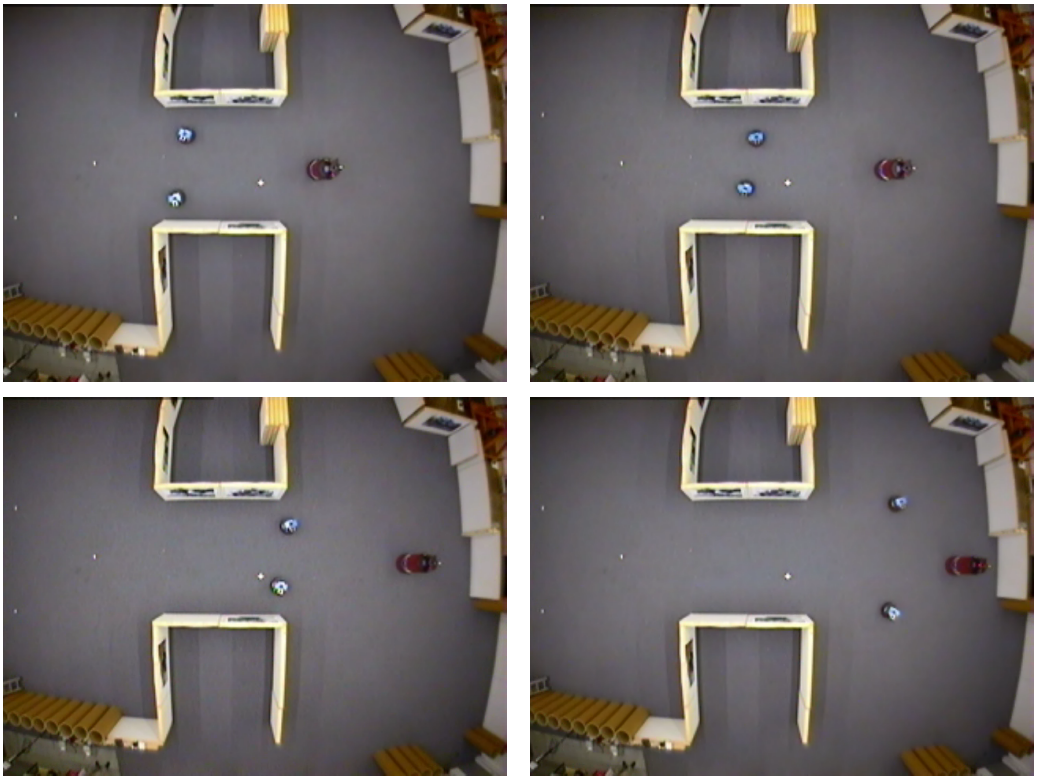

Figure 2-29. Snapshots of a directed triangle formation moving through a passage (top left to bottom right).

2.4 Summary

The foregoing section described the experiments that were conducted in order to test the fundamental framework of the formation approach.

The general behaviour of the non-directed and the directed potential field methods is shown regarding generation of formations, movement as a formation, and finally movement in the presence of obstacles. In the experiments, the directed approach was compared against the non-directed approach in various configurations.

The experiments substantiate that for simple trajectories and without obstacles, it is clearly application dependent, which one of these two behaviours is preferable. If there is some kind of leader-follower relationship among the robots of a group, it might be a requirement that the leader stays at the same position relative to the driving direction. On the other hand, for robot transport missions or with regular formations (e.g. circles) the individual positions of each robot might be of less importance.

This situation changes if the formation has to manage manoeuvres that are more complex. The advantage of using a directed force based method is that even large or complex formations can easily be defined and maintained, even in the presence of obstacles. This also holds for the cases where it comes to knotty trajectories. In sensing or transport missions, the robots must maintain an assigned position inside the

formation. The special formation problem of marching would not be possible with the non-directed method because changing a position inside the formation is not desired. Additionally, the directed method is able to solve the marching problem with a minimum of computation needed even for elaborate formations.

These circumstances become even more obvious when comparing the behaviour of the two approaches in the presence of obstacles. The non-directed approach turns out to be quite unstable regarding the formation positions depending on the repulsive obstacle forces. The robots tend to switch their positions inside the formation especially when passing through narrow passages. In such situations, the directed approach shows a preferable behaviour, which could be called “breathing”. This means that the formation shrinks and, again, inflates depending on the obstacle situation while continuously maintaining its shape and formation positions.

Overall, the experiments provided strong evidence that the potential field approach was successfully transferred from mathematical simulation to real world robot scenarios. It was also shown that the directed approach has several advantages over the non-directed approach especially in the presence of obstacles and for complex manoeuvres. In general, the approach is able to cope with intricate navigation situations using only little computing power and time. Additionally, because each robot calculates the forces for itself, the approach is completely decentralised. This results in low computing costs and makes the method very reactive and scalable.

The APF is computationally highly efficient even for larger formations because it is mainly based on evaluations of individual, independent potential functions for robots and obstacles. This is in contrast to the lately researched optimal control based approaches, which require a joint optimization of the objective function for all robots and for larger time horizons; the accuracy of the robot models used, is crucial in this process. For the APF approach, the relations between the entities of the formation are, in contrast, easy to model and do not introduce extra complexity (unlike e.g. spring damper techniques). Additionally it copes well with heterogeneous groups of robots unlike most of the leader-follower approaches.

3 Formation Navigation Metrics

The experiments performed in the previous section showed that in order to compare algorithms and methods it is important to have measures that allow a meaningful evaluation of the experimental data. The measure should allow performance comparisons of developed algorithms or methods. In the area of MRS formation navigation, only a few approaches to expedient metrics can be found. Various reasons for this include:

1. The complexity increases with the number of robots.
2. Most of the single robot methods cannot simply be scaled to MRS.
3. Access to larger real world MRS or adequate simulation is difficult.

These circumstances might explain the fact that only a few papers deal with systematic (real world) experiments in that field. The following section will focus on the problem of developing appropriate metrics for formation navigation.

3.1 Primary Remarks about Metrics for MRS

Metrics are to some extent determined by the scenario in which the MRS operates. Choosing the right parameters requires analysing the experimental set-up carefully. For simplicity in the rest of the discussion, it is assumed that:

1. the group of robots is made up of similar types of robots (e.g. all B21 or all Pioneers),
2. the robots have the ability to communicate with each other,
3. the robots have the ability to sense the environment and each other (e.g. through tracking),
4. all robots are real and operate in real environments (indoor or outdoor); simulations are not considered.

Most criteria are very much related to the environment. It has a great influence if the robots operate on an empty soccer field or in a crowded train station. However, most metrics work when measuring the effect of a modification (e.g. new algorithm or parameter set) in exactly the same experimental set-up and infrastructure (same robots, environment etc.).

Reasonable parameters for metrics are:

1. time
   - overall time in motion
   - time in/out of formation
   - time for setting up / establishing the formation
2. path
   - overall path length
   - path length being in/out of formation
   - path length for establishing the formation

3. position error
   - displacement in distance
   - displacement in angle
   - only for neighbours or for the whole formation
4. others
   Other parameters could be the amount of computation time, of communication, and of sensing.

Looking at the majority of papers in the area of formation navigation it is obvious that repeatability and reproducibility in the sense of a comparison is very difficult. Every real world set-up is unique even if it is "a typical office environment". If scientist CALVIN would like to compare his approach to scientist HOBBES, he will not be able to do so as long as he has a different set-up – at least if no Transmogrifier is at hand.
One solution for the metric problem might be to take the influence of the environment and other parameters into account. This, of course, would imply in most cases that a detailed map of the environment is available, as well as additional information about dynamic objects. This is difficult to achieve in unknown real world scenarios.

3.2 Common Metrics

This section describes the three commonly used metrics in the field of MRS. The discussed metrics are suitable for unmanned ground vehicles. Other metrics, for example for unmanned air vehicles, have not been taken into account because of the different obstacle situation.
Balch and Arkin [4] use three performance metrics for the evaluation of their formation experiments:

1. *Path length ratio* is the average distance travelled by the robots divided by the straight-line distance of the course.
2. *Average position error* is the average displacement from the correct formation position throughout the run.
3. *Percentage of time out of formation* reflects the time in which the robots fall out of their formation positions.

Naffin and Sukhatme [118] use similar criteria:

1. *Positional Error*: Given a formation, defined as the tuple <*G, h, d*>, where *G* is a connected geometric shape, *h* a desired heading, and *d* a desired inter-robot spacing, there exist *K* positions relative to the leader that represent the perfect formation. Given *N* robots attempting to construct this given formation, where $N \le K$, they define the formation's positional error as

   $$P = \frac{1}{N}\sum_{i=1}^{N} D(p_i, k_i),$$

   where p_i is the i^{th} robot's position, k_i its attempted formation position (both relative to the leader), and $D(p_i; k_i)$ is the Euclidean distance between these two positions. A given set of robots is "in formation" if $P < \varepsilon$, with a user-specified tolerance ε.

2. *Time to convergence* $T_c(N)$ is defined as the duration of time required for a formation to reach a given number of robots N and be in formation for that size.
3. *Percentage of time in Formation* is defined as $F = \frac{t_{in}}{t_{total}}$ where t_{in} is the time in formation and t_{total} is the total time elapsed since the formation reached its current size.

Fredslund and Matarić [56] and Lemay [97] use only the formation evaluation criterion *Percentage of time in Formation*. The robots are considered to be in formation when the following holds:

Given the positions of N mobile robots, an inter-robot distance $d_{desired}$, a desired heading h, and a connected geometric shape G (completely characterizable by a finite set of line segments and the angles between them), then the robots are considered to be in formation G if:

1. *Uniform dispersion*: The same distance is kept between all neighbouring robots with a maximum tolerance of ε_{d_1}.

   $\exists d$, such that $\forall$ pairs of immediate neighbours $\left(R_{i_1}, R_{i_2}\right)$ with distance $dist\left(R_{i_1}, R_{i_2}\right)$, $\left|d - dist\left(R_{i_1}, R_{i_2}\right)\right| < \varepsilon_{d_1}$ and $\left|d - d_{desired}\right| < \varepsilon_{d_1}$.
2. *Shape*: The robots are at the assigned positions depending on the desired formation with a maximal tolerance of ε_{d_2} around the desired position. No angle in the original shape must be stretched more than ε_a to make the data points fit.

   $\exists$ a "stretching function" f with $f(G) = \tilde{G}$, such that $\forall$ angles $\theta \in G, \left|f(\theta) - \theta\right| < \varepsilon_a$, and such that $\forall$ robots R_i, with distance $dist\left(R_i, \tilde{G}\right)$ to $\tilde{G}$, $dist\left(R_i, \tilde{G}\right) < \varepsilon_{d_2}$
3. *Orientation*: The stretching criterion 2 (shape) must not skew the heading more then ε_a.

   $\left|f(h) - h\right| < \varepsilon_a$; for small $\varepsilon_{d_1}, \varepsilon_{d_2}, \varepsilon_a > 0$

The three criteria allow measuring a "global" position error. Criteria 1 and 2 define tolerances for distance and angle measurements to be able to cope with noise and imprecision. Criterion 3 states that it should be possible to adjust desired distances and angles over the predetermined position so that all robots form the desired shape. The robots are allowed to move in a radius of ε_{d_2} away from their desired positions. This criterion enables the realisation of the desired shape even when each robot separately respects criteria 1 and 2.

When looking at the three presented approaches, basically, they all use the same metrics:

1. Position error
2. Percentage of time in formation

Every time and path parameter that is related to the shape of the formation, can only be calculated when a position error is measured. This reduces the number of elementary metrics for formation navigation to the position error criteria and the additional factor of time. However, as already stated above, these parameters are highly influenced by the structure of the environment. So, although Balch, Naffin, and Fredslund use similar metrics in the sense that they are all based on the position error, the results of the experiments cannot be directly compared.

The first part of the following experimental evaluation and discussion, namely sections 3.3.1 and 3.3.2, address the described common metrics, which do not consider any parameters of the environment. The last part, section 3.3.3, will then motivate the need for an extended, more generally applicable metric.

3.3 Experiments for Metrics in Formation Navigation

3.3.1 Experimental Setup

To evaluate the so far presented metrics, several experiments were conducted in simulation as well as in the robot lab. In both cases, two identical scenarios have been used. First, the robot formation had to pass a narrow passage of about 3m width and 4m length. In the second scenario, the robots had to move through an arrangement of pillars. The distance between two pillars of one row was about 3m and the distance between two rows was 2.5m. Figure 3-1 gives a graphical illustration of these two settings. In each figure, one simulated example run has been plotted. A formation of two or three robots started on the left side and passed the obstacles, thereby moving towards the goal point on the very right side.

The robots used to carry out the experimental runs were all circular with a diameter of 54cm. To get a better impression of the real world set-up look at the pictures in figure 3-2. A passage and a pillar scenario had to be passed by a triangle formation of one iRobot B21 and two Magellans. For the simulated runs, also round robots of 54cm in diameter were modelled. The motion model used in the multi-robot simulation environment corresponds to the B21 robot type.

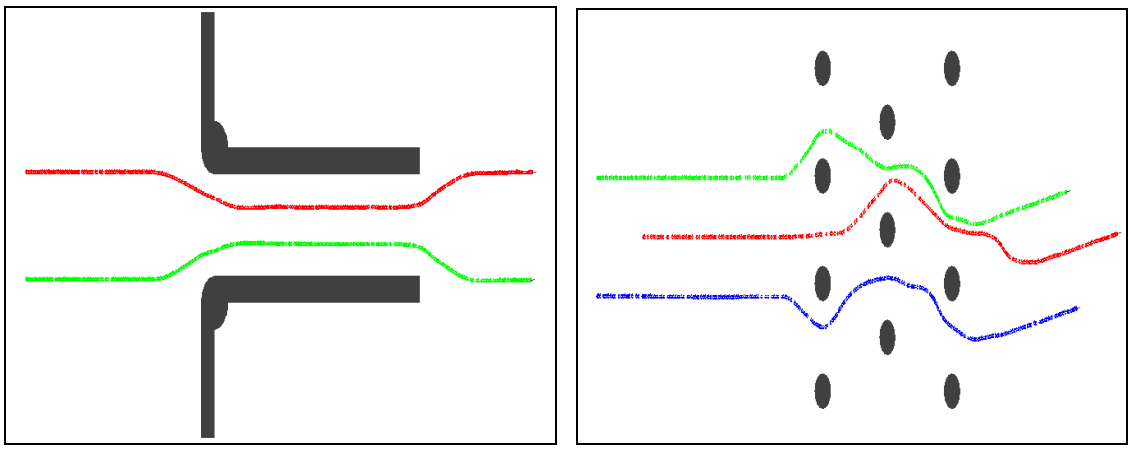

Figure 3-1. The passage scenario with an exemplarily chosen run of a two robot line formation (left). The pillar scenario with a three robot triangle formation (right). The formations started left and moved to the right towards the target coordinates.

In order to apply any metric it is, of course, necessary to acquire precise position information for each robot. Whereas it is simple to get the exact positions from the simulator at a fixed rate of, e.g., 10Hz, it is difficult to find such a ground truth for any real robot system. Common methods include vision-based approaches using ceiling cameras or installed beacons in the environment. Since all the used robots are equipped with two SICK laser scanners providing high precision 360 degree distance information, it was decided to use a standard SLAM method to correct odometry errors and compute global position information for the robots [45]. The localization step of the chosen SLAM algorithm runs at a much lower frequency than 10Hz and produces correction data only every two to four seconds. Therefore, from time to time gaps occur within the recorded paths of the real robots, because even in a four-second interval an additional odometry error of several centimetres can arise. The impact of these inaccuracies is discussed in more detail in the next section.

For both settings, passage and pillars, two different formations have been surveyed: a triangle formation made of three robots and a simple line formation of only two robots. Figure 3-2 provides two examples with these two formations. For each combination of the two formations and scenarios, 10 runs have been recorded, resulting in 40 simulated and 40 real world runs. This data is taken as a basis for the ongoing discussion of the metrics chosen for this multi robot application.

It should be emphasized that the real world experiments took place in a large experimental area with a size of about 14m x 17m. The setup included an office-like configuration of nearly real world dimensions. This large setup makes the comparison to experiments like those carried out by Lemay et al. [97], Naffin and Sukhatme [118], or Fredslund and Mataric [56] somewhat unbalanced. In their work, the typical multi-robot experimental lab environment is not larger than 5m x 5m.

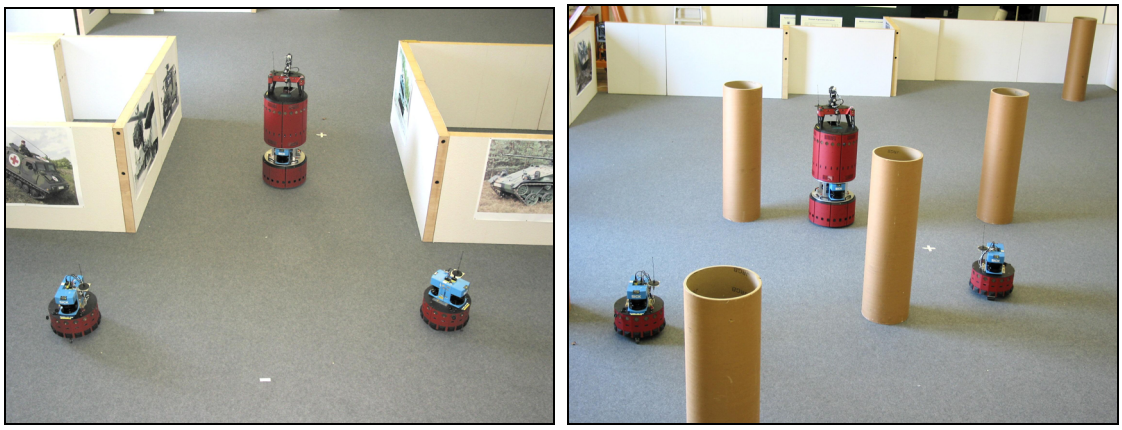

Figure 3-2. The passage (left) and the pillar scenario (right) in the lab environment. A triangle formation has to pass the obstacles.

3.3.2 Experiments with Common Metrics

In many cases, special characteristics of a formation algorithm are used to define a metric. Since the goal is a discussion of portability of metrics for different formation approaches, robot systems, and environmental conditions, it was tried to avoid this in the evaluation. The two metrics that have been used for the forthcoming experiments are formation position error and the percentage of time, for which the robots are "in formation". As stated in section 3.2 these are also the basic metrics used in the described approaches of Balch, Naffin and Fredslund.

In order to compute the formation position error, first an optimal formation position given the actual positions of the robots is calculated. Chapter 2 gives a detailed description of formation navigation approaches in general and of the used directed potential field method in particular. Because of this directed potential field approach, the actual target point determines the overall direction of the formation. For example, if the target formation is a triangle with one robot in the front, then the triangle formation is always turned with the leader's vertex pointing towards the goal.

This special feature of the formation algorithm simplifies the search for an "optimal" formation position with regard to the robots' actual positions at each time step. Since the formation direction only depends on the destination and the formation position, for the optimisation only the two-dimensional position parameters have to be considered. Therefore, the function of the added distances between each robot's actual position and its formation position is continuous and monotonically increasing. Thus, a simplex algorithm [95] with guaranteed termination was used to actually compute the minima.

The resulting (minimal) formation position error was used as input for the second metric, the so-called in-formation ratio. A threshold of 20cm per robot involved (leading to a 40cm threshold for two-robot formations and 60cm for three robots) was chosen to decide whether the robots were considered in or out of formation. Of course, these values are somewhat arbitrary, but produced feasible results for the example environment (see section 3.3.1). A more sophisticated solution should calculate these

thresholds automatically in order to keep the presented metrics generic. Influencing factors are, for example, size of robots and environment or density of obstacles (which is often unknown a priori).

Figure 3-3 and figure 3-4 provide two exemplary results for the passage scenario and the two-robot formation shown in figure 3-1 in the last section. Both figures are divided into an upper part, which displays the paths in Cartesian coordinates for both robots, and a lower part, which gives the results in terms of the chosen metrics. The solid line gives the total formation error for each time step, as described in section 3.3.2. Additionally, a dashed line is printed showing the limit beyond which the robots are considered to be out of formation. Note that this limit depends on the number of robots, for the two-robot case it is 40cm and for three robots 60cm.

Figure 3-3 presents data recorded with real robots in the multi robot lab, figure 3-4 refers to an arbitrarily chosen simulation run. As one can see, results are similar concerning both the total formation error as well as the in-formation ratio. Before a deeper discussion of the numerical results, examples for the other treated scenario will be given.

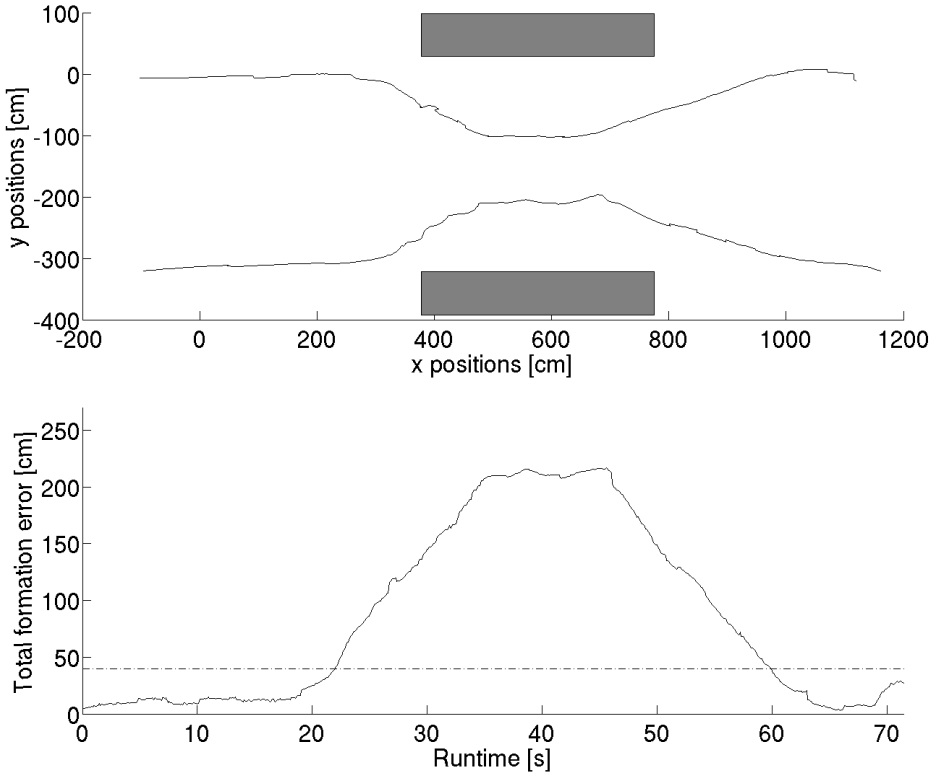

Figure 3-3: Results for a two-robot formation (two Magellan Pro) passing a small passage. In the following figures, the upper part gives the robot positions (obstacles are added for clarity). The lower part shows the formation error (in cm) over the runtime.

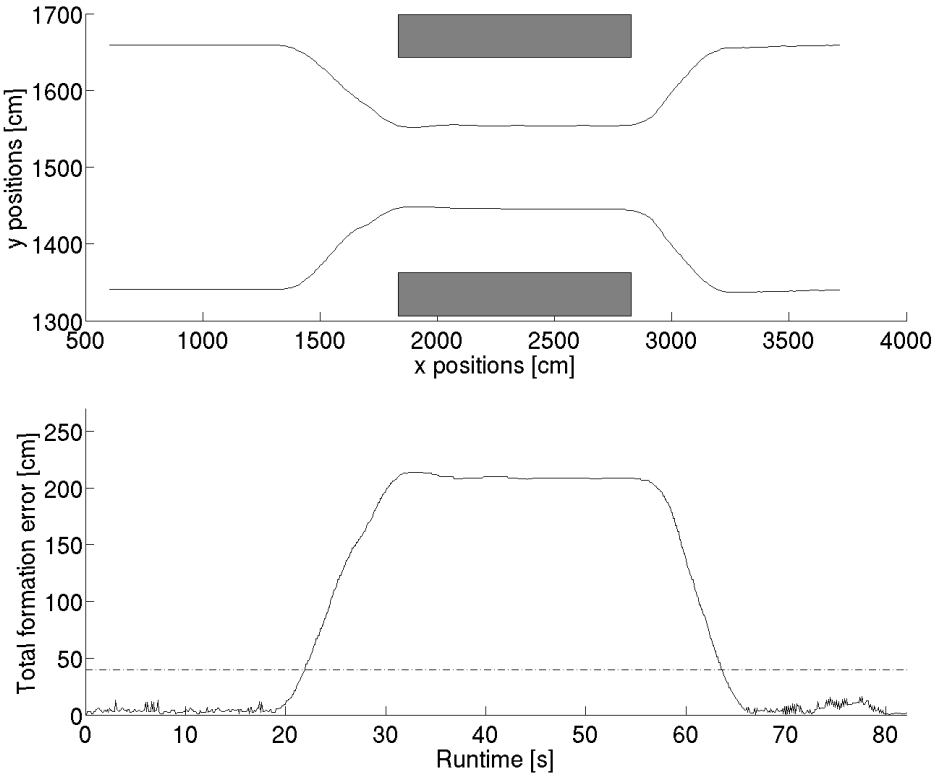

Figure 3-4. Simulation results for one example run with two robots in the passage scenario.

Figure 3-5 and figure 3-6 picture the data generated during two example runs of three robots in a triangle formation passing the pillar scenario. In contrast to the results from the passage, now there are major differences between real robots and simulation. Looking at the formation error chart, one can find that the mean error is smaller for the simulation run. On the one hand, this is because the simulated robots always move somewhat "smoother", especially near obstacles, which leads to slightly larger position errors for the real robots. On the other hand, as already stated in the last section, it is difficult to localize the robot positions exactly, especially in a real environment.

This additional error is hard to quantify, in terms of size as well as in terms of distribution. For a compensation of this error, a very precise localisation or additional information about the nature of the robots' odometry error is needed. Since both are hard to achieve in real world environments, the robot positions were treated as "precise".

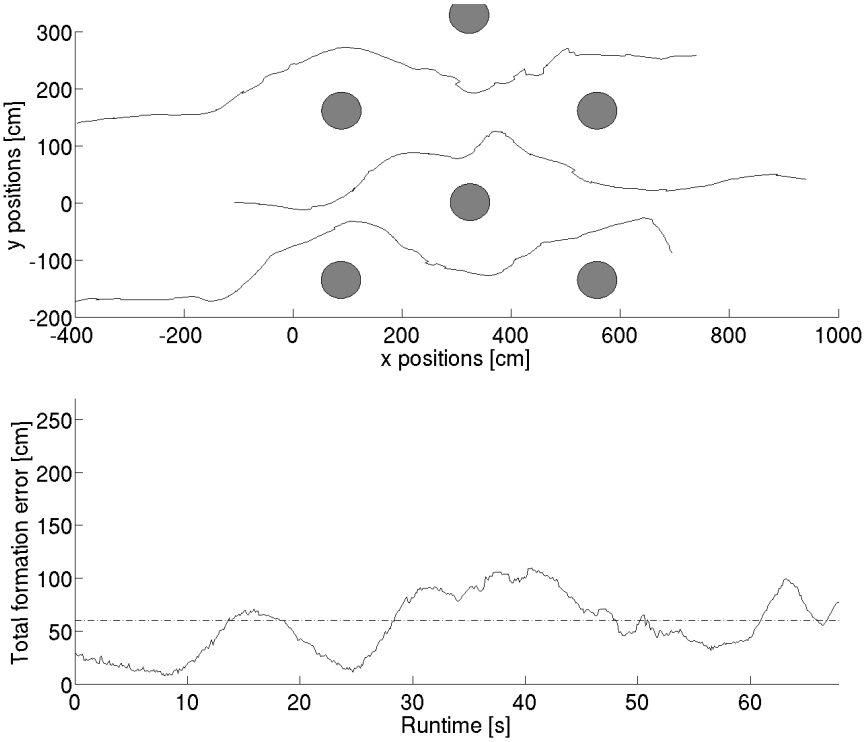

Figure 3-5. Three robots (one B21 and two Magellan Pro) in a triangle formation, pillar scenario.

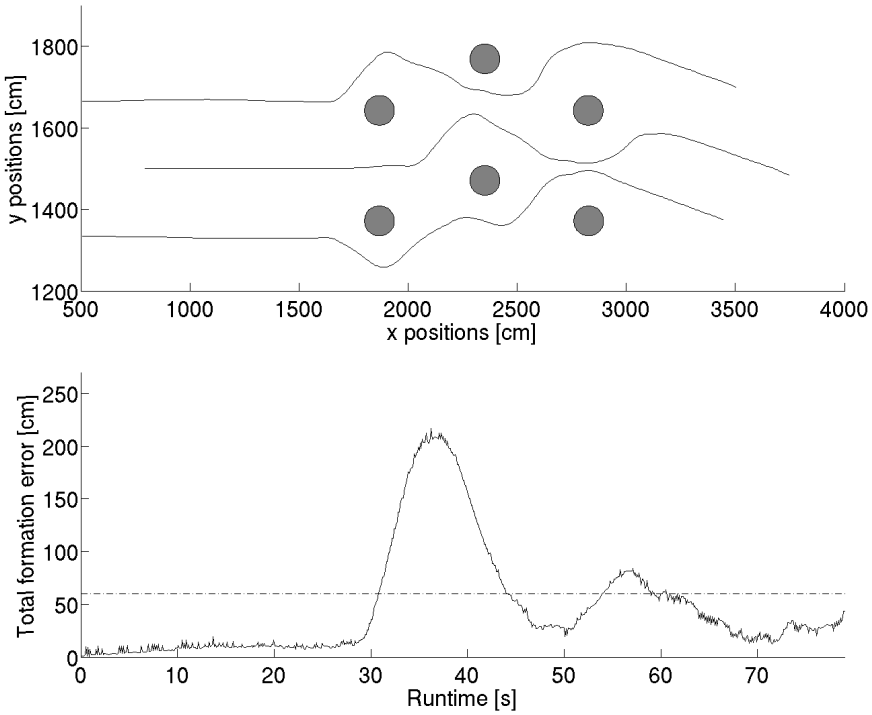

Figure 3-6. Example run for three simulated robots in the pillar scenario.

Although the mean error is smaller in simulation, the maximum of about 220cm is almost twice as large as in the real world run with real robots. The reason for this is obvious when taking a look at figure 3-7 and figure 3-8: these charts compare the robots' actual paths (solid line) and the computed optimal formation paths (dotted lines with different markers). See section 3.3.2 on how this calculation is done.

In figure 3-8, the simulated robot starting at the lower left formation position passes the first obstacle in an unforeseen way, compared to the optimal formation path. From its point of view, it circumnavigates the obstacle on the right instead of the left side, leading to a temporarily very large formation error. However, this type of wrong path decision occasionally happens for both, the real world runs as well as the simulation runs. Therefore, the mean of the 10 recorded runs is influenced in the same way for real world and simulation experiments.

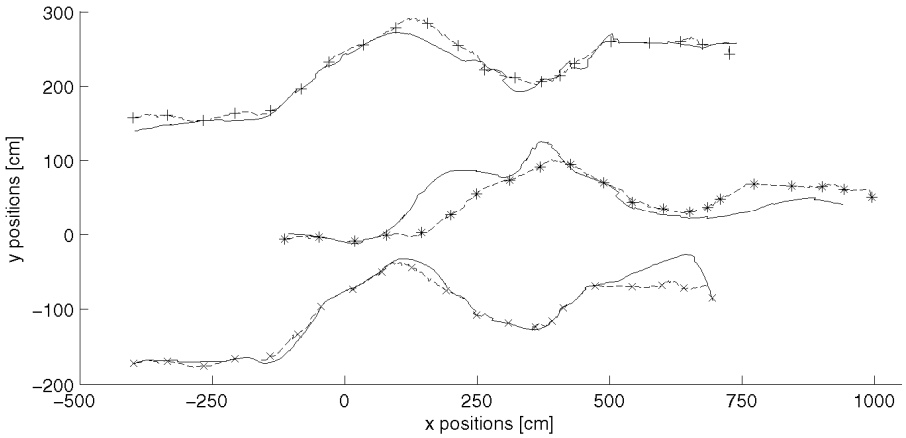

Figure 3-7. Real-robot example for the deviation between the paths of the three robots in the triangle formation (solid lines) and their optimal formation positions (dotted lines).

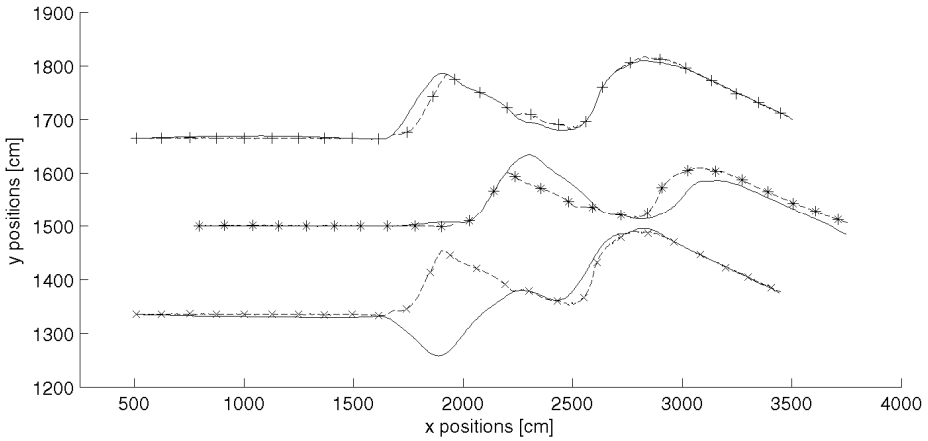

Figure 3-8. Simulation example for the deviation between the paths of the three robots in the triangle formation (solid lines) and their optimal formation positions (dotted lines).

Table 3-1 and table 3-2 provide some numerical results, namely the mean and the standard deviation for the two chosen metrics. Thereby, table 3-1 gives the results for the different scenarios and the different formations (two robots in a line, three in a triangle) for real laboratory runs, whereas table 3-2 lists these values for the simulation runs.

What can be seen corresponds well to the results stated so far. The formation error for the passage scenario is much larger than for the pillars, which is because while moving through the passage two robots are far out of formation. Nevertheless, results for real world and simulation are similar. On the other hand, for the pillar scenario simulation results are better, for the reasons mentioned before. However, because of the occasional large errors in this scenario (due to "wrong ways", see figure 3-8) the standard deviation is very large.

The in-formation ratio metric gives similar results. For the pillar scenario, the ratio is better, but at the same time, the standard deviation is much larger. It is worth mentioning, that the range of the resulting values is quite low. In most of the runs, the robots were out of formation for more than half of the time. This, of course, leads to the question whether this is a suitable metric for obstacle scenarios.

Note, however, that all mentioned differences in the results are solely caused by special characteristics of the environment. On the one hand, there is the rather small impact of simulated or real world runs. Everything else remains the same, including the algorithms, the robots, the simulator, and the laboratory. Just the choice of obstacles leads to the major changes in the results. Thus, it is worth asking what results the same metrics would have produced with another type of robots in another lab environment and other obstacles – and how comparable these results can be.

Although using the same robots and the same algorithms, the metrics produced very differing results – being highly dependent on the structure of environment and obstacles.

	Formation error (cm)	Std. dev.	Formation ratio	Std. dev.
Passage 2 robots	87.1357	2.3418	0.4527	0.0319
Passage 3 robots	116.0297	6.9447	0.3770	0.0325
Pillars 2 robots	49.0801	15.9714	0.5675	0.1477
Pillars 3 robots	71.5922	29.3875	0.4838	0.2271

Table 3-1. Numerical results for real world runs for all scenarios and formations. Mean formation error and in-formation ratio, 10 runs each, together with the standard deviation.

	Formation error (cm)	Std. dev.	Formation ratio	Std. dev.
Passage 2 robots	93.1811	0.4685	0.4974	0.0025
Passage 3 robots	121.7899	10.1445	0.4783	0.0085
Pillars 2 robots	38.8999	21.4419	0.6982	0.1787
Pillars 3 robots	56.0451	17.3125	0.7171	0.0786

Table 3-2. Numerical results for simulation, also 10 runs each.

3.3.3 Experiments with Enhanced Metrics

As shown in the previous section and mentioned in section 3.1 the next step towards a more general metric, i.e. one that is at least independent of the surroundings, is to use information about the environment as additional parameter. Meaning, if there are many obstacles then the formation error must be scaled down to be comparable to an empty environment where the error would be small. A suitable method could be a weighting factor, which is inverse proportional to the "density" of obstacles, so that the influence of the setting can be taken into account. Assuming that the environment is considered as a-priori unknown and possibly non-static, only actual sensor information can be used for these calculations.

In the presented approach, a method comparable to the computation of the repulsive obstacle force F_{rep} (see section 2.2.2.4 for details) is used to compute the weighting factor ρ_{obst}. Let o_i be the vector of a single laser beam that hits an obstacle in a distance smaller than d_{max}. Then ρ_{obst} is calculated as follows

$$\rho_{obst} = \left[\left(\sum_{i=1}^{n_{total}} \frac{\|o_i\|}{d_{max}} \right) \cdot 1 / n_{total} \right]^2,$$

where n_{total} is he number of laser measurements taken into account. Since for the formation error metric the actual positions of the obstacles are of no importance, only the magnitudes of the o_i are used in the formula. The resulting weighting factor ρ_{obst} is a scalar from the range [0; 1] and, therefore, the weighted total formation error is computed as follows:

weighted formation error := ρ_{obst} * non-weighted formation error

In the following, the developed weighting factor is used in fundamental experiments to show that it is a more general and setting-independent metric. In all of the figures, the upper part shows the robots' paths and the lower part compares non-weighted (solid line) and weighted (dashed line) total formation error. The dot-dashed line marks the in-formation threshold.

In figure 3-9 the formation error of an empty environment is shown. The non-weighted and the weighted formation error are equal, so the graphs are identical. This results from the fact that there are no obstacles in the vicinity of the robot that would have an influence on the weighting factor ρ_{obst}.

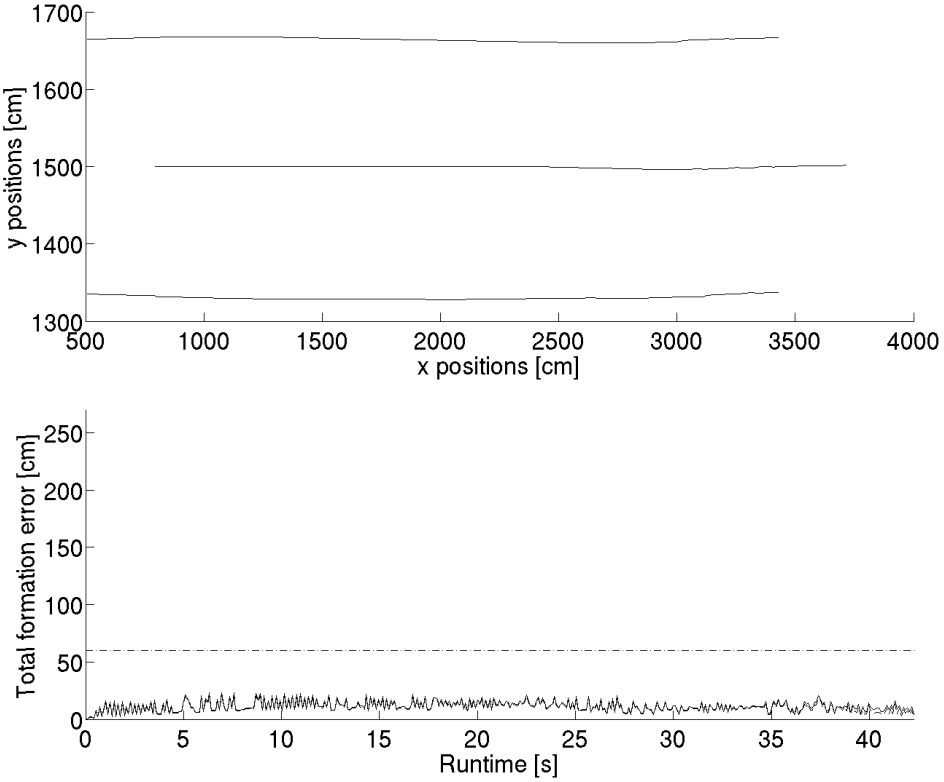

Figure 3-9. Non-weighted (solid line) and weighted total formation error (dashed line) for an empty hall scenario and a triangle formation.

Figure 3-10 shows that with this enhancement the (weighted) formation error metric now correctly reflects the fact that in the passage scenario the formation is only compressed (see 2.3.1.2 for details of experimental set-up). The overall shape of the formation is maintained. The error increases only in the breathing phase when the robots enter or leave the passage. The same holds for figure 3-11 that provides a similar example, in which a three-robot triangle formation avoids a wall-like obstacle on their left. In both cases the weighted formation error drops below the in-formation threshold during the whole run, meaning that the three robots are considered to form a still acceptable triangle formation while avoiding the obstacles (see section 3.2 for a detailed description of the in-formation ratio metric).

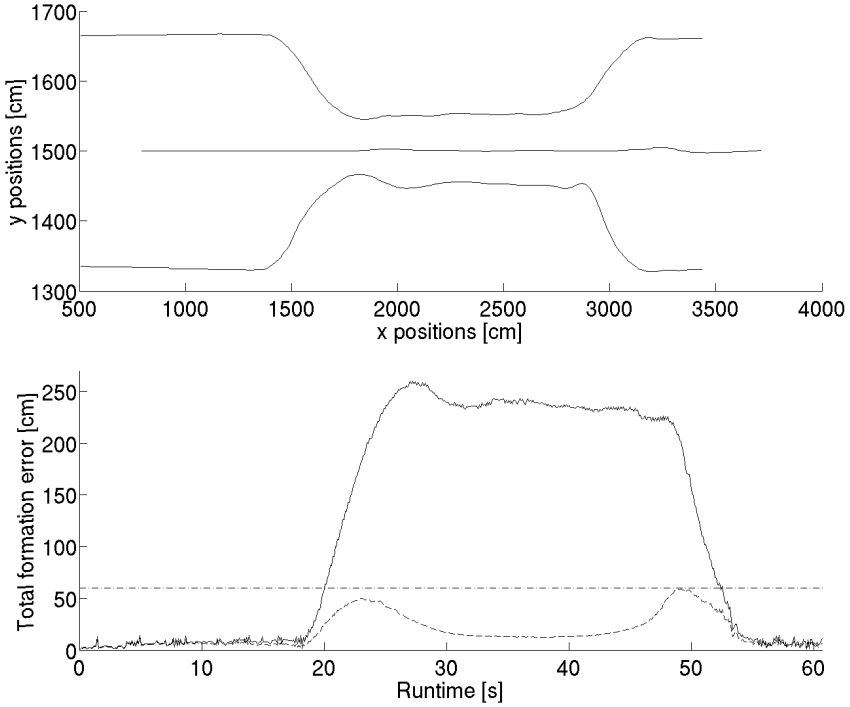

Figure 3-10. The weighted formation error (dashed line) for the passage scenario and a triangle formation; compare with figure 3-4

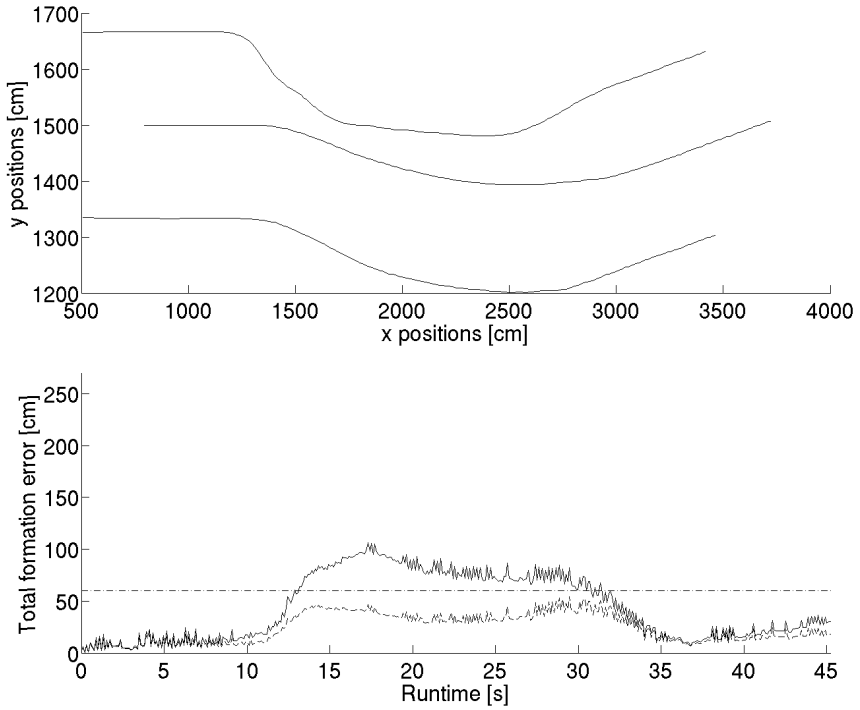

Figure 3-11. A triangle formation passing a wall on their left. Non-weighted (solid line) and weighted (dashed line) formation error.

Figure 3-12 gives an example of a triangle formation in the "pillar" scenario. See section 3.3.2, especially figure 3-6 and figure 3-8, for a detailed description of the environment. Now the weighted formation error metric adequately reflects the fact, that the formation is really distorted twice while passing the obstacles, meaning that the robots choose an opposite trajectory when they pass some of the pillars. Whenever this happens, the total formation error (non-weighted and weighted) grows up to 150cm or above, which is more than twice the in-formation threshold.

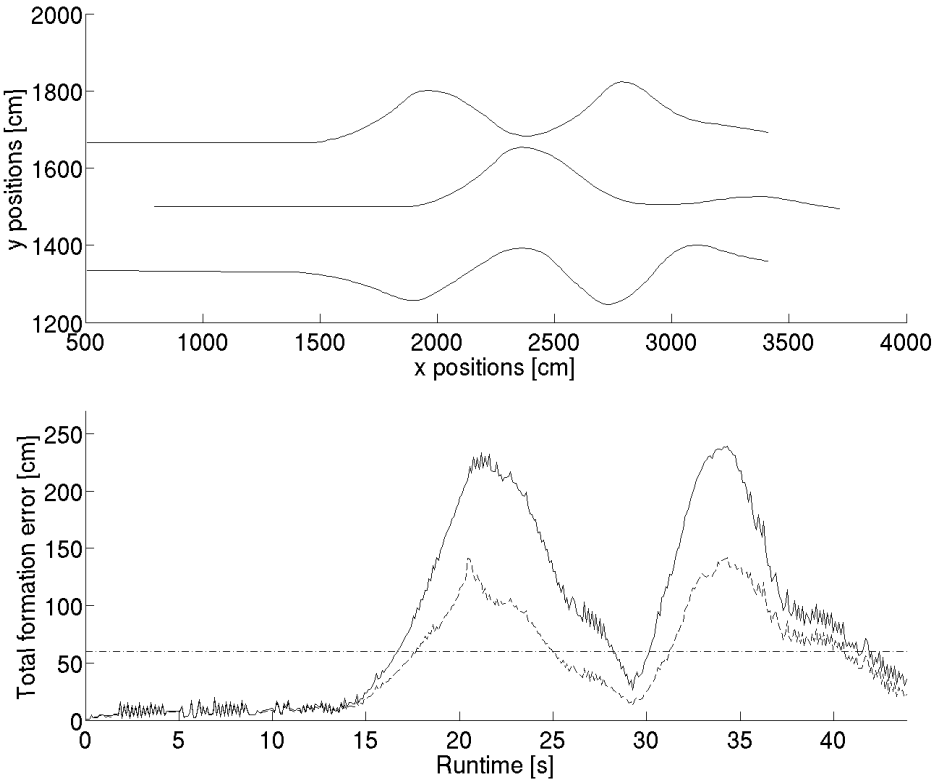

Figure 3-12. Non-weighted (solid line) and weighted total formation error (dashed line) for the pillar scenario and a triangle formation.

Table 3-3 summarizes the results of these experiments numerically. For all scenarios – "wall", "passage", "pillars", each with 3 robots in a triangle formation – 10 simulated runs were recorded. Additionally, the in-formation ratio, which is based on the formation error, mean values for the total formation error and the in-formation ratio, as well as their standard deviations are provided (see section 3.3.2). As stated above for the arbitrarily chosen example runs, when looking at the first two scenarios, the three robots are perfectly in formation throughout all of the "passage" and "wall" runs according to the weighted metric. For the "pillars", the mean formation error is also much lower using the weighted version of the metric. However, since the robots often leave their positions inside the triangle formation, by means of the in-formation ration they are still considered to be out of formation nearly half of the time. Note that parts of section 3.3 are based on earlier work published in [145].

	Un-weighted metrics				Weighted metrics			
	Formation error (cm)	Std. dev.	Formation ratio	Std. dev.	Formation error (cm)	Std. dev.	Formation ratio	Std. dev.
Field	10.4580	1.0444	1	0	9.4595	0.9275	1	0
Wall	42.2076	1.2901	0.6230	0.0431	22.9893	0.9714	1	0
Passage	109.0772	5.5965	0.4759	0.0077	16.4216	0.8488	1	0
Pillars	85.8374	17.4192	0.5087	0.0645	51.0063	10.5177	0.6346	0.0883

Table 3-3. Comparison between un-weighted and weighted formation metrics for different scenarios. For each scenario 10 simulation runs with three robots have been evaluated.

3.4 Summary

The foregoing section discussed the field of metrics for multi-robot systems with focus on the criteria for formation navigation.

Surveying the literature showed that a systematic discussion of metrics for formation navigation has not been done yet. In the following, a number of possible criteria were identified which all could be reduced to the parameters “position error” and “percentage of time in formation”.

The identified approaches were analysed and the proposed criteria for metrics extracted. With the factors formation position error and the percentage of time, several experiments were conducted in order to test the capabilities.

Although using the same robots and the same algorithms, those metrics produced very differing results – being highly dependent on the structure of environment and obstacles. Just the choice of obstacles led to major changes in the results. Thus, it is worth asking what results the same metrics would have produced with another type of robots in another lab environment and other obstacles – and how comparable these results can be.

However, all found approaches that were based on the tested criteria do not consider any environmental parameters and therefore fail to establish a general metric that allows a common method of comparison. Using the benefits from the potential field approach for formation navigation a novel weighting factor was developed that allows to consider environmental influences on the chosen metrics.

The conducted experiments showed that the new weighting factor adequately models the influence of the environment. The formation error is close to zero if there is no influence through obstacles. If the formation is just deformed, as in the case of a narrow passage or doorway, the formation error is correctly scaled down to extricate the influence of the surroundings. Nevertheless, if the formation is really distorted the formation error raises, exceeds the threshold, and indicates that the formation is disfigured.

Although these results look promising, for a sensible comparison of different approaches, tested with different robots in different laboratories, even more parameters have to be taken into account. However, the developed metric is already an appropriate tool to compare different formation navigation approaches in dissimilar settings and environments.

4 Relative Localisation

When using a multi-robot system in which the robots have to fulfil a cooperative task, two typical positioning problems arise:

1. robust position estimation for each robot itself, and
2. relative position estimation of the other group members.

The first problem can be typically solved by some kind of simultaneous localisation and map building (SLAM) method. An important precondition for these methods is that the environment provides enough distinguishable features (e.g. landmarks) to give the localisation "a handle to grip on". This, however, is not necessarily the case in open space like large hallways, barren land, or long monotone corridors.

The second problem, in particular, arises when the robots do not have a common co-ordinate system, which is often the case if GPS is not available. Common reference points like landmarks or predefined co-ordinate systems must often be specified by an operator.

Therefore, the multi-robot positioning problem asks if it is possible for an autonomous vehicle to start at an unknown location in an unknown environment, and then to incrementally estimate its own position and the relative locations of the other robots using only sensor information. The answer would be a robust, fast, and precise method that does not need any preconditions or specific assumptions about the environment. In this chapter an approach to relative position estimation in a group of robots is presented, which is based on sensor and odometry information only.

4.1 Related Work

4.1.1 Local Localisation

Local localisation means evaluating the position and the orientation through integration of self-contained information provided by encoders or inertial sensors.

The integration is started from the initial position and orientation and is continuously updated in time. Local localisation is also known as dead reckoning. There are two basic approaches for dead reckoning: odometric systems and inertial navigation systems. In most mobile robots, odometry is implemented by means of optical encoders that monitor the wheel revolutions and steering angles of the robot wheels. Using simple geometric equations (kinematic model of the vehicle), the encoder data are then used to compute the momentary position of the vehicle relative to a known starting position. Inertial navigation systems are widely used in aviation and lately in outdoor robots. Most of them consist of gyroscopes and accelerometers that provide angular rate and velocity rate information. By integrating this rate information, inertial navigation systems calculate the position and orientation of the vehicle. Its simplicity has made dead reckoning a widely used technique, but it shows major drawbacks and has been

proven unreliable when travelling for long distances. Due to inaccurate models, sensor drift and noise, there is an error in the calculation of the vehicle's position and orientation. This error generally grows unbounded with time. Typical techniques of dead reckoning can be found in [19, 49, 10]. Substantial improvement is provided by applying Kalman filtering techniques [58]. However, local localisation can usually not be applied to MRS.

4.1.2 Global Localisation

Global localisation is based on a metric and/or topological map and uses sensors information to re-localise the robot with respect to these maps.

The problem of single robot localisation is widely studied in the literature [45, 103, 161]. Most of the approaches to simultaneous localisation and mapping (SLAM) or concurrent mapping and localisation (CML) can roughly be classified by the kind of sensor data processed and the matching algorithms that are used. One method is to extract landmarks out of the data and match these landmarks to localize the robot in the map being learned. The other set of approaches use raw sensor data and perform a dense matching of the scans. All these approaches have the ability to cope with a certain amount of noise in the sensor data, but it is assumed that the environment is almost static during the mapping process. Local and global localisation approaches both have drawbacks. To cope with these drawbacks, the methods are often combined [166, 35], introducing Kalman filter [65, 70] and Monte Carlo Localisation (MCL) [22, 40]. Kalman filtering, MCL and other localisation methods are comparatively reviewed in [69, 71].

In the recent years, the problem was extended to multi-robot localisation (see e.g. [55, 128, 161, 105]), using sequential Monte Carlo methods [46, 77] (also known as particle filters) for both multi-robot global localisation [55] and real-time CML using SICK laser scanner data. Also feature-based representations [27, 67] as well as topological representations [33, 29] have been investigated. Mourikis and Roumeliotis have studied the time evolution of the position estimates' covariance in Cooperative Simultaneous Localization and Mapping (C-SLAM) [115], and thus obtain analytical upper bounds for the positioning uncertainty.

4.1.3 Absolute Localisation

Absolute localisation uses a technique that permits the vehicle to determine its position directly through a provided exterior reference system.

These methods rely usually on satellite-based signals like Global Positioning System (e.g. GPS, GLONASS or Galileo) or navigation beacons, active or passive landmarks. Since GPS-like systems do not have the accuracy needed for most robotic tasks, absolute localisation is often combined with one of the other localisation techniques using Kalman-filter methods [116]. A typical non-differential GPS was tested by Cooper and Durrant-White [36] and yielded an accumulated position error of over 40m (131 ft) after extensive filtering. Systems likely to provide the best accuracy are those

that combine GPS with Inertial Navigation Systems (INS), because the INS position drift is bounded by GPS corrections [113]. Similarly, the combination of GPS with odometry and a compass was proposed by Byrne [23]. The main advantage of this localisation method is the fact that it introduces a common coordinate and reference system for all vehicles. A brief survey of GPS localisation techniques and issues can be found in [21].

4.1.4 Relative Localisation

Relative localisation uses sensor observations to localise the robot with respect to other robots – without having an environmental model.

There is one major difference between this approach and the other presented methods. Most of them make use of maps and/or landmarks with the intention of generating a globally consistent world co-ordinate system. The aim of relative localisation is to maintain relative positioning only among the robots.

The work by [102] is an example of how to recover the relative movement of the robot between two time points. Localisation is done without knowing where the robot actually is in the model using only laser range scans. The key idea is to register a scan to a previous scan and obtaining thereby the relative movement. To carry out the registration, the method calculates tangent lines at the scan points, which help to define correspondences between them. Some authors worked on similar concepts in order to reduce the odometry error of a single robot system. Murray [117] and Braithwaite [20], for example, use a movable stereo camera system to follow special points of interest (POI) in the surrounding environment. Using the measured distances and rotation angles of the camera, they calculate the actual movement of the robot.

In several approaches, these results are transferred from a single to a multi robot system [125, 91]. Because in these works the aim is to generate and maintain a global co-ordinate system, a great accuracy is needed. Just one robot moves at any given period of time while the others are standing still, thereby functioning as ‘temporary’ landmarks. Some authors add additional global information sources like GPS to achieve greater accuracy [65, 131], whereas others observe only the robot group itself. Kurazume et al., for example, develop a so-called Cooperative Positioning System (CPS) [91, 93], other similar ideas can be found in [125, 126].

Suzuki and Yamashita [156] present an approach to building a common co-ordinate system in which all robots may move simultaneously, but the atuhors use a simulated and somewhat idealised robot system. In their simulation, for example, every robot has a full 360-degree view and is capable of error-free measurement of the relative positions of the other robots.

An example of a system that is designed for cooperative localization is presented in [91]. The authors acknowledge that dead reckoning is not reliable for long traverses due to the error accumulation and introduce the concept of “portable landmarks”. A group of robots is divided into two teams in order to perform cooperative positioning. At each

time instant, one team is in motion while the other remains stationary and acts as landmark. In the next phase, the roles of the teams are reversed. This process continues until both teams reach the target. This method can work in unknown environments and the conducted experiments suggest accuracy of 82.3mm (i.e. 0.38%) for the position estimate and 1 degree for the orientation after a total travel distance of the master robot of 21.6m [92]. Improvements on this system and optimum motion strategies are discussed in [93]. In many of the newer work on cooperative localization the precondition of some robots remaining stationary has been dropped. Therefore, some other authors have discussed the problem of suitable motion strategies or special formations for cooperative localization [74, 178, 163].

In [66] only one robot moves, while the rest of the team of small-sized robots forms an equilateral triangle of localization beacons in order to update their pose estimates. Another realization is presented in [125, 126]. The authors deal with the problem of exploration of an unknown environment using two mobile robots. In order to reduce the odometric error, one robot is equipped with a camera tracking system that allows it to determine its relative position and orientation with respect to a second robot carrying a helix target pattern and acting as a portable landmark. Both previous approaches have the following limitations: (a) Only one robot (or team) is allowed to move at a certain time instant, and (b) the two robots (or teams) must maintain visual contact at all times.

In [127] the authors have explored the effect of different robot tracker sensing modalities on the effectiveness of cooperative localization. Statistical properties were derived from simulated results for groups of robots of increasing size N when only one robot moved at a time. In their subsequent work [133] the authors examined upper bounds on the localization uncertainty also for the more realistic case of all robots moving simultaneously. However, their assumption of homogeneity and the requirement that every robot continuously measures the relative position of all other robots in the team still limits the applicability of this approach. Mourikis and Roumeliotis [114] further relax these assumptions and study the time evolution of the positioning uncertainty in heterogeneous robot teams with an arbitrary topology of, what they call, the Relative Position Measurement Graph (RPMG), roughly meaning arbitrary mutual relative position measurements of the robot team members.

A Kalman filter-based implementation of a cooperative navigation schema is described in [137]. In this work, the effect of the orientation uncertainty in both the state propagation and the relative position measurements is ignored resulting in a simplified distributed algorithm. The improvement in localization accuracy is computed after only a single update step with respect to the previous values of uncertainty. In [131, 132] a Kalman filter pose estimator is presented for a group of simultaneously moving robots. The Kalman filter is decomposed into a number of smaller communicating filters, one for each robot, processing sensor data collected by its host robot. It has been shown that when every robot senses and communicates with its colleagues at all times, every member of the group has less uncertainty about its position than the robot with the best (single) localization results. Because many real world sensors are not able to provide

relative observations consisting of both, range, and bearing information, in [107] special EKF equations are derived to integrate more generic relative observations. Then, three different types of relative observations are considered, relative bearing, relative distance, and relative orientation.

Fox [55] describes an approach to multi-robot localization in which each robot maintains a probability distribution describing its own pose (based on odometry and environment sensing), but is able to refine this distribution through the observation of other robots. This approach extends earlier work on single-robot Markov/Monte-Carlo localization techniques [54] and an implementation of a collaborative multi-robot localization scheme, which is presented in [53]. The authors had extended the single Monte Carlo localization algorithm to the case of two robots when the same map of the area is available to both robots. When these robots detect each other, the combination of their belief functions facilitates their global localization task. The main limitation of this approach is that it can be applied only within known indoor environments

The aim of the approach of Howard et al. [76] is pure relative localization, as it is described at the beginning of this section. In his work, the robots do not attempt to determine their pose with respect to some external global co-ordinate system. Each robot rather tries to determine the pose of every other robot in the team, relative to itself. In their approach, each robot uses a set of independent particle filters to represent the relative pose distribution of the other robots. For each new observation, one or more of these particle filters have to be updated. In the experiments, laser scanners and pan-tilt cameras are used together to detect and identify special markers placed on the robots. It is important to notice, that in contrast the goal of most authors presented beforehand is global localization. They use mutual measurements of the robots only as a means for decreasing uncertainty about each robot's pose.

In order to acquire mutual relative measurements between the members of a robot group a wide variety of possible techniques is used. Apart from the resulting precision, these techniques differ mainly in the kind of data provided, distance, or bearing information or both of them. Støy [153], for example, performs simple relative localization between collaborators using directional beacons. Vision-based cooperative localization is widespread because in addition to distance and/or bearing information it can provide a means of distinguishing the other team members. In [152] vision is used by a team of vehicles tasked with cooperatively trapping and moving objects. Tracking via vision is also used for relative localization of collaborators in an autonomous mobile cleaning system [81]. In [109] the authors use a stereo vision system, and in [111] information is gathered from omni-directional cameras combined with the motion of the vehicles themselves.

In [110] the trajectories described by unidentifiable moving objects and observed by different robots are the base for mutual position estimates of the robots themselves. [100] presents a method for estimating the relative poses of a team of mobile robots using only acoustic sensing. The relative distances and bearing angles of the robots are estimated using the time of arrival of audible sound signals on stereo microphones. The

robots emit specially designed sound waveforms that simultaneously enable robot identification and time of arrival estimation. Some papers [152, 39] present solutions for the relative multi-robot localization problem by combining information exchanged by the robots using least squares optimisation.

4.2 Camera-Based Relative Localisation Approach

One way to set up a common co-ordinate system in a group of robots is to equip at least one robot within the group with a camera that is continuously taking pictures of the surrounding robots. Based on these images the relative positions of all visible robots can be calculated. Whenever a robot moves and therefore its position inside the camera image changes, the movement with respect to the watching robot's co-ordinate system can be computed. By comparing this movement with the one, the moving robot itself reports it is possible to calculate the transformation matrix between the co-ordinate system of that robot and the common relative co-ordinate system. This common co-ordinate system might be the system of the camera-equipped robot as well as some arbitrarily chosen reference co-ordinate system.

The method presented here is based on Suzuki's and Yamashita's ideas [156] but works under more realistic conditions. Because the relative positions retrieved from a real vision system are not precise, an additional error model is developed in order to weight and correct each measurement. By these means, the resulting co-ordinate system is improved which makes it possible to maintain it over longer periods.

4.2.1 Description of the Algorithm

A two-step approach is used to establish the common co-ordinate system and share it between a group of robots. The first step consists of a vision process in which one or more camera-equipped robots continuously grab images of the surrounding robots and hence calculate their relative positions. In the second step, the position information in combination with the robots' movement data is used to establish and share the so-called 'relative' common co-ordinate system.

4.2.1.1 Calculation of Robot Positions

The images necessary for the mutual localisation are continuously acquired by the mounted camera systems and then analysed and segmented in order to extract the different objects visible in the picture. The criteria relevant for the segmentation are:

- brightness of neighbouring pixels,
- size and shape of objects,
- special movement parameters.

Figure 4-1 shows an example of such an image segmentation. In the left picture an image containing one of the robots can be seen, the right one presents the complete segmentation generated from the original. All robots have special two coloured markers

mounted on top of the laser rangefinders, which can be found as easily distinguishable areas in the upper part of the segmented image as well.

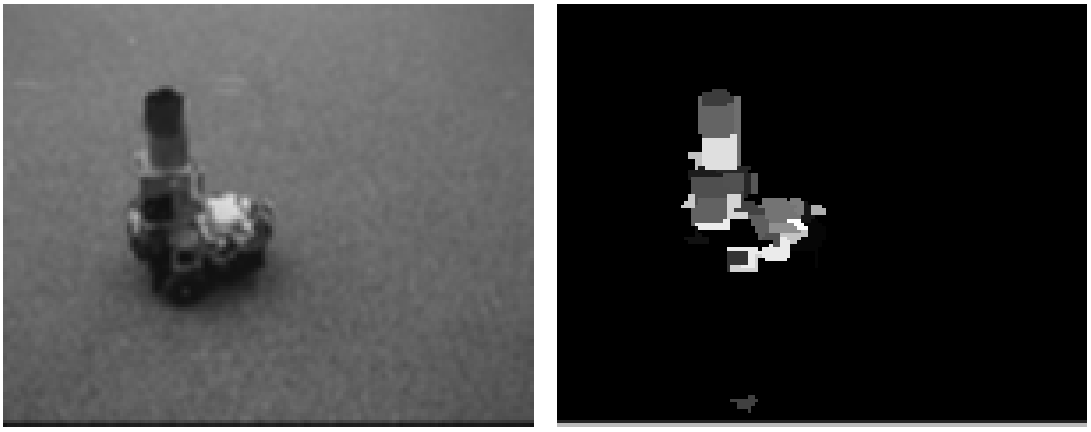

Figure 4-1: Image segmentation example.

The segmentation process generates a list of objects within the segmented image. For each object in this list its size, its position and its colour coding is stored and compared to the characteristics of each robot. If one or more objects found in an image segmentation can be identified as part of a robot or – to be more precise – as belonging to the mounted marker, their relative positions are computed. A standard photogrammetric projection algorithm as, for example, described in [88] is applied to calculate the robot's relative co-ordinates based on its position inside the image.

For each image, taken by one of the robots' cameras, first its projection centre (which roughly means the position of the camera lens) is computed. Afterwards the current position of the image with reference to the robot's local co-ordinate system has to be calculated. Since the camera is mounted on a pan/tilt system its current viewing direction, i.e. the rotation angles ω, φ, and κ around the *x*-, *y*-, and *z*-axis are used to calculate a spatial rotation matrix *R*. Let R_ω, R_φ, and R_κ be the usual 3-dimensional rotation matrices

$$R_\omega = \begin{pmatrix} 1 & 0 & 0 \\ 0 & \cos\omega & \sin\omega \\ 0 & -\sin\omega & \cos\omega \end{pmatrix}, R_\varphi = \begin{pmatrix} \cos\varphi & 0 & -\sin\varphi \\ 0 & 1 & 0 \\ \sin\varphi & 0 & \cos\varphi \end{pmatrix}, R_\kappa = \begin{pmatrix} \cos\kappa & \sin\kappa & 0 \\ -\sin\kappa & \cos\kappa & 0 \\ 0 & 0 & 1 \end{pmatrix} \quad (16)$$

As $\varphi = 0$ because the camera is mounted exactly upright, it is $R_\varphi = I_3$. That leads to

$$R_{\omega,\kappa} = R_\omega R_\varphi R_\kappa = R_\omega R_\kappa = \begin{pmatrix} \cos\kappa & \sin\kappa & 0 \\ -\cos\omega\sin\kappa & \cos\omega\cos\kappa & \sin\omega \\ \sin\omega\sin\kappa & -\sin\omega\cos\kappa & \cos\omega \end{pmatrix} = \begin{pmatrix} r_{11} & r_{12} & r_{13} \\ r_{21} & r_{22} & r_{23} \\ r_{31} & r_{32} & r_{33} \end{pmatrix} \quad (17)$$

Let X_O, Y_O, and Z_O denote the co-ordinates of the formerly computed projection centre, ξ_0 and η_0 the pixel co-ordinates of the image centre point, ξ and η the pixel co-ordinates of a relevant image segment, and c the so called "camera constant", then the corresponding object co-ordinates X and Y (in the plane) can be derived from the two equations (18) and (19) (see [88]):

$$X = X_O + (Z - Z_O)\frac{r_{11}(\xi - \xi_0) + r_{12}(\eta - \eta_0) - r_{13}c}{r_{31}(\xi - \xi_0) + r_{32}(\eta - \eta_0) - r_{33}c} \tag{18}$$

and

$$Y = Y_O + (Z - Z_O)\frac{r_{21}(\xi - \xi_0) + r_{22}(\eta - \eta_0) - r_{23}c}{r_{31}(\xi - \xi_0) + r_{32}(\eta - \eta_0) - r_{33}c}. \tag{19}$$

As the height of each robot and thereby the height of the relevant image segments belonging to the top mounted markers is well known, the Z co-ordinate has a constant value. Using this additional knowledge it is possible to assign a unique point in the robot's local co-ordinate system to each relevant image segment and – as a result – compute the relative position of every visible robot.

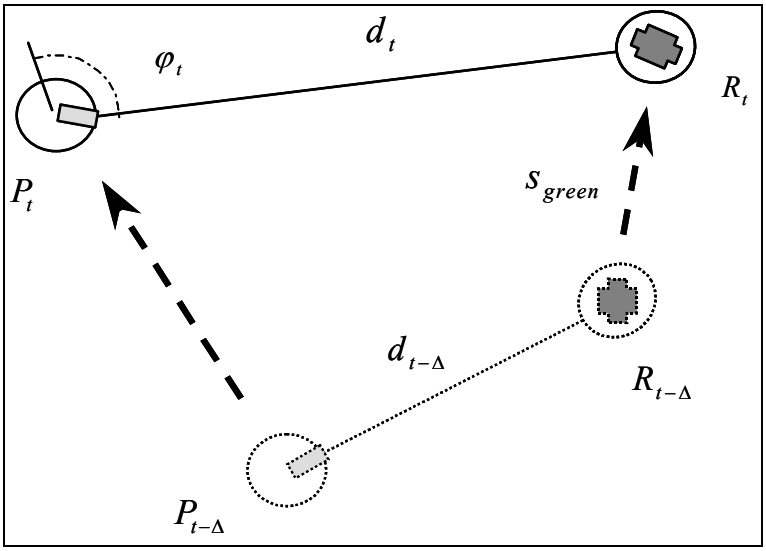

Figure 4-2: Camera equipped robot watching another robot while both are moving.

4.2.1.2 Establishing the Relative Common Co-ordinate System

Using the relative positions of the other robots, which are computed by the vision process described in the last section, it is possible to establish a so-called "relative" common co-ordinate system for all visible robots. In this context, the attribute "relative" means that there is no reference to any fixed global co-ordinate system but instead the

robots just share a common co-ordinate system among each other. Figure 4-2 schematically describes the process leading to this relative co-ordinate system.

One camera equipped robot observes another robot and calculates its relative positions while it is moving from position $R_{t-\Delta}$ to R_t during a time interval Δ. In the same time the observer itself might be moving from point $P_{t-\Delta}$ to point P_t. In order to establish a common co-ordinate system for these two robots, the watched robot functions as some kind of moving landmark. The following paragraphs present a closer look at this idea.

First, it is considered that the camera-equipped robot is not moving but stands still at a given position throughout the observation process. Whenever a new position for another robot is accepted by the vision and evaluation process, the total movement during a specified period of time is computed based on the last few measurements.

As figure 4-3 illustrates, the starting point $R_{t-\Delta}$ and the end point R_t of this movement can be expressed as points in a global reference co-ordinate system. For the same period of time, the movement of the robot measured by its odometry sensors is transferred over a communication link. $\hat{R}_{t-\Delta}$ and $\hat{R}_t$ represent this route with respect to the local co-ordinate system of that robot. Using these four points a (2-dimensional) transformation matrix can be computed which transfers the communicated vector into the observed one and thus transfers the local co-ordinate system of one robot into the reference co-ordinate system.

In a next step the pre-condition of the camera-equipped robot standing still at one position is dropped. If the observing robot itself has moved while watching the other robot, this additional translation and rotation has to be taken into account when calculating the vector from point $R_{t-\Delta}$ to point R_t. The other steps of the calculation remain unchanged but the resulting transformation matrix of course suffers from the additional odometry error, which enters the calculation process.

Obviously the whole process does not need and use any information about the environment (apart from the knowledge of which robot uses which marker). The resulting reference co-ordinate system therefore is not ‘global’ in the sense that it has a fixed reference to world co-ordinates. It is called a ‘relative’ common co-ordinate system because it is just shared among the participants of the robot group and can diverge from world co-ordinates over time. Once the common co-ordinate system is established the robots can start working on their task. During the work of the robot group the whole process must be repeated regularly in order to maintain and correct the transformations between the robots’ local co-ordinate systems and the reference co-ordinate system.

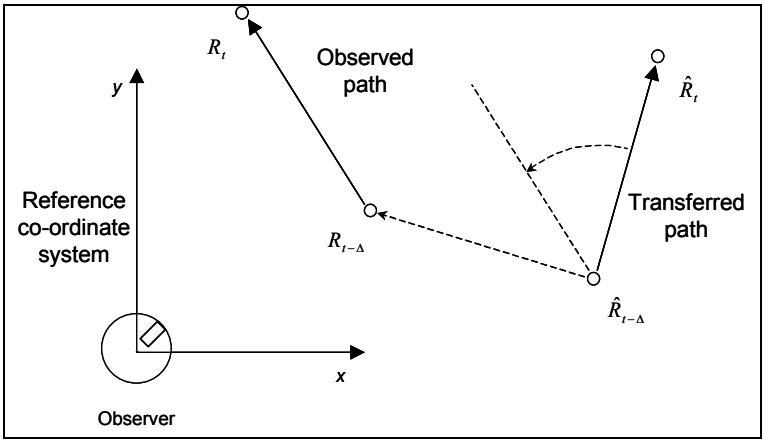

Figure 4-3: Transformation from robot's local co-ordinate system into reference co-ordinate system.

Since the used camera system, of course, only has a limited opening angle, it was mounted on a pan/tilt platform. Therefore, it is not necessary to move the whole robot in order to take images of the surrounding robots. Simply the camera is moved towards the direction in which a robot is expected to be found. A simple prediction algorithm was implemented to derive the probable course of a robot from its last observed positions. With the help of this prediction algorithm the sequence of measured robots as well as the direction the camera has to be moved to in order to point towards a special robot can be optimised. As a result, the frequency of measurements can be increased and thus the mean accuracy of the resulting relative co-ordinate system can be improved.

If a robot is not visible over a longer period of time because it works behind some obstacle or too far away, it might become necessary to use an additional, globally referenced localisation method. For such a task, a vision-based approach is probably not the best choice.

4.2.2 Experimental Implementation

To prove the usability of the presented approach several experiments have been performed. First, as a supplement for the multi-robot simulation environment a very simple camera simulation was added. With this rough simulation of the vision part of the algorithm the rest of the algorithm could already be implemented and tested. In parallel the vision system was installed in order to undertake first real world experiments.

4.2.2.1 Simulation Results

As already stated a simple simulation component for the multi-robot simulation environment was added, which delivers relative positions of the robots inside a virtual camera field of view. In order to emulate the inherent inaccuracy of this vision-based process a simple randomly distributed error offset is added to each position information.

Additionally, the multi-robot simulation models the odometry error for the robots, thus providing a rather realistic environment for testing complex higher-level algorithms for multi-robot systems.

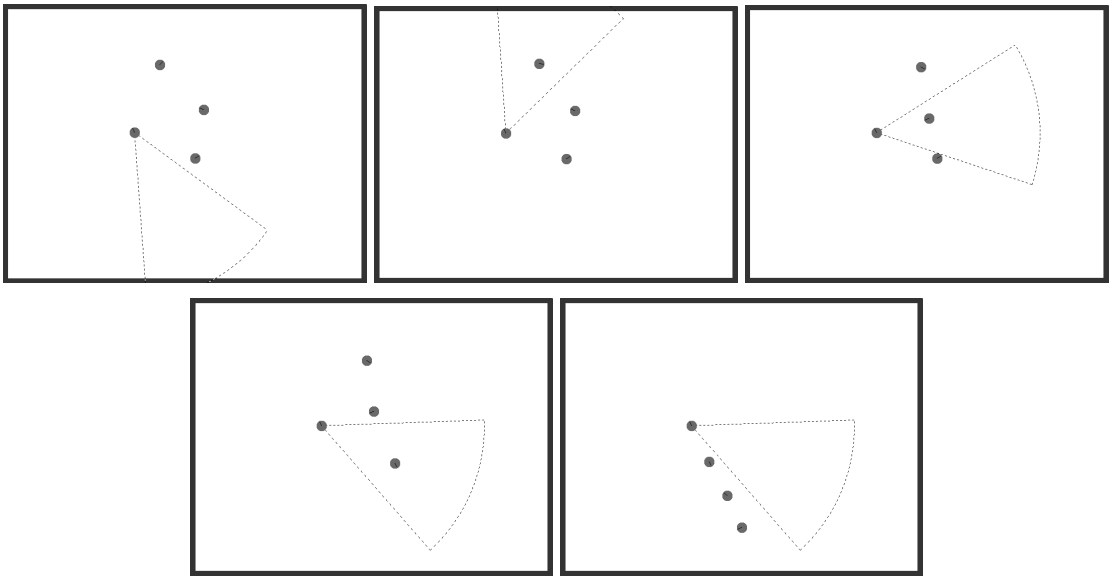

Figure 4-4: Example simulation run – one camera equipped robot co-ordinates three other group members. Pictures are ordered from upper left to lower right.

Figure 4-4 shows an example run of the complete co-ordination algorithm inside the simulation environment. The robot group in this example consists of four robots, of which one is equipped with a top mounted and movable camera system. This robot takes the role of a group leader throughout this run. The task for the group is to set up a common co-ordinate system and build a line formation behind the leading robot. This formation is generated by simply sending each robot a target position with reference to the shared co-ordinate system.

The five pictures in figure 4-4 are sorted upper left to lower right and shall describe the complete procedure. As a first step the group leader turns its camera until all participants are found. Then it successively commands each robot to move forward about one meter. Pictures 2 to 4 present these steps of the algorithm. As described in section 4.2.1.2 the observer generates a common relative co-ordinate system by comparing the travelled path it observed with the path reported by each robot.

Each resulting transformation matrix is sent to the corresponding robot. With this matrix, the robots are able to transform movement commands expressed in terms of the common co-ordinate system into locally referenced steering commands. The last picture presents the result for the given task – all robots line up behind the group leader. Because of the imprecise relative positioning and the inherent odometry errors this is, of course, not a perfect line but is somewhat deformed.

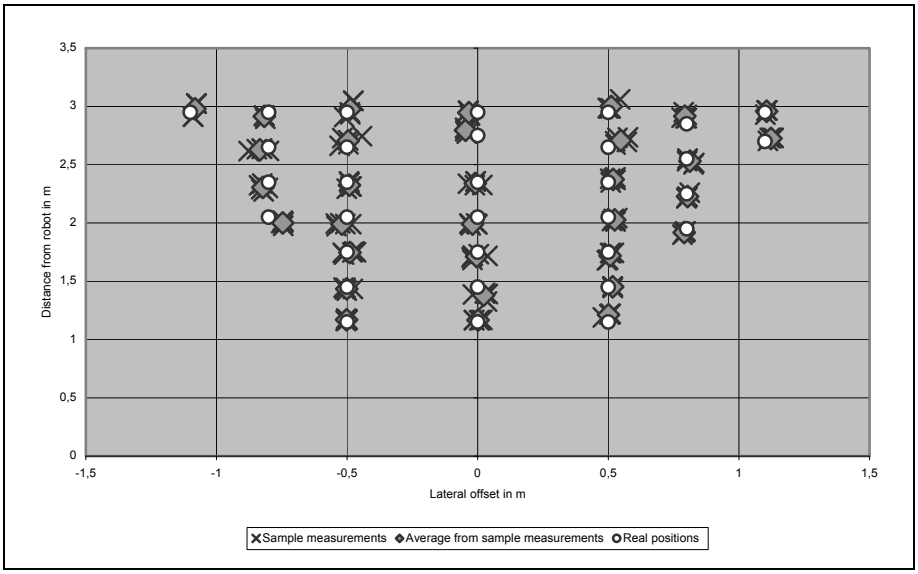

Figure 4-5: Measured positions of a specially marked robot using a real camera system.

4.2.2.2 Experiments with Real Robots

Since the results from simulation looked rather promising, the approach was implemented on the real robot system. It consisted of one B21 robot by RWI Inc., which is equipped with a camera system mounted on top of a pan/tilt platform, and four RWI Pioneer I robots. Special two-coloured markers were mounted on top of the Pioneers which made them distinguishable for the vision process. After implementing the basic vision algorithms for locating and identifying a robot inside a camera picture as described in section 4.2.1.1, the evaluation of the quality of the delivered relative position information was conducted.

The first result was a large number of wrong and deviating segmentations nearly for every measurement. The main reason for the variation of the segmentation results is that, depending on the lighting of the scene, a single red coloured area is often segmented into more than one partition. In order to use all these segments and to distinguish them from erroneous segments, a simple selection algorithm was developed: The circle (of the robot's diameter) in which the most correctly coloured segments are found is considered to be the position of the robot. Of course, this method still is error prone but – as figure 4-5 shows – produces already good results. One Pioneer robot was positioned at different positions spread over the camera's field of view (marked by the small circles inside the chart). Then five pictures were taken and the relative position of the robot was calculated (marked by the small crosses). The average computed from these five measurements is marked by the small diamond shaped figures inside the chart.

In order to clarify the quality of the localization process figure 4-6 and figure 4-7 both show the mean error and the standard deviation (in metres) of the measured positions. Figure 4-6 presents error and deviation with reference to the lateral offset of a robot, i.e. distance to the left or to the right from the line of sight of an observer's camera; figure 4-7 presents the same with reference to the distance from the observer. In both cases, there is no obvious trend in the mean error or the deviation. In the whole camera field of view the algorithm produces results of sufficient accuracy.

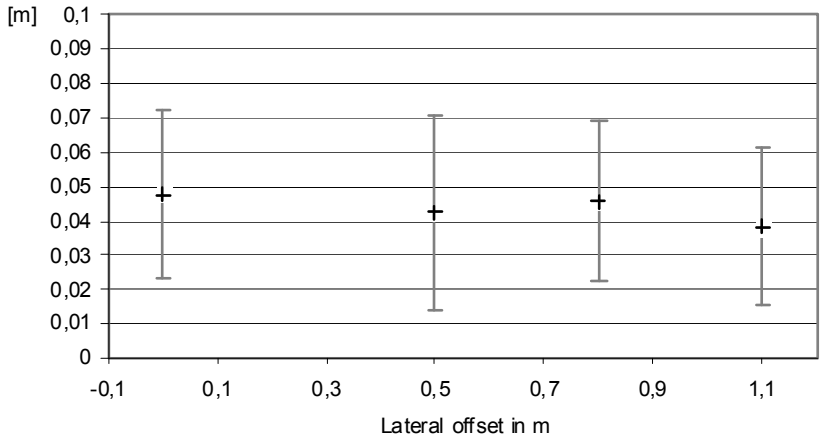

Figure 4-6: Mean error and standard deviation with reference to the lateral offset of a robot.

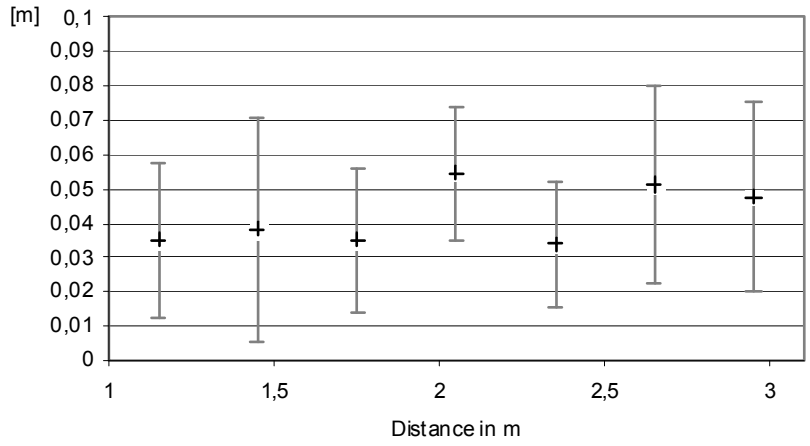

Figure 4-7: Mean error and standard deviation with reference to the distance of a measured robot.

The next experimental set-ups are with moving robots. Figure 4-8 shows the first set-up by three pictures ordered from left to right representing one example run. A Pioneer I robot crosses the field of view of the observing B21 robot. Each picture was augmented

with a little overlay representing the field of view of the camera mounted on top of the robot. The Pioneer robot moved very slowly at a speed of about 15 cm per second in order to get several measurements while passing through the camera's view.

Although the resulting positions seem to be rather steady, the probability of completely wrong measurements increases when more than one robot is visible on the same image. In order to reduce the probability of such errors an additional testing algorithm was implemented. With every measurement, the last positions computed for a robot are compared to its current position. If the new position is impossible, e.g. because the robot's maximum speed would have been exceeded, or unlikely, e.g. because it differs strongly from the direction the robot had before, a repetition of the last measurement is initiated.

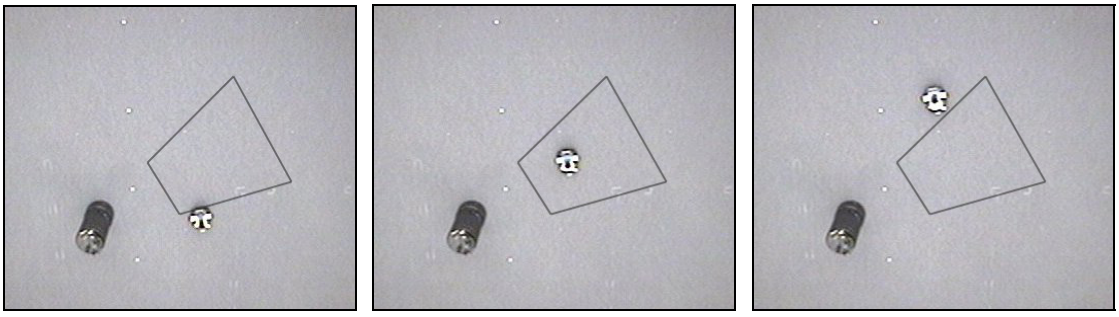

Figure 4-8: A robot crossing the field of view of a still standing observer.

4.2.3 Conclusions

Within this chapter, a new approach to the problem of establishing and maintaining a common co-ordinate system for a group of robots was presented. A camera system mounted on top of a robot and vision algorithms are used to calculate the relative position of each surrounding robot. The watched movement of each robot is compared to the reported movement that is sent over some communication link. From this comparison, the co-ordinate transformation is calculated.

The method was tested inside a multi-robot simulation environment, which fully models the odometry errors of the robot vehicles. The inaccuracy of the vision process is only modelled by a very simple random variation of the resulting relative positions.

Experiments with real robots and a real camera system were performed and produced fair results. The vision process generates consistent position information for the other visible robots.

Several problems occurred throughout the implementation process. For example, the segmentation process ceased to work properly because of decreasing image quality when the watched vehicles and especially the camera-equipped robot moved too fast. At the moment, the range in which a robot's position can be calculated from a camera image is limited to a few meters.

When performing the real world experiments with the vision based relative localisation approach, several drawbacks turned up:

1. Vision process
    a. Vision based algorithms suffer from intrinsic problems. Changing light conditions, for example, require frequent camera calibrations. Thus, although looking only at indoor robots, reliable detection even of marker-equipped robots is often difficult.
    b. To overcome the problem of looking into the "right" direction either an intelligent vision process (e.g. active perception) or a combination of omni-directional and measuring cameras is needed.
    c. The whole vision process needs a considerable amount of computing power, which makes it difficult to use on small robots.
2. Precision
    The process of estimating the position of another robot through a vision process is inherently imprecise. The factors that affect the estimation are the camera parameters, the design of the markers, viewing angle, and additionally the pan/tilt head.

The sum of these circumstances and the fact that all used robots are equipped with laser-based distance measurement devices led to a more promising approach described in the next section. The work presented in this section has been partially published beforehand [173].

4.3 Laser-Based Relative Localisation Approach

This method to estimate the positions and to establish the common co-ordinate system is divided into two stages. First, each robot scans its surrounding environment for other robots. Whenever a robot moves and therefore its position inside the sensor field changes, the movement with respect to the sensing robot's co-ordinate system can be measured. Based on the distance and angular information for every robot and its observers, an initial position estimation for each observer is generated. A simple geometrical algorithm is used to fulfil this task. The results of these observations are then communicated to the other robots. By comparing that movement with the one the moving robot itself reports, it is possible to calculate the transformation matrix between the co-ordinate system of that robot and the common relative co-ordinate system.

Based on these initial estimations each robot can estimate the relative positions of all visible robots and use them as landmarks to improve its own position estimation. This again results in better estimates for the localisation of the other robots, which in turn results again in a better localisation for the robot itself. An Extended Kalman Filter (EKF, see e.g. [9] and [82] for basic concepts) is used to continuously update the position of the robot as well as position and orientation of its observers. If all robots run this position estimation in parallel, a common co-ordinate system with reference only to the robots themselves can be established.

While most localisation techniques are based on global strategies that make use of special landmarks or other kinds of a priori knowledge, the described method uses only local information.

The approach also allows introducing a method for establishing a common co-ordinate system with reference only to the robots themselves; (this will be called a 'relative' common co-ordinate system throughout the rest of this manuscript). Since it is not possible to map such a relative co-ordinate system to any system of global world co-ordinates, it is of course not useful for all multi robot applications. Nevertheless, for most navigation problems it is sufficient, for example moving in formation and exploration.

4.3.1 Mathematical Background

4.3.1.1 Initial Estimation of Robot Positions

In this section, the basic steps for the initial estimation of the robot positions are briefly sketched. Since the scientific topic behind this problem is one of the major fields of work even in the tracking community, a detailed elaboration is far beyond the scope of this work, see [148, 172] for more information.

Each of the robots is equipped with odometry sensors and a laser scanner. This enables the robots to roughly orientate themselves and to measure distances to other objects. By using a laser scanner it is also possible to detect moving objects in the field of view. This tracking process provides the information, distance, and angle about the other robots that are needed for the position estimation process. The result of the tracking process is a list of distances and bearings describing where in the sensed area a robot has moved. This information is now communicated to all other group members. This means that each robot knows about what the others are "seeing".

In the next stage, this information is used to estimate the position of the other robots. Since the distances measured by the other robots are known, they can be used just like the sensor information from the robot's own sensors. If someone tells you that you are 5 meters away from him, you know that he is also 5 meters away from you, even if it is not your own measurement. The only information missing is the bearing, meaning that there is no information where on a circle with 5 meter radius the sensing took place.

If a robot is moving from position P_{t-1} to position P_t and an observer measured the state vectors $\langle d_{t-1}, \vartheta_{t-1} \rangle$ and $\langle d_t, \vartheta_t \rangle$, consisting of belonging distance and angular information, then the location of the observer itself can be derived (see figure 4-9). Taking two circles $K_{t-1}(P_{t-1}, d_{t-1})$ and $K_t(P_t, d_t)$ with centre P_{t-1} and radius d_{t-1}, respectively P_t and d_t, their intersections can be calculated. Aside from errors due to sensor faults, there are always two intersection points because of the limited robot velocity and the high data rate of a laser sensor. Since the observations not only contain distances but also angular information ϑ_{t-1} and ϑ_t, the difference $\Delta\vartheta$ of those two

angles can be used to decide which of the two possible intersection points must be the position of the observer. This step is repeated several times during the beginning of the robot's movement, until the probability of an erroneous guess falls below some lower bound. Figure 4-10 shows all measurements taken by one observer during an example run, drawn as circles around the robot positions. For the initial step, only a small subset of them would be needed. The results of this stage are the estimated initial positions of the other group members. In the next stage, these are used to correct the position of the moving robot itself.

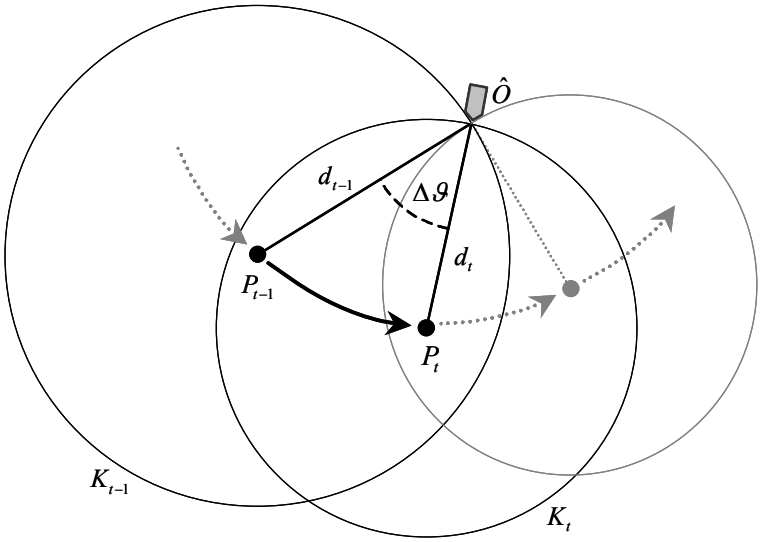

Figure 4-9: A robot moving from P_{t-1} to P_t is seen by an observer.

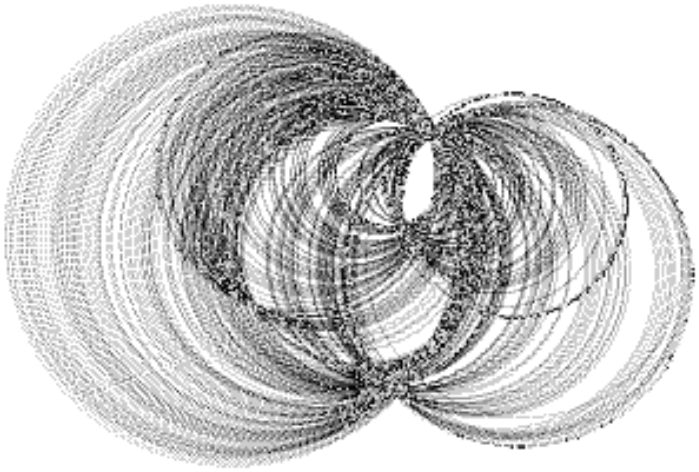

Figure 4-10: Example scans measured by one observer, painted as circles around the robot positions.

4.3.1.2 Position Update Process Using an Extended Kalman-Filter

The position estimation described in the last section is used to create an initial state estimation for the ongoing update and correction process. Additional position information generated by the tracking process is used to update the position estimates of the robots as well as for the observers.

An Extended Kalman Filter (EKF) is employed in order to combine all different measurements into one global state estimate. The state vector describing the localization information in a robot group of n robots at time step k is denoted as

$$x(k) = \begin{bmatrix} p_1(k) & \dots & p_n(k) \end{bmatrix}^T, \tag{20}$$

where $x(k) \in \mathbb{R}^{3n}$ and

$$p_i(k) = \begin{bmatrix} p_{i,x}(k) & p_{i,y}(k) & p_{i,\vartheta}(k) \end{bmatrix} \tag{21}$$

means position and orientation of the i^{th} robot. The initial error covariance P_0 for the initial state x_o (acquired as described in the last section) is defined as

$$P_0 = \begin{pmatrix} \sigma_t^2 & & & & & & \\ & \sigma_t^2 & & & 0 & & \\ & & \sigma_o^2 & & & & \\ & & & \ddots & & & \\ & & & & \sigma_t^2 & & \\ & 0 & & & & \sigma_t^2 & \\ & & & & & & \sigma_o^2 \end{pmatrix}, \tag{22}$$

with σ_t the translational and σ_o the rotational error. Unless otherwise stated for all experiments carried out in this work $\sigma_t = 7\,[cm]$ and $\sigma_o = \frac{10\pi}{180}$ is assumed. The used values have been ascertained by extensive empirical analyses, which provided strong evidence that the magnitude is reasonable. Even for notably larger initial errors the algorithm produces good results.

In order to explain the EKF update step one has to consider the following situation. Each time one of the robots gathers a relative measurement of one of the others this information is deployed into the EKF in order to update the overall system state. For explanation of update step k, without loss of generality, look at the case that the i^{th} robot got a new measurement $z = \begin{bmatrix} d & \alpha \end{bmatrix}^T$ of the robot with index 1, in which d means the distance between them and α the direction of a vector from the observer to robot no. 1.

Keep in mind that these indices are arbitrarily chosen. The whole process works identically for any pair of robots.

First, the information gained from the odometry sensors of the two involved robots is used for the prediction step of the EKF. Let

$$u_1(k+1) = \begin{bmatrix} \Delta p_{1,x}(k+1) & \Delta p_{1,y}(k+1) & \Delta p_{1,\vartheta}(k+1) \end{bmatrix} \tag{23}$$

be the way the 1st robot moved from time step k to $k+1$ expressed in Cartesian coordinates and an additional turning angle, and

$$u_i(k+1) = \begin{bmatrix} \Delta p_{i,x}(k+1) & \Delta p_{i,y}(k+1) & \Delta p_{i,\vartheta}(k+1) \end{bmatrix} \tag{24}$$

be the same for the i^{th} robot. Then the state prediction can be written as

$$x^-(k+1) = \begin{bmatrix} p_1(k)+u_1(k+1) & \dots & p_i(k)+u_i(k+1) & \dots \end{bmatrix}^T. \tag{25}$$

Accordingly, the projection of the error covariance is simply defined as

$$P^-(k+1) = P(k) + Q(k+1). \tag{26}$$

The process noise covariance $Q(k+1)$ in the approach is not constant over the course of the filter, but depends on the distances the two involved robots travelled since their state has been updated the last time. The further they moved the larger is the uncertainty on this movement because of possible odometry errors. This consideration leads to the following definition:

$$Q(k+1) = \begin{pmatrix} Q_1 & & & & & & \\ & \hat{Q} & & & & 0 & \\ & & \ddots & & & & \\ & & & \hat{Q} & & & \\ & & & & Q_i & & \\ & & & & & \hat{Q} & \\ & 0 & & & & & \ddots \\ & & & & & & & \hat{Q} \end{pmatrix}, \tag{27}$$

with $\hat{Q} = \begin{pmatrix} \hat{q}_t^{\,2} & 0 & 0 \\ 0 & \hat{q}_t^{\,2} & 0 \\ 0 & 0 & \hat{q}_o^{\,2} \end{pmatrix} \in \mathbb{R}^{3\times 3}$, $\hat{q}_t$ and $\hat{q}_o$ small positive constants, as well as for $Q_1 \in \mathbb{R}^{3\times 3}$ and $Q_i \in \mathbb{R}^{3\times 3}$

$$Q_1(k+1) = \begin{pmatrix} \left(s_t \Delta p_{1,x}(k+1) + \hat{q}_t\right)^2 & 0 & 0 \\ 0 & \left(s_t \Delta p_{1,y}(k+1) + \hat{q}_t\right)^2 & 0 \\ 0 & 0 & \left(s_o \Delta p_{1,\vartheta}(k+1) + \hat{q}_o\right)^2 \end{pmatrix}, \quad (28)$$

respectively

$$Q_i(k+1) = \begin{pmatrix} \left(s_t \Delta p_{i,x}(k+1) + \hat{q}_t\right)^2 & 0 & 0 \\ 0 & \left(s_t \Delta p_{i,y}(k+1) + \hat{q}_t\right)^2 & 0 \\ 0 & 0 & \left(s_o \Delta p_{i,\vartheta}(k+1) + \hat{q}_o\right)^2 \end{pmatrix}. \quad (29)$$

Here s_t represents the mean error for translational movement of the robots and s_o the same for rotations. As long as all robots show the same error characteristic those values may remain constant, otherwise they should depend on the actual robot to which they belong. The $\hat{q}_t$ and $\hat{q}_o$ in (27) represent the inherent uncertainty of the position information for every robot; this grows even if the odometry reports no movement at all.

After this, the EKF prediction step is finished. Thereupon, the new measurement $z(k+1) = [d \quad \alpha]^T$ of robot no. 1 obtained by the i^{th} observing robot is now used for the correction step of the EKF:

$$x(k+1) = x^-(k+1) + K(k+1)\left[z(k+1) - h\left(x^-(k+1), 0\right)\right], \quad (30)$$

where $K(k+1)$ denotes the Kalman gain (34) and the function $h(x,v)$ relates a state vector x, defined as in (20), to a measurement $z = [d \quad \alpha]^T$, given the current measurement noise v. For $h(x,v)$ a standard mixed coordinate EKF approach [9] is used, which in this example case writes to

$$h(x,\nu)=\begin{pmatrix} h_1(x,\nu) \\ h_2(x,\nu) \end{pmatrix}=\begin{pmatrix} \sqrt{\left(p_{1,x}-p_{i,x}\right)^2+\left(p_{1,y}-p_{i,y}\right)^2}+\nu_d \\ \arctan\left(\dfrac{p_{1,y}-p_{i,y}}{p_{1,x}-p_{i,x}}\right)-p_{i,\vartheta}+\nu_\vartheta \end{pmatrix}. \tag{31}$$

When (25) is redefined as $\begin{bmatrix} \tilde{p}_{1,x} & \tilde{p}_{1,y} & \tilde{p}_{1,\vartheta} & \cdots & \tilde{p}_{i,x} & \tilde{p}_{i,y} & \tilde{p}_{i,\vartheta} & \cdots \end{bmatrix}^T = x^-(k+1)$ and

$$P_1=\sqrt{\left(\tilde{p}_{1,x}-\tilde{p}_{i,x}\right)^2+\left(\tilde{p}_{1,y}-\tilde{p}_{i,y}\right)^2}=\left\|\begin{pmatrix} \tilde{p}_{1,x} \\ \tilde{p}_{1,y} \end{pmatrix}-\begin{pmatrix} \tilde{p}_{i,x} \\ \tilde{p}_{i,y} \end{pmatrix}\right\|, \tag{32}$$

then for the Jacobian matrix $H(k+1)$ needed for the remaining EKF step this leads to

$$H(k+1)=\begin{pmatrix} \dfrac{\tilde{p}_{1,x}-\tilde{p}_{i,x}}{P_1} & \dfrac{\tilde{p}_{1,y}-\tilde{p}_{i,y}}{P_1} & 0 & \cdots & 0 & \dfrac{\tilde{p}_{i,x}-\tilde{p}_{1,x}}{P_1} & \dfrac{\tilde{p}_{i,y}-\tilde{p}_{1,y}}{P_1} & 0 & 0 & \cdots \\ \dfrac{\tilde{p}_{i,y}-\tilde{p}_{1,y}}{P_1^2} & \dfrac{\tilde{p}_{1,x}-\tilde{p}_{i,x}}{P_1^2} & 0 & & 0 & \dfrac{\tilde{p}_{1,y}-\tilde{p}_{i,y}}{P_1^2} & \dfrac{\tilde{p}_{i,x}-\tilde{p}_{1,x}}{P_1^2} & -1 & 0 & \end{pmatrix}. \tag{33}$$

Note that $\dfrac{\partial h_1}{\partial \tilde{p}_{1,\vartheta}}\left(x^-(k+1),0\right)=H_{1,3}(k+1)=0$ and $\dfrac{\partial h_2}{\partial \tilde{p}_{1,\vartheta}}\left(x^-(k+1),0\right)=H_{2,3}(k+1)=0$, which means that no update on the orientation of the observed robot takes place during the filter step. This is, of course, because due to the hardware set-up the observer cannot measure orientation information. However, as long as all participating robots at least occasionally generate measurements on their own, orientation information for all robots is updated.

As usually, the Kalman gain $K(k+1)$ is computed as

$$K(k+1)=P^-(k+1)H^T(k+1)\left[H(k+1)P^-(k+1)H^T(k+1)+R\right]^{-1}. \tag{34}$$

As one can see, the measurement noise covariance *R* is considered as constant in this approach. Special efforts have been undertaken to acquire reasonable values for the matrix *R*. This has been difficult because *R* does not refer to some well-known specification for a hardware device like a laser scanner, but describes the quality of the underlying tracking algorithm. Unless otherwise stated always

$$R=\begin{pmatrix} r_t & 0 \\ 0 & r_o \end{pmatrix}, \tag{35}$$

with $r_t = 3[cm]$ and $r_o = \frac{3\pi}{180}$ is used. These values produced good results for nearly all inspected situations.

Finally, the filter step ends with the update of the error covariance matrix

$$P(k+1) = \left[I_{3n} - K(k+1) H(k+1) \right] P^{-}(k+1). \tag{36}$$

As a result, $x(k+1)$, as computed in (30), contains updates for the position of the first robot, which has been observed, and updates for position and orientation of the i^{th} robot, which in this case played the role of the observer. In other words, starting with initial position estimations the EKF maintains the relative positions for all robots during the on-going run.

It is important to mention that, so far, the EKF approach is implemented as centralised algorithm. All measurements *z* coming from individual robots are received by a central component and processed sequentially. Only one system state is maintained and broadcast back to the group members. Of course, this leads to the requirement of reliable communication among the robots, only temporarily limited disconnections are allowed. Decentralised solutions could be implemented in which each robot computes its own system state, but such an approach would generally require some agreement between the different state vectors. The pseudo-code of algorithm 1 describes the centralised EKF implementation. Primary work on this particular EKF based approach to relative localisation and some of its mathematical foundations have been published beforehand [139].

Algorithm 1. Relative Localisation, centralised EKF implementation

1: **whenever** a new measurement *z* with timestamp *k* arrives from robot *i*
2: Acquire odometry data Δp_i at time *k* from robot *i*
3: Calculate state prediction $x^-(k+1)$ and error projection $P^-(k+1)$
4: Compute $H(k+1)$ and the Kalman gain $K(k+1)$
5: Update system state $x(k+1)$ and error covariance matrix $P(k+1)$
6: Transmit $x(k+1)$ to all robots
7: **end whenever**

4.4 Experiments

4.4.1 Non-moving Observer

In these first experiments three Pioneer I robots were used as the observing robots. The B21 was used as the moving target to be observed by the other robots. Four different routes were in the experiments, see figure 4-11 for details.

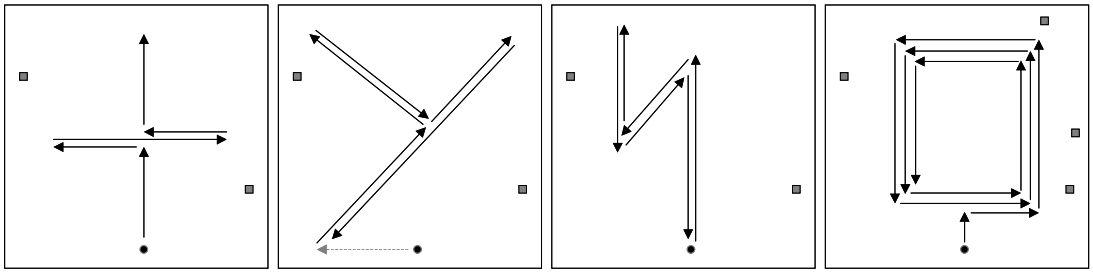

Figure 4-11: Some of the conducted experiments.
The arrows show the paths travelled by the moving B21, the black dots mark the observers' positions.

Figure 4-12 presents one example of the results of the position estimation process with two observers. Starting with a nearly perfect match between odometry and "filtered" positions, one can clearly indicate a deviation at the other three endpoints of the cross. The inaccuracy in the angular odometry sensors accumulates to about 20cm at the left end and 15cm at the upper and right end and vanishes while the robot drives back to the centre of the cross.

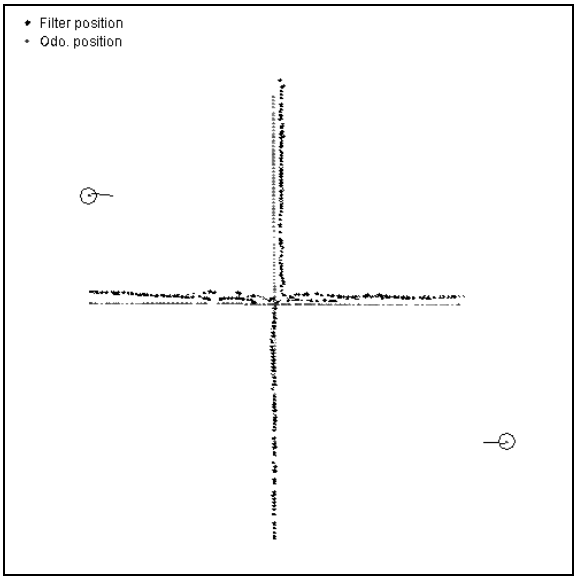

Figure 4-12: Example run with two observers. The dark points are the results of the filtering process;
the grey points give the positions as seen by the odometry.

The results of a more interesting example run are shown in figure 4-13. In this experiment, four observers are arranged around one moving robot, which runs in a square-sized manner several times. Like in figure 4-12 the upper left part of figure 4-13 shows the deviation between the results of the odometry sensors and of the position estimation. It is the typical situation, which most autonomous vehicles face when travelling a "closed" path. Because of wheel slip and rotation error the real moved path differs further from the odometry estimation with each cycle.

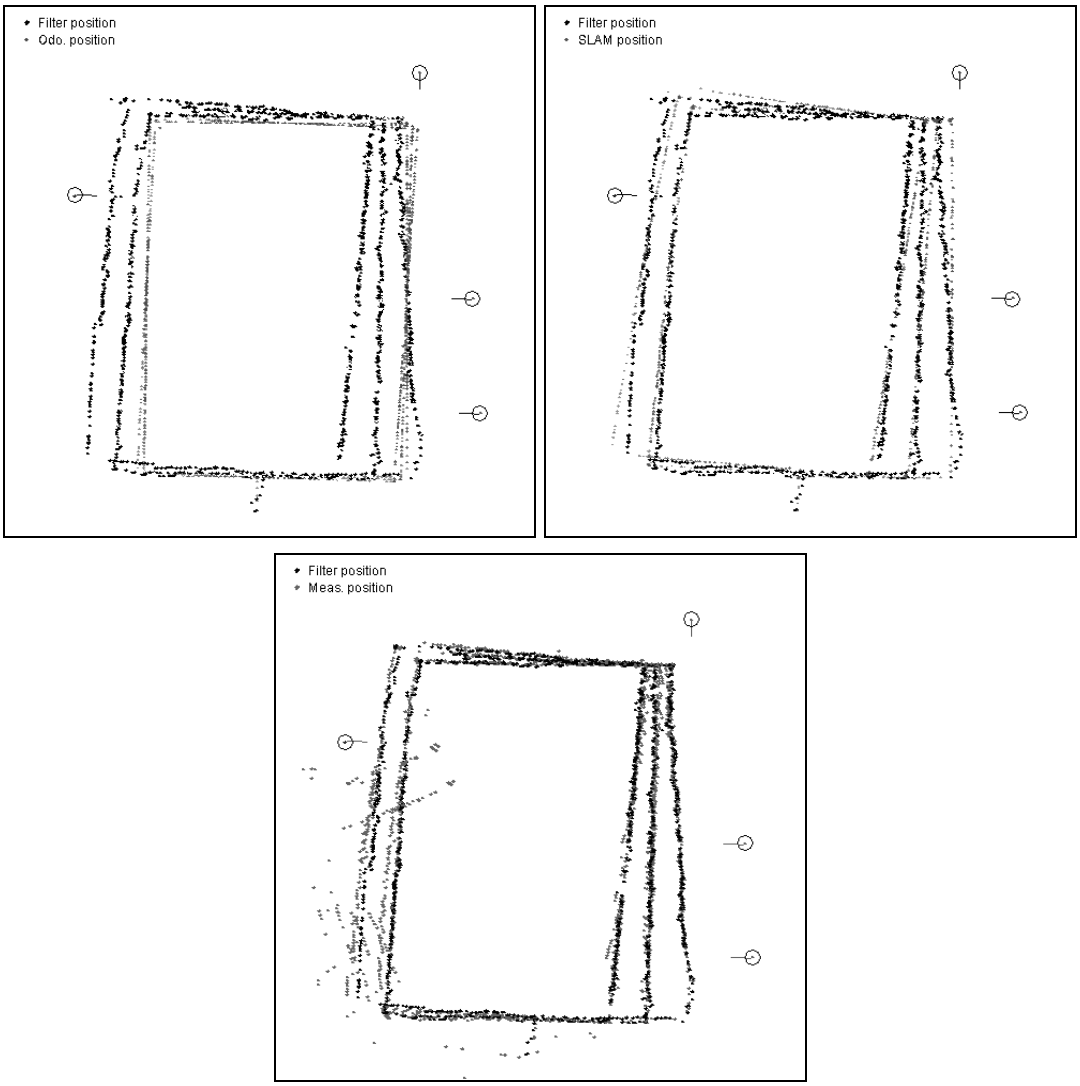

Figure 4-13: A square sized run with four observers.
The upper left figure shows the estimated positions compared with pure odometry data, the upper right one compares them with the result of a global SLAM algorithm. The lower figure compares the raw measurements of the observers with the positions estimation by the filter.

The upper right figure compares the results of the sensor based EKF with a typical global SLAM method [45]. As one can see there are several parts of the track, where the estimations of the filter and the SLAM algorithm match quite well. However, some segments show a significant deviation between the two estimates. This can have several reasons (apart from the trivial one that SLAM goes wrong, which can be precluded for this experiment). The bulge at the lower right corner, for example, is caused by the initially wrong guessed and then corrected position of the lower right observer. The deviation in the upper part of all paths is also originated in slightly wrong initial position estimations. Nevertheless, since these wrong estimates coincide for all upper observers, their positions are not corrected this time – instead the moving robot's path is displaced.

When looking at the error in the lower left part of the path one can find the reason in the lower picture of figure 4-13. This figure shows the raw measurements taken by the four observers. Especially in the lower left quadrant there is a huge amount of cluttered and partially completely wrong measurements, which produce problems for the filtering algorithm.

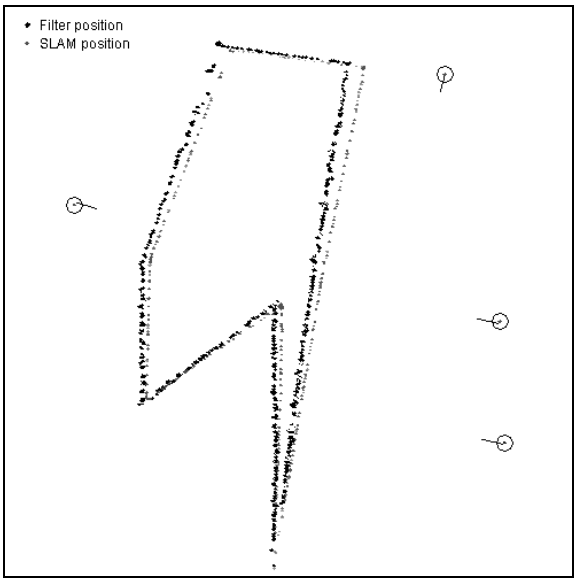

Figure 4-14: Example of a globally deviated common co-ordinate system.

Figure 4-14 gives a good example for the relative nature of the position estimation process. In this figure, again the result of the EKF is compared to the position information generated by a SLAM algorithm. Four observers watch the movement of the B21. The result is a precise position estimation for the B21 as well as for the four observers, but every position differs from its real counterpart as delivered by the SLAM method. (Instead of using SLAM, the positions of the B21 could have been measured manually but that, of course, would have disturbed the observers' laser readings.) In fact, although distance and bearing between each observer and every position of the B21

is correctly estimated, the resulting relative co-ordinate system is rotated by about two degrees counter-clockwise around some virtual turning point below the figure.

Finally, figure 4-15 shows an experiment where three observers were used to track a B21. The B21 moved in a large square with 10x6 meters. In this figure all three positions estimations are drawn in one diagram. While the green track shows the "estimate" of the robots odometry, the red (Kalman-Filter) and the blue line (SLAM) sketch the driven track as estimated through the measurements by the laser scanner data. On the first few meters and after the first left turn the three methods are still pretty close. Starting with the second turn left (upper right corner) the Kalman-Filter as well as the SLAM begin to deviate quite strongly from the odometry. On the opposite, the Kalman-Filter and SLAM results are nearly congruent with each other.

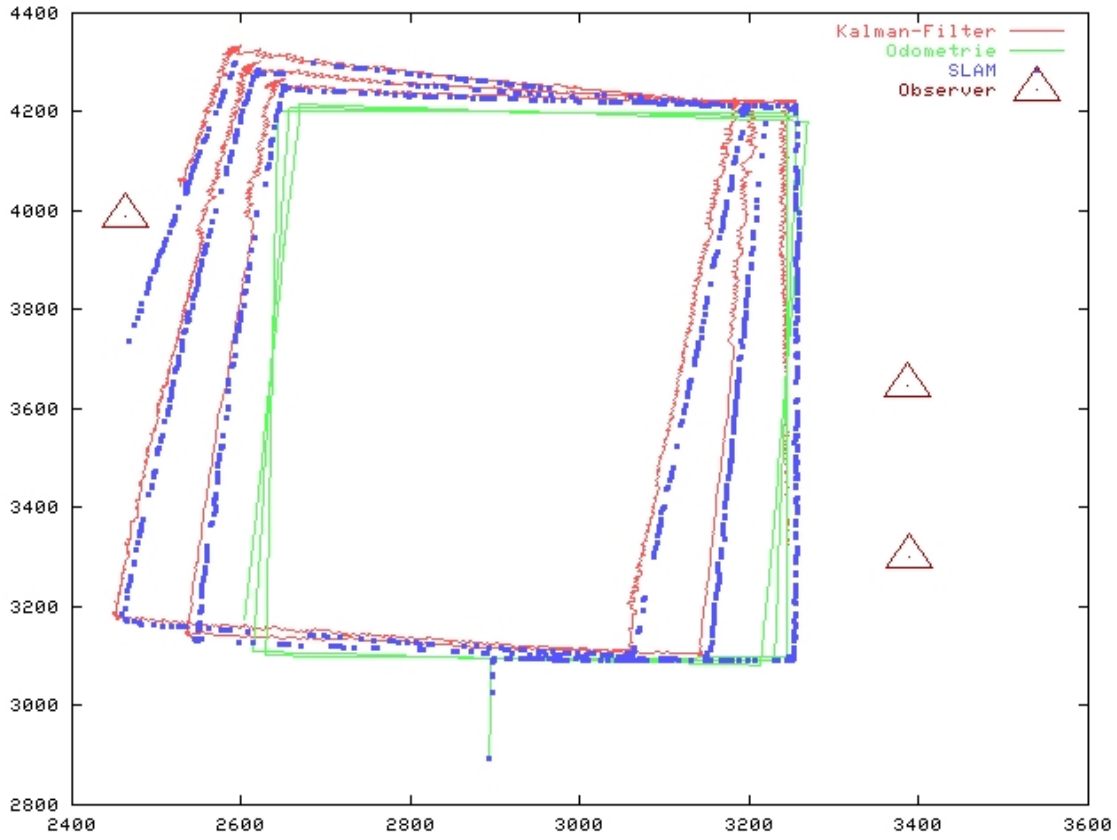

Figure 4-15: Experimental comparison of three position estimation methods.

4.4.2 Moving Observers

After getting these quite promising results, the next step was the usage of moving observers. In order to get reproducible results and to further tune the filtering process, first some experiments with the multi-robot simulation environment were conducted. Figure 4-16 presents one example of these simulation runs with four observers positioned just around one moving robot.

First, the observers remain stationary, exactly like described in the previous sections. Then after a few seconds, two of the four observers start to move, while at the same time the observed robot also continues its movement. The right part of figure 4-16 shows the situation after another few seconds. All robots participating in the experiment are still correctly tracked. Note that the experimental validation presented in the previous sections is partially based on work published in [144].

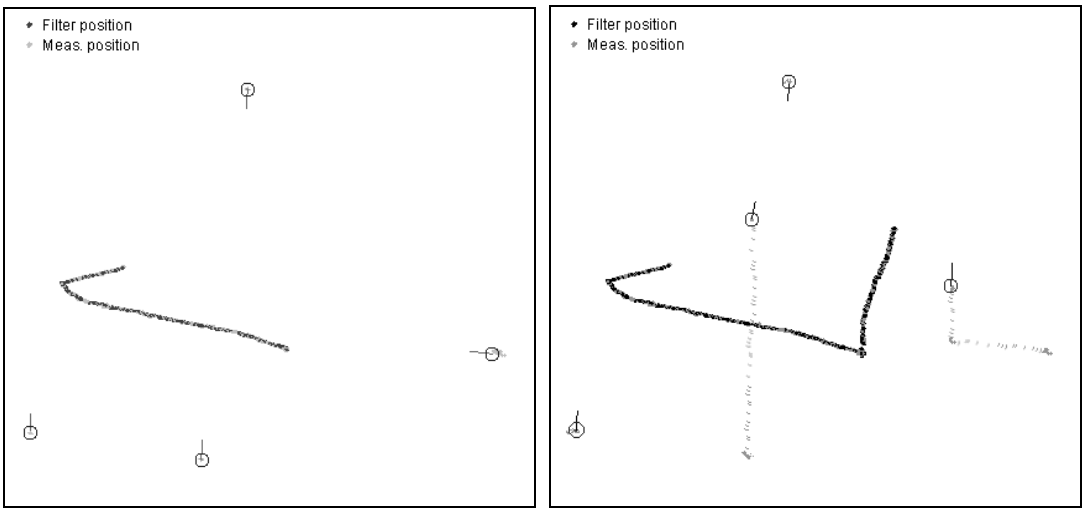

Figure 4-16: Example run with moving observers, before (left) and after (right) observers started to move.

4.4.3 Precision Evaluation with Moving Robots

Looking on co-operative position estimation the question whether the number of robots sharing the common relative co-ordinate system has any influence on the precision of the resulting relative localisation is one of the core issues.

On one hand, since each robot measures distance and direction to every other robot in the group, the amount of mutual measurements rapidly increases. On the other hand, apart from the errors caused by the odometry sensors of each robot, there is also a possibly growing number of faulty measurements due to temporary occlusions while the robots work together and share a common working area.

In the experimental set-up, the underlying sensor device is a standard, widely used laser range finder, which delivers distance information at a very high precision and with an angular resolution up to 0.5 degree. Thus, any sophisticated tracking method using this data as input delivers accurate position information for the other group members. See for example [146] for a comprehensive comparison of different tracking approaches under such conditions.

In contrast, the aggregated odometry error within a robot group grows only linearly in the number of group members. The frequency of mutual occlusions depends on the kind of task the robots have to fulfil, but normally such occlusions have only a very limited

duration, happening for example while two robots are passing each other or while a robot is turning. Therefore, the expectation was that the increasing number of mutual position measurements outweighs the growing number of possible error sources. Thus, it can also be expected that the overall precision of the relative localisation should increase with the size of the robot group.

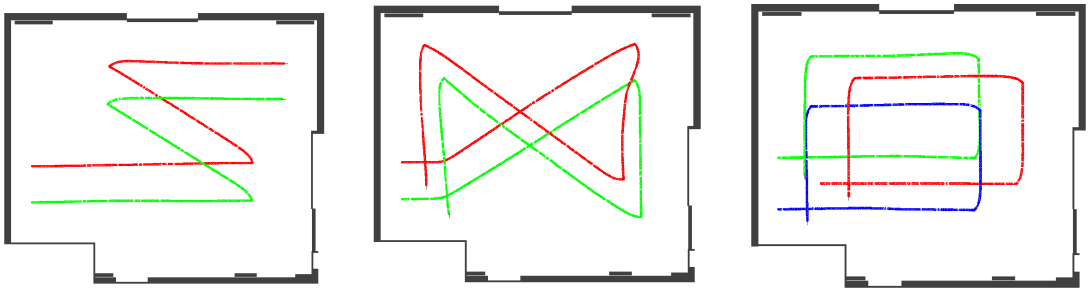

Figure 4-17: Three different shapes on which the robots had to move.

4.4.3.1 Design Decisions and Necessary Preconditions

The experiments were fully conducted in simulation. Apart from the obvious reason that a simulation with well-known parameters yields reproducible and comparable results, some other important reasons lead to this decision. First, the simulation provides an exact ground-truth in form of absolute position information for each robot, far better than any means of positioning for "real" robots.

Additionally, it was planned to compare group sizes of at least five robots, which means a great challenge with experimental robot systems and a lab environment of limited size. And the goal was not to record some impressive demonstration runs but to obtain data from a large number of runs for each scenario in order to establish a meaningful basis for further evaluation.

With different group sizes from two to five robots, at least three different driving scenarios and a minimum of 20 runs for each combination, this already results in a total of 240 experiments, not considering any possible technical troubles or problems in the design of the experiments. Realistically, this easily leads to hundreds of additional trials, consuming weeks of laboratory time. In simulation, the original design regarding group size and driving scenarios was retained. Thus, in principle all results of these experiments could be validated using the real platforms and a large experimental hall. In simulation, each of the scenarios described in the following section was conducted 60 times.

The three different paths on which the robots moved along are pictured in figure 4-17. The left figure shows a group of two robots (red and green line) moving along some Z-like shape. The middle one presents the second scenario, a shape like a horizontal eight with corners. In the right figure a formation of three robots (red, green and blue

line) drives on a rectangular path. Throughout the remainder of this chapter these scenarios will be mostly referred to as “Z”, “eight”, and “rectangle”.

The three paths look similar in terms of driving distance, covered area, or overall turning angle, and in fact they are to some extend arbitrarily chosen. However, there are also relevant characteristics in which the scenarios differ, mainly the kind of turns, which the vehicles have to follow. For many robot platforms, and for the ones used as well, any rotation induces a potentially large odometry error, and each rotational error sums up to a growing displacement as the robot continues its movement.

Another observation, at least for the used different types of robots, is the influence of the turning direction on the aggregated odometry error. Throughout longer experiments, it sometimes happens that the rotational odometry error increases and decreases in turn. Especially if a robot drives to some goal point and returns afterwards the error grows until the goal is reached and nearly diminishes during its way back. This seems to be because odometry errors caused by clockwise and counter-clockwise turns often cancel out each other.

The multi-robot simulator was configured to use a realistic odometry error model, reflecting the foregoing considerations. Each robot had its own error characteristic with a normally distributed translational error ($\sigma = 3cm$ per 1m translation), and an orientation error spread normally around a small systematic fault ($\mu \in [1.5, 2.5]$, $\sigma = 0.3°$ per 90° turn). Especially the systematic fault causes the typical displaced odometry data. Figure 4-18 presents some characteristic example runs. In these examples, only two robots have been recorded in order to simplify the illustrations. Data from groups of more than two robots does not differ in principle.

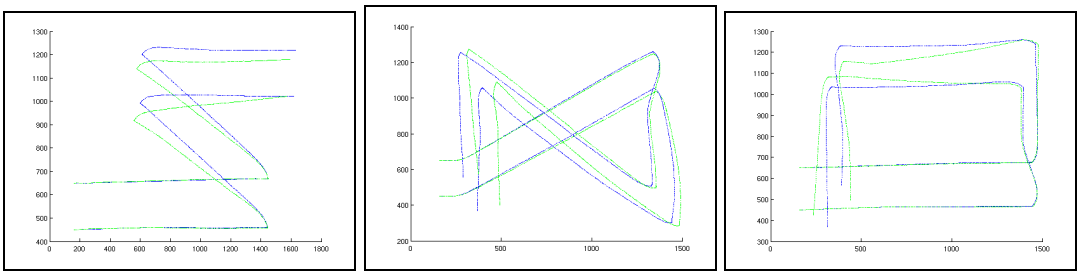

Figure 4-18: Comparison of true positions (blue path) with information from odometry (green path).

The blue line gives the robots’ exact positions in the simulation environment. The three figures correspond to the “Z”, “eight”, and “rectangle” scenario described above. In contrast, the green lines present the faulty positions of the robots as they are recorded by the simulated odometry sensors.

The leftmost figure, thereby, shows a good example for the before mentioned decreasing odometry error. The lower of the two robots nearly ends at its exact position, even though with faulty orientation information and the odometry position of the upper robot also approaches to the real one. This is a recurrent behaviour in this first scenario,

possibly because in this scenario the robots have to turn exactly by the same angle of about 110° in both directions, first counter-clockwise and then clockwise. Contrarily, it only rarely happens in the other two scenarios.

In the eight and rectangle scenario the overall driving distance for each robot is between 30m and 40m, and the accumulated odometry error at the end is often more than 1m, sometimes even more than 2m. As the right figure demonstrates, this deviance often points into opposite directions, due to the independent error model for each robot. As a result, looking only at the pure odometry data the distance (and orientation) error between any pair of robots easily reaches the magnitude of several metres during and, especially, at the end of a run. Deviances of this dimension mainly happen in the rectangle scenario, again possibly because of the kind of necessary turns. In the rectangle scenario, the robots have to turn only counter-clockwise, three times about 90°. Altogether, it can be stated that the average odometry error should be smallest in the Z-scenario, largest in the rectangle scenario and somewhere in between for the eight.

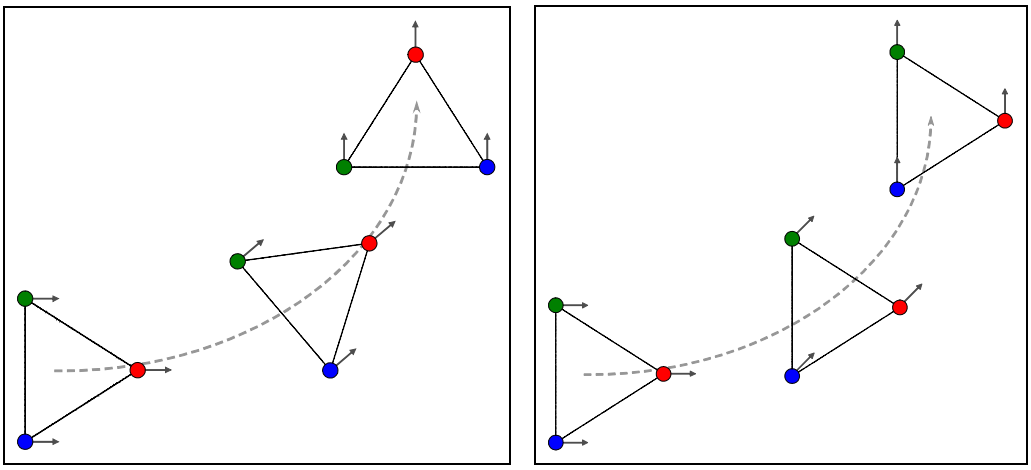

Figure 4-19: Different modes of turning a formation: "normal" (left) – whole formation turns, "fixed" (right) – only the robots turn around.

It is important to mention one more time that, although the presented data is simulation generated, it very well matches the experiences when collecting odometry data from different "real" robot systems. Of course, one might argue that the odometry error model is only empirically founded, but deeper research on this topic is certainly beyond the scope of this work.

Apart from the differences and impacts of the entire paths, which the robots had to follow in the three scenarios "Z", "eight", and "rectangle", it is worth discussing the exact mode in which the robot group had to move during the experiments. Of course, since all robots had to follow the same path, special co-ordination was necessary. Different approaches are conceivable and have been considered.

One possibility, for example, is to assign exactly the same path to each robot and then let them start consecutively from the same starting position at a fixed time interval. This

should lead to the robots driving one after another in a train-like manner. The obvious disadvantage is the nearly permanent mutual occlusion of robots, which are moving along the same line of sight. Apart from the turning points, only direct neighbours can see each other and produce mutual position and orientation measurements. For relative localisation this, of course, might be an interesting case, but not the right choice for evaluating the overall precision of the approach.

Another idea was to supply the goal or turning points for the different paths to the robots, set them up at distinct start positions, and let them start simultaneously, leaving the remaining co-ordination to the collision avoidance. However, apart from the confusion this method probably leads to near the turning points, the lack of a pre-defined and reproducible behaviour for each robot is a problem for the goal of precision measurement. Unexpected variations in the quality of the resulting localisation are hard to explain if the driven paths are too chaotic and, therefrom, the number of factors taking influence on the results gets to large.

Thus, it was decided to use fixed formations, which the robots had to maintain while following the three pre-defined paths, “Z”, “eight”, and “rectangle”. The idea of using robot formations in the context of relative localisation is based on earlier work presented in [141]. Here, “fixed” formation characterises a special manner of movement in formation. It means that, whenever the formation reaches a turning point, instead of completely turning the shape of the formation only the robots themselves turn around. Figure 4-19 illustrates this difference.

On the one hand, this is still a realistic scenario, giving results, to some extent, with immediate transferability into real life. On the other hand, especially this fixed formation approach produces well-defined and predictable tracks for each robot and comparable results for the mutual position measurements in all three scenarios. Additionally, mutual occlusions, in terms of location, duration, and frequency, are also predictable as well as reproducible.

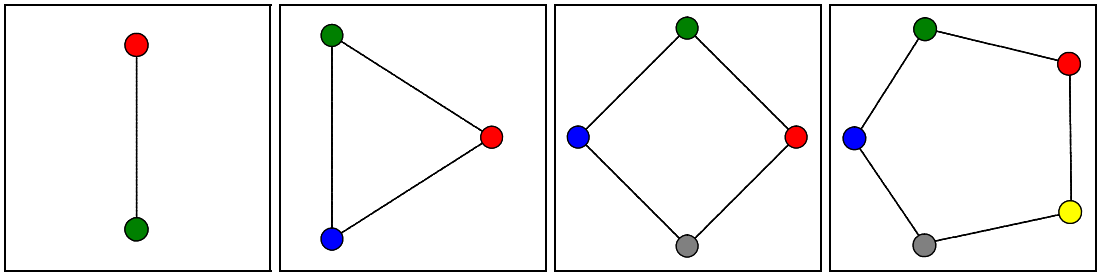

Figure 4-20: Formation shapes used for the different robot group sizes.

The intended formations for the different group sizes can be seen in figure 4-20. They are straightforward from the 2-robot line over a triangle and rectangle shape leading to a pentagon for five robots. The minimal distances, as found between neighbouring robots, are 2 metres for the line shape, 2.25 metres for the rectangles and about 2.7 metres for the two other shapes. The largest distance of about 4.25 metres can be found in the pentagon formation.

As mentioned above the formation algorithm was configured to generate fixed formation shapes in order to obtain regular and straight paths for all robots. The simulated environment was a part of the indoor robot lab, namely the large experimental hall of about 15 x 18 metres in size. This gives the possibility to repeat at least some of the trials in a physical environment. Figure 4-21 presents some arbitrarily chosen example runs, the "Z" with four robots, the "eight" with three robots, and the "rectangle" with five robots. The different colours correspond to the different robots in the same way as in figure 4-20. As one can see, the formation algorithm very well steers the robot formations along the defined paths, keeping all robots strictly at their specified formation positions. Moreover, as intended, this leads to predictable and reproducible tracks for each robot. For the very most of the recorded experimental runs, also the number of occlusions was limited and well defined. Those phases during which a robot was not able to see and, therefore, to directly measure distance and direction of one or more of its group members nearly exclusively happened at the turning points of the formation. Of course, especially with the four and five robot formations sometimes disturbances in the formation lead to temporary occlusions not only when the formation changed their direction. Altogether, it can be stated that the number of measurement errors and discontinuities due to mutual occlusions was small and was only slightly affected by the size of the robot group. This fact matches the expectations formulated at the beginning of this chapter and should make the recorded data a good basis for the ongoing precision evaluation.

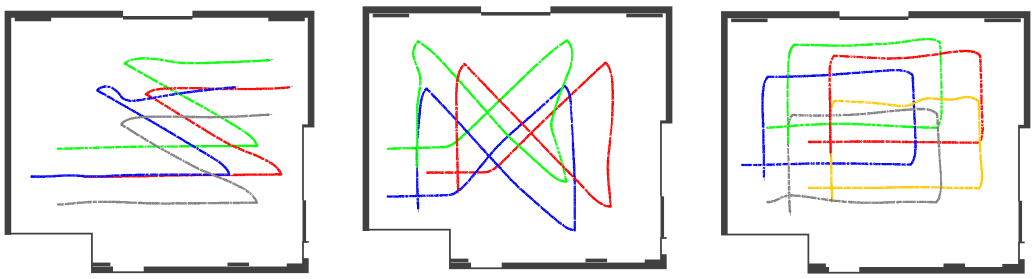

Figure 4-21: Example runs for formations of three (middle), four (left), and five (right) robots.

4.4.3.2 Collecting Data

As already stated, the indoor robots are equipped with standard SICK laser range finders, and this equipment is also modelled in the multi-robot simulation environment. According to the official specification by SICK [101], the LMS200 laser devices, which were used, deliver distance information with 10mm resolution and an error of less than 15mm. In the configuration, the angular information has a resolution of 1° with a typical error of about 0.4°. Although occasionally these values seemed slightly optimistic, especially in the presence of partly reflecting or metallic surfaces, a detailed verification was not conducted. Therefore, the simulated laser scanners compute their sensor data with this error characteristic.

In order to derive position information for other robots from the raw laser readings, in the very beginning a straightforward stateless geometric algorithm was used. Possible choices for more sophisticated tracking methods are, for example, addressed in detail in [146]. Nevertheless, evaluating the resulting position information, it turned out to be nearly of equal quality compared to real tracking algorithms. A mean error of about 5mm for the relative distance between two robots and less than 0.5° for the measured direction from one robot to another was achieved. According to [146], this is in a similar range as sophisticated probabilistic trackers like Probabilistic Data Association Filtering (PDAF) or Probabilistic Multi Hypothesis Tracking (PMHT), both customized especially for extended targets. Consequently, the implementation of other tracking algorithms was omitted and, instead, the simple geometric method was still used.

Figure 4-22 presents exemplary results for the mutual observation and measuring process in terms of quantity of position measurements. The average number of relative positions and orientation measurements, which one robot of the group took from all other group members during one experimental run was counted. The y-axis gives this number and the x-axis splits the results for the three different scenarios and the different group sizes from two up to five robots.

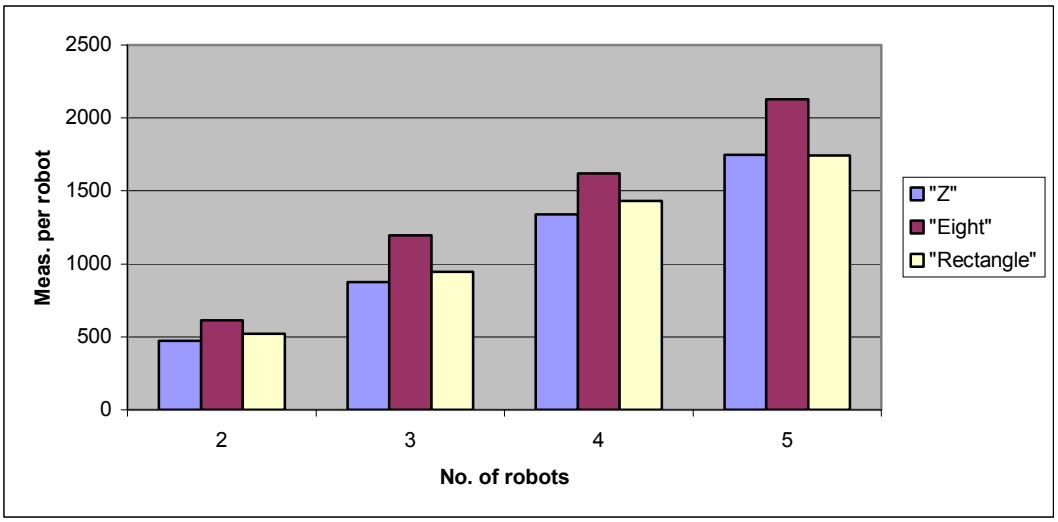

Figure 4-22: Amount of mutual position measurements (y-axis) for the three scenarios and the different number of robots (x-axis).

With only two robots both generate about 500 measurements for all scenarios, a bit less for the “Z”, a bit more for the “eight” due to different run times and driving distances. In the absence of any occlusions between the robots, one can expect the double number with three robots, triple with four and four times more measurements in the five-robot group. Actually, in the “Z” scenario for two robots each one measures its counterpart’s position at an average of 474 times during one experimental run. In a group of three robots, each of them generates an average of 875 measurements, 1340 position values for four robots, and in the five-robot group the mutual observation process delivers 1747

measurements per robots, which nearly fits to the stated expectation of $474 \cdot 4 = 1896$ values. As figure 4-22 illustrates the situation is similar for the other scenarios.

In summary, the design of the experiments should be adequate to analyse the influence of the robot group size on the resulting precision of the relative localisation. Due to the way the robots moved, a predictable and comparable behaviour for all scenarios could be achieved. The number and duration of mutual occlusions is limited and reproducible, leading to the expected result of more measurements per robot with growing group size. Although simulation based, the laser-driven position measurements and the robots' odometry sensors have realistic accurateness and error characteristics. The aggregated odometry error for the robot group differs between the scenarios, being larger for the "rectangle" and smaller for the "Z", but in all cases it grows only linearly in the number of group members.

Consequently, it was expected that the increasing number of mutual position measurements outweighs the growing odometry error and, thus, the overall precision of the relative localisation would increase with the size of the robot group.

The foregoing paragraphs described the simulation experiments in detail. Thereafter, the necessary input for the EKF-based relative localisation among the robots could be easily taken from the recorded simulation data. The position measurements derived from the simulated laser readings can be directly used for the EKF update step. In contrast to the more general values stated in section 4.3.1.2, in this special simulation set-up a different measurement noise covariance R could be used. As mentioned above, due to the characteristics of the simulated laser device and the special geometric tracking algorithm throughout these experiments the values $r_t = 0.5cm$ and $r_o = 0.5°$ were used.

The odometry data needed as basis for the EKF update step is also directly delivered by the multi-robot simulator. The scalar coefficients s_t and s_o, which are needed to calculate the translation respectively the orientation part of the process noise covariance $Q(k+1)$, are set to $s_t = 5cm$ and $s_o = 5°$. Finally, the scalar constants σ_t and σ_o, defining the translation respectively the orientation part of the error covariance P_0 for the initial state x_o, are set to $\sigma_t = 3cm$ and $\sigma_o = 3°$.

4.4.3.3 Evaluation of the Results

As mentioned earlier a total of 60 runs was conducted for each robot group size and each different driving scenario, leading to an overall number of 720 simulation-based datasets, which had to be evaluated. In accordance with the general guidelines for multi-robot system metrics, as formulated in section 3.1, the Mean Localisation Error (MLE) was developed for an quantitative assessment of the resulting relative localisation. To calculate the MLE, for each single localisation step the estimated robot positions were compared to the exact positions as delivered by the simulator. Since the focus is at relative localisation, simply comparing the absolute positions was not appropriate. Instead, for each pair of robots the difference between estimated and true distance was

summed up. This deviation was then weighted by the number of robots to get a measure independent of the group size. Finally, an average over the entire dataset was computed, resulting in one MLE per run.

Admittedly, this definition of the Mean Localisation Error is worth a discussion. One potential drawback is that orientation errors for each robot as well as in the line-of-sight between two robots are not addressed. In fact, some different approaches, including some complex and mathematically demanding methods derived from metrics for robot groups as described in [145] and [119] have been tried. However, since these approaches produced similar results as the computationally simple MLE, this approach was kept. For a general introduction to the field of metrics for robot groups and formations refer to section 3.2.

Looking at table 4-1 one can find the average MLE and the corresponding standard deviation calculated from the 60 runs for each scenario and each robot group size. First of all, it is obvious that the resulting relative localization among the robots is very accurate. The mean error per time step for one robot consistently lies below 1.8cm. Considering only the tracking process with its +/-0.5cm distance error and +/-0.5° angular error, then for typical robot distances between 2m and a bit more than 4m the angular error delivers displacements from 1.74cm in the near case and 3.48cm for the larger distances. Adding the perpendicular distance error, this already leads to errors ranging from +/-1.81cm up to +/-3.52cm, thereby not even taking into account the errors caused by the odometry.

"Z"	*no. of robots*	2	3	4	5
	mean MLE [cm]	1,542	1,552	1,364	1,441
	σ MLE	0,274	0,165	0,106	0,092
"eight"	*no. of robots*	2	3	4	5
	mean MLE [cm]	1,435	1,496	1,522	1,457
	σ MLE	0,078	0,160	0,132	0,085
"rectangle"	*no. of robots*	2	3	4	5
	mean MLE [cm]	1,695	1,781	1,501	1,541
	σ MLE	0,294	0,194	0,137	0,095

Table 4-1. Average MLE (in cm) and corresponding standard deviation per 60 runs for different group sizes and the three driving scenarios.

Unfortunately, the results from table 4-1, which in addition are plotted in figure 4-23, do not fully reflect the key expectation that the localisation precision increases with the number of robots. For the "eight" scenario there is no improvement at all, for the other scenarios there is at most a tendency of less than 0.2cm between the average MLE with

two robots and with five robots. This might be due to the fact that even with only two robots the accuracy of the laser based mutual tracking outweighs the errors of the odometry sensors. At least the standard deviation of the MLE calculated for the full runtime shows some improvement with larger group sizes. Again, for each combination of group size and scenario the table contains average values per 60 recorded example runs. Except for the "eight" scenario with two robots, the standard deviation shows less variations and therefore an improved stability in the relative localisation.

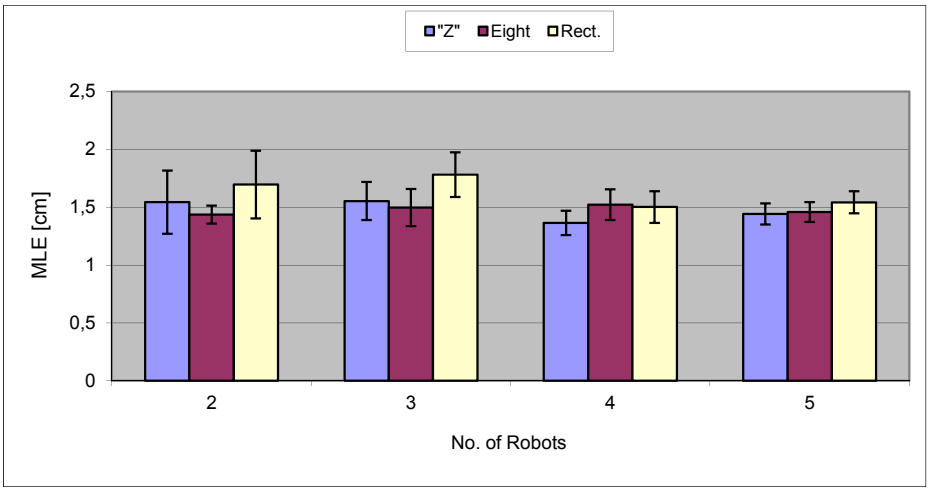

Figure 4-23: Plot of the average MLE (in cm) and corresponding standard deviation.

For a detailed analysis of the results, a closer look at the changes of the Mean Localisation Error (MLE) over runtime was taken. Figure 4-24 gives two typical examples, plotting the MLE in cm on the y-axis and the index of the localisation step on the x-axis. Based on this data it was possible to check whether the error remains constant over time or whether there are peaks corresponding, for example, to turns of single robots resp. of the whole formation, or to temporary occlusions of some of the robots.

The left part of figure 4-24 presents one of the 60 datasets for the "eight" scenario and the two-robot formation, the right chart shows the same for five robots. One can see that, actually, the MLE fluctuates much less if more robots take part in the relative localisation. During a further inspection of the error peaks no general correlation to regular incidents like turnings or occlusions could be identified. Neither sharp turns nor temporary occlusions of some of the robots seem to be the reason for the changes in the MLE. Instead, the variations seem to be arbitrarily spread over the whole runtime.

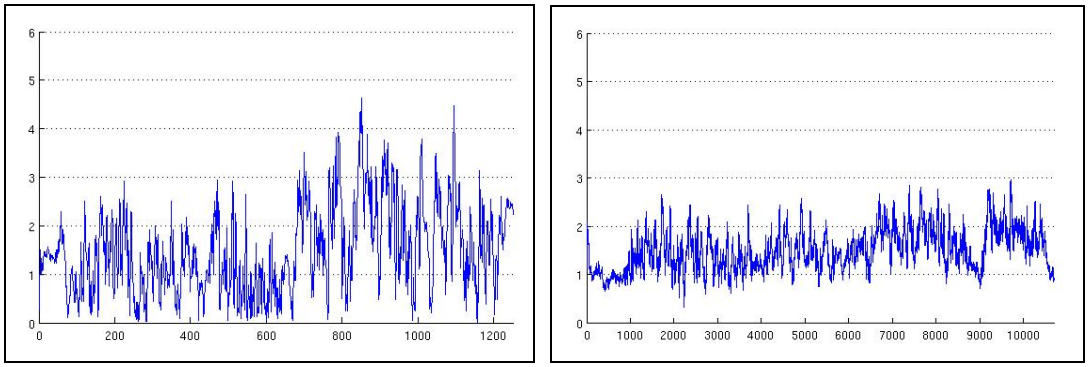

Figure 4-24: Example plot of the MLE in cm (y-axis) for the "eight" scenario with two (left) and five robots (right); the x-axis runs through the localisation steps resp. the duration of the run. The error for two robots shows more variations, fitting well to the larger standard deviation.

The only point, which occasionally recurs, is an increase of the MLE near the end of a run. In the left example in figure 4-24 the impression of a slightly higher error in the second half starting from time step 700 can be proven by numerical evaluation as well. The Mean Localisation Error is more than 0.5cm higher in the second half of the run. Figure 4-25 presents more examples of this effect. The left part is taken from a "rectangle" scenario with three robots, in the right part four robots move along the "Z" path. The results of the "rectangle" example are reflecting the previously described findings. From time step 1700 the standard deviation of the MLE starts growing and from step 2300 the error increases by more than 1cm. The other example gives an even larger growth of the MLE of nearly 2cm. But in this case this does not go along with larger fluctuations of the localisation error, instead a constant increase of the error can be seen. An explanation of this effect is an occasional above-average odometry error aggregation, which leads to very bad state predictions in the localisation EKF. The performance evaluation presented in this chapter is based on work published in [147].

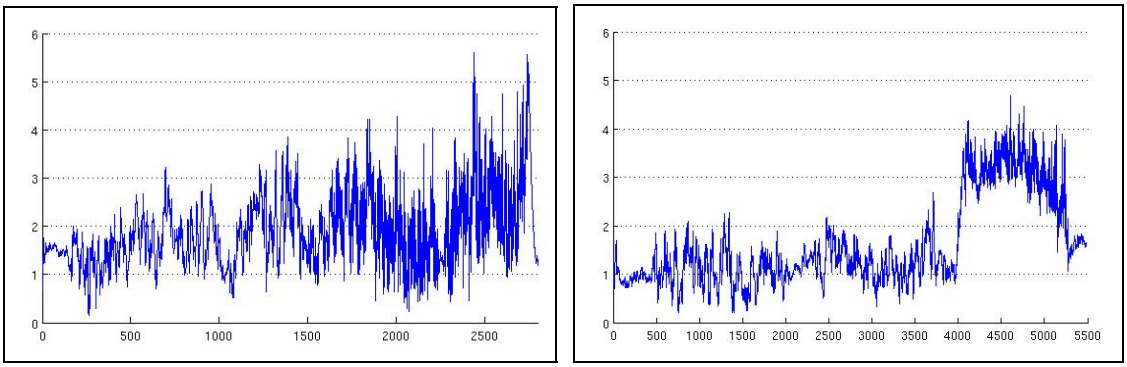

Figure 4-25: Example MLE for the "rectangle" with three (left) and the "Z" with four robots (right), axes as above, showing larger variations or sections with constantly large errors near the end of a run.

4.5 Summary

The foregoing sections describe the research that was done in the field of relative localisation. The focus was on establishing a common co-ordinate system between the different robots without using any external absolute references.

First, a comprehensive review of the different localisation methods was given and reviewed under the special circumstances of a multi-robot system.

To facilitate the set-up and maintenance of a formation as described in chapter 2

a) robust position estimation for each robot itself, and
b) relative position estimation of the other group members

were needed.

The first attempt to establish such a technique was a vision-based method. A two-step approach was used to establish the common co-ordinate system within the group of robots. The first step consists of a process in which one or more camera-equipped robots calculate their relative positions based on imagery. A standard photogrammetric projection algorithm is applied to calculate the robot's relative co-ordinates based on its position inside the image. In the second step, the position information in conjunction with the robots' movement data is used to generate the relative common co-ordinate system. Experiments with real robots were performed and showed good results. The vision process generates consistent position information for the other visible robots. However, due to the limitations inherent to the vision based process (changing light conditions, limited field of view, and performance) an alternative approach was developed.

The second approach was based on distance measurements produced by laser scanners, which were already mounted on the robots for collision avoidance.

Again, a two-step process was used. Whenever a robot moves and changes its position inside the sensor field, the movement with respect to the sensing robot's co-ordinate system is measured. Based on the distance and angular information an initial position estimation for each observer is generated and communicated to the other robots. By comparing these movements with the own robot movements, it is possible to calculate the transformation matrix between the co-ordinate system of that robot and the common relative co-ordinate system. Based on these initial estimations each robot can estimate the relative positions of all visible robots and use them as landmarks to improve its own position estimation. An Extended Kalman Filter is used to continuously update the position of the robot as well as position and orientation of its observers. Since all robots run this position estimation in parallel, a common co-ordinate system with reference only to the robots themselves is established.

The method was first tested with non-moving observers. Here a comparison to a standard SLAM based localisation method showed that the proposed relative localisation performs at least as good as the former.

The extensive experiments with moving observers confirmed that the design of the experiments is valid and appropriate to gain the necessary information for the evaluation. The data gathered in the experiments substantiate that for all of the testing patterns the Mean Localisation Error was significantly better than 2cm regardless of the number of robots involved. Interestingly, the number of robots did not improve the accuracy of the localisation but nevertheless improved the overall stability in the localisation process.

In general, the experiments provided strong evidence that the developed technique is valid and suitable. It was also shown that the laser scanner based approach has several advantages over the implemented vision approach, especially concerning the covered distance and for complex manoeuvres. The approach is able to handle even dispersed groups of robots using only little computing power and time.

5 Conclusions and Outlook

Co-operative action is one of the most relevant topics, when proceeding from single to multiple robots. The domain of robotic security systems holds typical applications for a multi-robot system (MRS), as for example reconnaissance and surveillance. Possible scenarios are safety and security issues on airports, harbours, large industry plants, or museums. Correspondingly, the field of environmental supervision is an up-coming issue.

Inherent to these applications is the need for the robots to move in an organised way. The main problem arises from the fact that due to the unknown and changing environment the local arrangement of the robots cannot be a rigid one. The desired formation should maintain its configuration but also must be able to temporarily adapt to the local circumstances. Additionally, the setting in which the group operates often is uncooperative, making typical localisation methods infelicitous.

This thesis focused on mobile robots, which not only share their workspace but also co-operatively navigate and localise each other. To make the methods feasible for even small robots special attention was given to a low impact on computing power. To meet the operational requirements the approach also had to enable the establishing and maintaining of a formation, while moving in a continuous manner and at a reasonable speed. Since the task of cooperative navigation involves multiple robots methods that are easily distributable were developed.

Formation navigation in its beginnings has been studied mostly on a theoretical basis concentrating on rather idealised geometrical problems and specialisations like the piano moving problem. This thesis successfully addressed the task of establishing and maintaining a specified configuration with real mobile robots even in the presence of obstacles. While typical approaches to this domain require a central planning component and severe computing power, the developed directed potential field method works without that.

The few existing approaches of using an artificial potential field for formation navigation use only forces to specify the distances between the robots. In contradiction to those un-directed formation forces, the proposed method also uses the orientation between the direct neighbours of the formation. Consequently, each robot has a designated position in the formation shape. It is therefore called directed potential field approach. This feature enables the formation to keep or reengage its desired configuration even after a serious distortion through e.g. obstacles.

Extensive experiments document that the method is capable to generate all different kind of formation shapes, even in the presence of dense obstacles. The trials with up to four robots also positively confirmed the functionality of the formation moving through a varying configuration of hurdles.

In the comparison of the two approaches, the non-directed approach turns out to be unstable regarding the formation positions. The robots strive to switch their positions inside the formation e.g. when passing through narrow passages. Under such conditions, the directed approach shows a preferable behaviour, which is called “breathing”. The formation shrinks or inflates depending on the obstacle situation while trying to maintain its shape and formation positions.

In summary, it was shown that the potential field approach was successfully transferred from mathematical simulation to real world robot scenarios. It was also shown that the directed approach has several advantages over the non-directed approach, especially in the presence of obstacles and for complex manoeuvres.

The evaluation of scientific work or the comparison of experiments and their results is one of the key issues in all domains of research. In the second part of this work, the problem of how to compare formation algorithms and methods is addressed. Within this thesis, a metric that allows a meaningful evaluation of the experimental data is motivated. The measure effectively allows a comparison on how well a developed formation algorithm or method performs.

An analysis of the corresponding literature through a comprehensive survey showed that a systematic discussion of metrics for formation navigation had not been done yet. Based on the details from the survey and the experiences gained from the experiments in formation navigation the parameters “position error” and “percentage of time in formation” were derived.

The problem of reproducibility increases when experiments take place in the real world settings, especially if the environment is unknown and dynamic or even non co-operative. Using the benefits from the potential field approach for formation navigation a novel weighting factor was developed that allows to consider environmental influences on the chosen metrics. The conducted experiments showed that the new weighting factor adequately modelled the influence of the environment.

While these outcomes are very encouraging, a more detailed comparison of other methods or algorithms might have to consider much more parameters. However, the developed metric is an appropriate tool to compare different formation navigation approaches in dissimilar settings and environments.

Localisation is a vital component in the process of co-ordination of navigation and movement. Almost any form of navigation is based on some sort of geometrical reference. This thesis presents a new relative localisation approach that uses sensor observations to localise the robot with respect to other objects – without having an environment model. In multi-robot systems, there is the inherent opportunity not to use the environment as reverence but to localise each robot with respect to the other team members.

While most of the literature is focussing on the application of SLAM with single robots, MRS based methods that consider environment detached approaches can be found very rarely. Most of the common approaches use maps and/or landmarks with the intention

of generating a globally consistent world co-ordinate system for the robot group. The aim of the considered relative localisation approach, on the other hand, is to maintain relative positioning only between the robots.

The presented method enables a group of mobile robots to start at an unknown location in an unknown environment, and then to incrementally estimate their own positions and the relative locations of the other robots using only sensor information. The result is a robust, fast, and precise approach that does not need any preconditions or special assumptions about the environment but sensor and odometry information only.

For the evaluation of the intensive testing with multiple real and simulated robots, the Mean Localisation Error (MLE) was introduced. The experiments included a comparison between the proposed Extended Kalman Filter and a standard SLAM based approach. It was shown that the developed method robustly delivering an accuracy less than 2cm and did perform at least as good as SLAM. The approach coped with scattered groups of robots while moving on arbitrarily shaped paths.

In summary, the presented research provides a framework for co-ordinated navigation in multi-robot systems. The results will facilitate the co-operative movements of robot groups as well as the relative localisation among the group members. In addition, a solid foundation for a non-environment related metric for formation navigation was introduced.

Despite these encouraging results, there is a variety of interesting issues for future research:

- A more comprehensive comparison between the classes of linear and non-linear stochastic methods for state estimation.
- The complex field of benchmarking and metrics has the potential for several further research topics especially when the combination of navigation and localisation is concerned.
- The directed formation navigation with artificial potential fields does not suffer severely from local minima but the use of harmonic potential fields could be of interest.

6 References

[1] R. Alur, A. K. Das, J. Esposito, R. Fierro, G. Grudic, Y. Hur, V. Kumar, I. Lee, J. P. Ostrowski, G. Pappas, B. Southall, J. Spletzer and C. J. Taylor, *A Framework and Architecture for Multirobot Coordination*, Proceedings of the International Symposium on Experimental Robotics, Hawaii, 2000, pp. 289-299.

[2] H. Ando, I. Suzuki and M. Yamashita, *Formation and Agreement Problems for Synchronous Mobile Robots with Limited Visibility*, Proceedings of the International Symposium on Intelligent Control, Monterey, 1995, pp. 453-460.

[3] T. Balch and R. C. Arkin, *Motor schema-based formation control for multiagent robot teams*, Proceedings of the 1st International Conference on Multiagent Systems, San Francisco, 1995, pp. 10-16.

[4] T. Balch and R. C. Arkin, *Behaviour-based Formation Control for Multi-robot Teams*, IEEE Transactions on Robotics and Automation, vol. 14, no. 6, 1998, pp. 926-939.

[5] T. Balch and M. Hybinette, *Social Potentials for Scalable Multi-Robot Formations*, Proceedings of the IEEE International Conference on Robotics and Automation (ICRA), San Francisco, 2000, pp. 73-80.

[6] T. D. Barfoot and C. M. Clark*, Motion planning for formations of mobile robots*, Robotics and Autonomous Systems, vol. 46, no. 2, 2004, pp. 65-78.

[7] L. Barnes, M. A. Fields and K. Valavanis, *Unmanned Ground Vehicle Swarm Formation Control Using Potential Fields*, Proceedings of the Mediterranean Conference on Control & Automation, Athens, 2007, pp. 1-8.

[8] J. Barraquand and J.-C. Latombe, *Robot Motion Planning: A Distributed Representation Approach*, International Journal of Robotics Research, vol. 10, no. 6, 1991, pp. 628-649.

[9] Y. Bar-Shalom and X.-R. Li, *Estimation and Tracking: Principles, Techniques and Software*, Artech House, 1993.

[10] B. Barshan and H. F. Durrant-Whyte, *Inertial navigation systems for mobile robots*, IEEE Transactions on Robotics and Automation, vol. 11, no. 3, 1995, pp. 328-342.

[11] C. Belta and V. Kumar, *Trajectory design for formations of robots by kinetic energy shaping,* Proceedings of the IEEE International Conference on Robotics and Automation (ICRA), Washington DC, 2002, pp. 2593-2598.

[12] G. Beni, *The Concept of Cellular Robotic Systems*, Proceedings of the 3rd IEEE International Symposium on Intelligent Control, Arlington, 1988, pp. 57-62.

[13] G. Beni and S. Hackwood. *Stationary waves in cyclic swarms*. Proceedings of the IEEE International Symposium on Intelligent Control, Glasgow, 1992, pp. 234-242.

[14] D. J. Bennet and C. R. McInnes, *Distributed control of multi-robot systems using bifurcating potential fields*, Robotics and Autonomous Systems, vol. 58, no. 3, 2010, pp. 256-264.

[15] A. Benzerrouk, L. Adouane, L. Lequievre and P. Martinet, *Navigation of Multi-Robot Formation in Unstructured Environment Using Dynamical Virtual Structures*, Proceedings of the IEEE/RSJ International Conference on Intelligent Robots and Systems (IROS), Taipei, 2010, pp. 5589–5594.

[16] J. Borenstein and Y. Koren, *Real-time Obstacle Avoidance for Fast Mobile Robots*, IEEE Transactions on System, Man and Cybernetics, vol. 19, no. 5, 1989, pp. 1179-1187.

[17] J. Borenstein and Y. Koren, *Real-time Obstacle Avoidance for Fast Mobile Robots in Cluttered Environments*, Proceedings of the IEEE International Conference on Robotics and Automation, Cincinnati, Ohio, 1990, pp. 572-577.

[18] J. Borenstein and Y. Koren, *The Vector Field Histogram – Fast Obstacle-Avoidance for Mobile Robots*, IEEE Journal of Robotics and Automation, vol. 7, no. 3, 1991, pp. 278-288.

[19] J. Borenstein and L. Feng, *Measurement and Correction of Systematic Odometry Errors in Mobile Robots*, IEEE Transactions on Robotics and Automation, vol. 12, no. 6, 1996, pp. 869-880.

[20] R. N. Braithwaite and B. Bhanu, *Robust Guidance of a Conventionally Steered Vehicle Using Destination Bearing*, Proceedings of the International Symposium on Intelligent Control, Chicago, 1993, pp. 382-387.

[21] N. Bulusu, J. Heidemann and D. Estrin, *GPS-less low cost outdoor localisation for very small devices*, Technical Report 00-729, University of Southern California, CS Department, 2000.

[22] W. Burgard, A. Deer, D. Fox and A. B. Cremers, *Integrating Global Position Estimation and Position Trackig for Mobile Robots: The Dynamic Markov Localisation Approach*, Proceedings of the IEEE/RSJ International Conference on Intelligent Robots and Systems (IROS), Victoria, 1998, pp. 730-736.

[23] R. H. Byrne, *Global Positioning System Receiver Evaluation Results*, Sandia Report SAND93-0827, Sandia National Laboratories, Albuquerque, 1993.

[24] Z. Cao, M. Tan, S. Wang, Y. Fan and B. Zhang, *The optimization research of formation control for multiple mobile robots*, Proceedings of the 4th World Congress on Intelligent Control and Automation, vol. 2, Shanghai, 2002, pp. 1270-1274.

[25] S. Carpin and L. E. Parker *Cooperative leader following in a distributed multi-robot system*. Proceedings of the IEEE International Conference on Robotics and Automation (ICRA), Washington DC, 2002, pp. 2994-3001.

[26] S. Carpin and L. E. Parker, *Cooperative Motion Coordination Amidst Dynamic Obstacles*, In: Distributed Autonomous Robotic Systems 5, H. Asama, T. Arai, T. Fukuda, and T. Hasegava (Eds.), Springer, 2002, pp. 145-154.

[27] J. A. Castellanos and J. D. Tardos, *Mobile Robot Localisation and Map Building: A Multisensor Fusion Approach*, Kluwer Academic Publishers, Boston, 2000.

[28] R. Castro, J. Alvarez and J. Martinez, *Robot formation control using backstepping and sliding mode techniques*, Proceedings of the 6th International Conference on Electrical Engineering, Computing Science and Automatic Control, Toluca, 2009, pp. 1-6.

[29] S. Chao-xia, H. Bing-rong and W. Yan-qing, *Cooperative Exploration by Multi-robots without Global Localization*, International Journal of Advanced Robotic Systems, vol. 4, no. 3, 2007, pp. 339-348.

[30] Q. Chen and J. Y. S. Luh, *Distributed Motion Coordination of Multiple Robots*, Proceedings of the International Conference on Intelligent Robots and Systems (IROS), Munich, 1994, pp. 1493-1500.

[31] Q. Chen and J. Y. S. Luh, *Coordination and Control of Small Mobile Robots*, Proceedings of the IEEE International Conference on Robotics and Automation (ICRA), San Diego, 1994, pp. 2315-2320.

[32] J. Cheng, W. Cheng and R. Nagpal, *Robust and self-repairing formation control for swarms of mobile agents*, Proceedings of the American Conference on Artificial Intelligence (AAAI), Pittsburgh, 2005, pp. 59-64.

[33] H. Choset and K. Nagatani, *Topological Simultaneous Localisation and Mapping (SLAM): Toward Exact Localisation without Explicit Localisation*, IEEE Transactions on Robotic and Automation, vol. 17, no. 2, 2001, pp. 125-137.

[34] S. Cifuentes, J. M. Giron-Sierra and J. Jimenez, *Robot Navigation Based on Discrimination of Artificial Fields: Application to Robot Formations*, Advanced Robotics, vol. 26, no. 5-6, 2012, pp. 627-652.

[35] A. Clerentin, L. Delahoche, C. Pegard and E. B. Gracsy, *A Localisation Method Based on Two Omnidirectional Perception System Cooperation*, Proceedings of the IEEE International Conference on Robotics and Automation (ICRA), San Francisco, 2000, pp. 1219-1224.

[36] S. Cooper and H. Durrant-Whyte, *A Kalman Filter for GPS Navigation of Land Vehicles*, Proceedings of the IEEE/RSJ International Conference on Intelligent Robots and Systems (IROS), Munich, 1994, pp. 157-163.

[37] Y. Dai and S.-G. Lee, *The leader-follower formation control of nonholonomic mobile robots*, International Journal of Control, Automation, and Systems, vol. 10, issue 2, 2012, pp. 350-61.

[38] A. K. Das, R. Fierro, V. Kumar, J. P. Ostrowski, J. Spletzer and C. Taylor, *A vision based formation control framework,* IEEE Transactions on Robotics and Automation, vol. 18, no. 5, 2002, pp. 813–825.

[39] A. K. Das, J. Spletzer, V. Kumar and C. Taylor, *Ad Hoc Networks for Localization and Control*, Proceedings of the 41st IEEE Conference on Decision and Control, vol. 3, 2002, pp. 2978-2983.

[40] F. Dellaert, D. Fox, W. Burgard and S. Thrun, *Monte Carlo Localisation for Mobile Robots*, Proceedings of the IEEE International Conference on Robotics and Automation (ICRA), Detroit, 1999, pp. 1322-1328.

[41] A. De Luca and G. Oriolo. *Local Incremental Planning for Nonholonomic Mobile Robots*. Proceedings of the IEEE International Conference on Robotics and Automation (ICRA), vol. 1, San Diego, 1994, pp. 104-110.

[42] J. P. Desai, J. P. Ostrowski and V. Kumar, *Controlling formations of multiple mobile robots,* Proceedings of the IEEE International Conference on Robotics and Automation (ICRA), vol. 4, Leuven, 1998, pp. 2864-2869.

[43] T. Dierks and S. Jagannathan, *Asymptotic Adaptive Neural Network Tracking Control of Nonholonomic Mobile Robot Formations*, Journal of Intelligent & Robotic Systems, vol. 56, issue 1-2, 2009, pp. 153-176.

[44] T. Dierks, B. Brenner and S. Jagannathan, *Near optimal control of mobile robot formations*, Proceedings of the IEEE SSCI Symposium on Adaptive Dynamic Programming and Reinforcement Learning, Paris, 2011, pp. 234–241.

[45] G. Dissanayake, H. Durrant-Whyte and T. Bailey, *A Computationally Efficient Solution to the Simultaneous Localisation and Map Building (SLAM) Problem*, Proceedings of the IEEE

International Conference on Robotics and Automation (ICRA), vol. 2, San Francisco, 2000, pp. 1009-1014.

[46] A. Doucet, N. de Freitas and N. Gordan, Eds., *Sequential Monte Carlo Methods in Practice*, Springer, 2001.

[47] G. Dudek, M. Jenkin, E. Milios and D. Wilkes, *A taxonomy for swarm robots*, Proceedings of the IEEE/RSJ International Conference on Intelligent Robots and Systems (IROS), vol. 1, Yokohama, 1993, pp. 441-447.

[48] O. Egecioglu and B. Zimmermann. *The one dimensional random pairing problem in a cellular robotic system,* Proceedings of the IEEE International Symposium on Intelligent Control, Arlington, 1988, pp. 76-80.

[49] H. R. Everett, *Sensors for Mobile Robots*, AK Peters, 1995.

[50] M. Farrokhsiar and H. Najjaran, *An Unscented Model Predictive Control Approach to the Formation Control of Nonholonomic Mobile Robots*, Proceedings of the IEEE International Conference on Robotics and Automation (ICRA), St Paul, 2012, pp. 1576-1582.

[51] R. Fierro, A. K. Das, V. Kumar and J. P. Ostrowski, *Hybrid Control of Formations of Robots*, Proceedings of the IEEE International Conference on Robotics and Automation (ICRA), vol. 1, Seoul, 2001, pp. 157-162.

[52] R. Fierro, P. Song, A. Das and V. Kumar, *Cooperative Control of Robot Formations*, In: Cooperative Control and Optimization: Series on Applied Optimization, R. Murphey and P. Paradalos (Eds.), Kluwer Academic Press, 2002, pp. 79-93.

[53] D. Fox, W. Burgard, H. Kruppa and S. Thrun, *Collaborative Multi-Robot Localisation,* Proceedings of the 23rd Annual German Conference on Artificial Intelligence (KI) and the 21st Symposium on Pattern Recognition (DAGM), Bonn, 1999, pp. 15-26.

[54] D. Fox, W. Burgard and S. Thrun, *Markov Localization for Mobile Robots in Dynamic Environments*, Journal of Artificial Intelligence Research, vol. 11, 1999, pp. 391-427.

[55] D. Fox, W. Burgard, H. Kruppa and S. Thrun, *A Probabilistic Approach to Collaborative Multi-Robot Localization*, Autonomous Robots, vol. 8, no. 3, 2000, pp. 325-344.

[56] J. Fredslund and M. J. Matarić, *A general algorithm for robot formations using local sensing and minimal communication,* IEEE Transactions on Robotics and Automation, vol. 18, no. 5, 2002, pp. 837-846.

[57] J. Fredslund and M. J. Matarić, *Robots in Formation Using Local Information*, Proc. of the 7th International Conference on Intelligent Autonomous Systems (IAS-7), Marina del Rey, March 2002, pp. 100-107.

[58] Y. Fuke and E. Krotkov, *Dead Reckoning for a Lunar Rover on Uneven Terrain*, Proceedings of the IEEE International Conference on Robotics and Automation (ICRA), vol. 1, Minneapolis, 1996, pp. 411-416.

[59] G. W. Gamage, G. K. I. Mann and R. G. Gosine, *Formation Control of Multiple Nonholonomic Mobile Robots Via Dynamic Feedback Linearization*, Proceedings of the 14th International Conference on Advanced Robotics, Munich, 2009, pp. 1-6.

[60] X. Gao, Q. Huang, M. Wan, C. Liu, *Sliding Mode Formation Control of Nonholonomic Robots*, Proceedings of the International Conference on Artificial Intelligence and Computational Intelligence, Sanya, 2010, pp. 67-71.

[61] S. Garrido, L. Moreno and PP U. Lima, *Robot formation motion planning using Fast Marching*, Robotics and Autonomous Systems, vol. 59, issue 9, 2011, pp. 675-683.

[62] S. S. Ge and Y. J. Cui, *New Potential Functions for Mobile Robot Path Planning,* IEEE Transactions on Robotics and Automation, vol. 16, no. 5, 2000, pp. 615-620.

[63] S. S. Ge and Y. J. Cui, *Dynamic Motion Planning for Mobile Robots Using Potential Field Method*, Autonomous Robots, vol. 13, no. 3, 2002, pp. 207-222.

[64] V. Genovese, P. Dario, R. Magni and L. Odetti, *Self-organizing Behavior and Swarm Intelligence in a Pack of Mobile Miniature Robots in Search of Pollutants*, Proceedings of the IEEE International Conference on Intelligent Robots and Systems (IROS), Raleigh, 1992, pp. 1575-1582.

[65] P. Goel, S. I. Roumeliotis and G. S. Sukhatme, *Robust Localisation Using Relative and Absolute Position Estimates*, Proceedings of the IEEE/RSJ International Conference on Intelligent Robots and Systems (IROS), Kyongju, 1999, pp. 1134-1140.

[66] R. Grabowski, L. E. Navarro-Serment, C. J. Paredis and P. K. Khosla, *Heterogeneous Teams of Modular Robots for Mapping and Exploration*, Autonomous Robots, vol. 8, no. 3, 2000, pp. 293-308.

[67] J. Guivant and E. Nebot, *Optimization of the Simultaneous Localisation and Map Building Algorithm for Real Time Implementation*, IEEE Transactions on Robotics and Automation, vol. 17, no. 3, 2001, pp. 242-257.

[68] J. Guo, Z. Lin, M. Cao and G. Yan, Adaptive Leader-Follower Formation Control for Autonomous Mobile Robots, Proceedings of the American Control Conference, Baltimore, 2010, pp. 6822-6827.

[69] J.-S. Gutmann, W. Burgard, D. Fox and K. Konolige, *An Experimental Comparison of Localization Methods*, Proceedings of the IEEE/RSJ International Conference on Intelligent Robots and Systems (IROS), vol. 2, Victoria, 1998, pp. 736-743.

[70] J.-S. Gutmann, T. Weigel and B. Nebel, *Fast, Accurate, and Robust Self-Localization in Polygonal Environments*, Proceedings of the IEEE/RSJ International Conference on Intelligent Robots and Systems (IROS), vol. 3, Kyongju, 1999, pp. 1412-1419.

[71] J.-S. Gutmann and D. Fox, *An Experimental Comparison of Localisation Methods Continued*, Proceedings of the IEEE/RSJ International Conference on Intelligent Robots and Systems (IROS), vol. 1, Lausanne, 2002, pp. 454-459.

[72] K. Hengster-Movricacute, S. Bogdan and I. Draganjac, *Bell-shaped potential functions for multi-agent formation control in cluttered environment*, Proceedings of the 18th Mediterranean Conference on Control & Automation, Marrakech, 2010, pp. 142-147.

[73] E. G. Hernandez-Martinez and E. Aranda-Bricaire, *Multi-agent formation control with collision avoidance based on discontinuous vector fields*, Proceedings of the 35th Annual Conference of IEEE Industrial Electronics, Porto, 2009, pp. 2283-2288.

[74] Y. S. Hidaka, A. I. Mourikis and S. I. Roumeliotis, *Optimal Formations for Cooperative Localization of Mobile Robots*, Proceedings of the IEEE International Conference on Robotics and Automation (ICRA), Barcelona, 2005, pp. 4137-4142.

[75] S. P. Hou, C. C. Cheah, J. J. E. Slotine, *Dynamic Region Following Formation Control for a Swarm of Robots*, Proceedings of the IEEE International Conference on Robotics and Automation (ICRA), Kobe, 2009, pp. 1929–1934.

[76] A. Howard, M. J. Matarić and G. S. Sukhatme, *Cooperative Relative Localization for Mobile Robot Teams: An Egocentric Epproach*, In: Multi-Robot Systems: From Swarms to Intelligent Automata, A. C. Schultz and L. E. Parker, and F. E. Schneider (Eds.), Kluwer, 2003, pp. 65-76.

[77] A. Howard, *Multi-robot Simultaneous Localization and Mapping using Particle Filters*, International Journal of Robotics Research, vol. 25, no. 12, 2006, pp. 1243-1256.

[78] M. A. Hsieh, V. Kumar, and L. Chaimowicz, *Decentralized controllers for shape generation with robotic swarms*, Robotica, vol. 26, 2008, pp. 691-701.

[79] M. A. Hurni, P. Sekhavat, M. Karpenko, and I. M. Ross, *Autonomous Multi-Vehicle Formations Using A Pseuodospectral Optimal Control Framework*, Proceedings of the IEEE/ASME International Conference on Advanced Intelligent Mechatronics, Montreal, 2010, pp. 980-986.

[80] R. T. Jonathan, R. W. Beard and B. J. Young, *A decentralized approach to formation maneuvers*. IEEE Transactions on Robotics and Automation. vol. 19, no. 6, 2003, pp. 933-941.

[81] D. Jung, J. Heinzmann and A. Zelinsky, *Range and Pose Estimation for Visual Servoing on a Mobile Robotic Target*, Proceedings of the IEEE International Conference on Robotics and Automation (ICRA), vol. 2, Leuven, 1998, pp. 1226-1231.

[82] R. E. Kalman, *A New Approach to Linear Filtering and Prediction Problems*, Transactions of the ASME-Journal of Basic Engineering, vol. 82 (Series D), 1960, pp. 35-45.

[83] O. Khatib, *Real-time obstacle avoidance for manipulators and mobile robots,* International Journal of Robotics Research, vol. 5, no. 1, 1986, pp. 90-98.

[84] D. H. Kim, H.-W. Lee, S. Shin and T. Suzuki: *Local Path Planning Based on New Repulsive Potential Functions with Angle Distributions*. Proceedings of the 3rd International Conference on Information Technology and Applications, vol. 2, Sydney, 2005, pp. 9-14.

[85] D. H. Kim, H. Wang and S. Shin, *Decentralized Control of Autonomous Swarm Systems Using Artificial Potential Functions: Analytical Design Guidelines*, Journal of Intelligent and Robotic Systems, vol. 45, no. 4, 2006, pp. 369-394.

[86] Y. Koren and J. Borenstein, *Potential Field Method and Their Inherent Limitations for Mobile Robot Navigation*, Proceedings of the IEEE International Conference on Robotics and Automation (ICRA), Sacramento, 1991, pp. 1398-1404.

[87] W. Kowalczyk and K. Kozlowski, *Artificial Potential Based Control for a Large Scale Formation of Mobile Robots*, In: Climbing and Walking Robots, Part II, Springer, 2005, pp. 191-199.

[88] K. Kraus, *Photogrammetrie – Band 1: Grundlagen und Standardverfahren*, Dümmlers Verlag, Bonn, 1994.

[89] B. H. Krogh, *A Generalized Potential Field Approach to Obstacle Avoidance Control,* Proceedings of the International Robotics Research Conference, Bethlehem, PA, 1984, pp. 1150-1156.

[90] B. H. Krogh and C. E. Thorpe, *Integrated Path Planning and Dynamic Steering Control for Autonomous Vehicles*, Proceedings of the IEEE International Conference on Robotics and Automation (ICRA), San Francisco, 1986, pp. 1664-1669.

[91] R. Kurazume, S. Nagata, and S. Hirose, *Cooperative Positioning with multiple robots*, Proceedings of the IEEE International Conference on Robotics and Automation (ICRA), vol. 2, San Diego, 1994, pp. 1250-1257.

[92] R. Kurazume, S. Hirose, S. Nagata and N. Sashida, *Study on Cooperative Positioning System (Basic Principle and Measurement Experiment)*, Proceedings of the IEEE International Conference on Robotics and Automation (ICRA), vol. 2, Minneapolis, 1996, pp. 1421-1426.

[93] R. Kurazume and S. Hirose, *An Experimental Study of a Cooperative Positioning System*, Autonomous Robots, vol. 8, no. 1, 2000, pp. 43-52.

[94] J.-W. Kwon and D. Chwa, *Hierarchical formation control based on a vector field method for wheeled mobile robots*, IEEE Transactions on Robotics, vol. 28, no. 6, 2012, pp. 1335-1345.

[95] J. C. Lagarias, J. A. Reeds, M. H. Wright and P. E. Wright, *Convergence Properties of the Nelder-Mead Simplex Method in Low Dimensions*, SIAM Journal of Optimization, vol. 9, no. 1, 1998, pp. 112-147.

[96] J. C. Latombe, *Robot Motion Planning,* Kluwer, 1991.

[97] M. Lemay, F. Michaud, D. Létourneau and J.-M. Valin, *Autonomous Initialization of Robot Formations*, Proceedings of the IEEE International Conference on Robotics and Automation (ICRA), vol. 3, New Orleans, 2004, pp. 3018-3023.

[98] M. A. Lewis and K.-H. Tan, *High Precision Formation Control of Mobile Robots Using Virtual Structures*, Autonomous Robots, vol. 4, 1997, pp. 387–403.

[99] P. Liang and G. Beni, *Robotic Morphogenesis*, Proceedings of the IEEE International Conference on Robotics and Automation (ICRA), Nagoya, 1995, pp. 2175-2180.

[100] Y. Lin, P. Vernaza, J. Ham and D. D. Lee, *Cooperative Relative Robot Localization with Audible Acoustic Sensing*, Proceedings of the IEEE/RSJ International Conference on Intelligent Robots and Systems (IROS), Edmonton, 2005, pp. 3764-3769.

[101] LMS200/211/221/291 Laser Measurement Systems – Technical Description, doc. 8008970/ QI72/2006-12, SICK AG, Germany, 2006.

[102] F. Lu and E. E. Milios, *Robot Pose Estimation in Unknown Environments by Matching 2D Range Scans*, Proceedings of the IEEE Conference on Computer Vision and Pattern Recognition, Seattle, 1994, pp. 935-938.

[103] F. Lu and E. E. Milios, *Globally Consistent Range Scan Alignment for Environment Mapping*, Autonomous Robots, vol. 4, no. 4, 1997, pp. 333–349.

[104] E. Z. MacArthur, C. D. Crane, *Compliant formation control of a multi-vehicle system*, Proceedings of the IEEE International Symposium on Computational Intelligence in Robotics and Automation, Jacksonville, 2007, pp. 479–484

[105] R. Madhavan, K. Fregene and L.E. Parker, *Distributed Cooperative Outdoor Multirobot Localization and Mapping*, Autonomous Robots, vol. 17, no. 1, 2004, pp. 23-39.

[106] A. Manz, R. Liscano and D. Green, *A comparison of real-Time Obstacle Avoidance Methods for Mobile Robots*. In: Experimental Robotics II, R. Chatila and G. Hirzinger (Eds.), Lecture Notes in Control and Information Sciences 190, Springer, 1993, pp. 299-316.

[107] A. Martinelli, F. Pont and R. Siegwart, *Multi-Robot Localisation Using Relative Observations*, Proceedings of the IEEE International Conference on Robotics and Automation (ICRA), Barcelona, 2005, pp. 2797-2802.

[108] N. Michael, J. Fink, S. Loizou, and V. Kumar, *Architecture, abstractions, and algorithms for controlling large teams of robots: Experimental testbed and results*, Robotics Research, Springer Tracts in Advanced Robotics, vol. 66, 2011, pp. 409-419.

[109] A. Milella, F. Pont and R. Siegwart, *Model-Based Relative Localization for Cooperative Robots Using Stereo Vision*, Proceedings of the IEEE Conference on Mechatronics and Machine Vision in Practice, Manila, 2005.

[110] L. Montesano, W. Burgard and L. Montano, *Relative Localization for Pairs of Robots Based on Unidentifiable Moving Features*, Proceedings of the IEEE/RSJ International Conference on Intelligent Robots and Systems (IROS), vol. 2, Sendai, 2004, pp. 1537-1543.

[111] L. Montesano, J. Gaspar, J. Santos-Victor and L. Montano, *Cooperative Localization by Fusing Vision-Based Bearing Measurements and Motion*, Proceedings of the IEEE/RSJ International Conference on Intelligent Robots and Systems (IROS), Edmonton, 2005, pp. 2333-2338.

[112] H. P. Moravec and A. Elfes, *High Resolution Maps form Wide Angle Sonar*, Proceedings of the IEEE International Conference on Robotics and Automation (ICRA), St. Louis, 1985, pp. 116-121.

[113] B. Motazed, *Measure of the Accuracy of Navigational Sensors for Autonomous Path Tracking*, In: SPIE - The International Society for Optical Engineering, vol. 2058, Mobile Robots VIII, W. H. Chun and W. J. Wolfe (Eds.), 1993, pp. 240-249.

[114] A. I. Mourikis and S. I. Roumeliotis, *Performance Analysis of Multirobot Cooperative Localization*, IEEE Transactions on Robotics, vol. 22, no. 4, 2006, pp. 666-681.

[115] A. I. Mourikis and S. I. Roumeliotis, *Predicting the Performance of Cooperative Simultaneous Localization and Mapping (C-SLAM)*, International Journal of Robotics Research, vol. 25, no. 12, 2006, pp.1273-1286.

[116] A. Moutinho and J. R. Azinheira, *Comparison and fusion of odometry and GPS navigation for an outdoor mobile robot*, Proceedings of the IEEE International Conference on Advanced Robotics, Coimbra, 2003, pp. 1290-1295.

[117] D. W. Murray, I. D. Reid and A. J. Davison, *Steering and Navigation Behaviours using Fixation*, Proceedings of the 7th British Machine Vision Conference, Edinburgh, 1996, pp. 635-644.

[118] D. Naffin and G. Sukhatme, G. *Negotiated Formations*. Proceedings of the International Conference on Intelligent Autonomous Systems, Amsterdam, 2004, pp. 181-190.

[119] I. Navarro and F. Matía, A *Proposal of a Set of Metrics for Collective Movement of Robots*, Proceedings of the Workshop on Good Experimental Methodology in Robotics, Robotics: Science and Systems (RSS) Conference, Seattle, 2009.

[120] L. E. Parker, *Designing Control Laws for Cooperative Agent Teams*, Proceeding of the IEEE International Conference on Robotics and Automation (ICRA), Atlanta, 1993, pp. 582-587.

[121] L. E. Parker. *Cooperative Robotics for Multi-Target Observation*, Intelligent Automation and Soft Computing, vol. 5, 1999, pp. 5-19.

[122] A. Poty, P. Melchjor and A. Oustaloup, *Dynamic Path Planning for Mobile Robots using Fractional Potential Field*, Proceedings of the 1st International Symposium on Control, Communications and Signal Processing, Hammamet, 2004, pp.557-561.

[123] E. Pruner, D. Necsulescu, J. Sasiadek and B. Kim, *Control of decentralized geometric formations of mobile robots*, Proceedings of the 17th International Conference on Methods & Models in Automation & Robotics, Miedzyzdroje, 2012, pp. 627-632.

[124] B. Ranjbar-Sahraei, F. Shabaninia, A. Nemati and S.-D. Stan, *A Novel Robust Decentralized Adaptive Fuzzy Control for Swarm Formation of Multiagent Systems*, IEEE Transactions on Industrial Electronics, vol. 59, issue 8, 2012, pp. 3124-3134

[125] I. M. Rekleitis, G. Dudek and E. E. Milios, *Multi-Robot Exploration of an Unknown Environment, Efficiently Reducing the Odometry Error*, Proceedings of the International Joint Conference in Artificial Intelligence, vol. 2, Nagoya, 1997, pp. 1340-1345.

[126] I. M. Rekleitis, G. Dudek and E. E. Milios, *Multi-Robot Collaboration for Robust Exploration*, Annals of Mathematics and Artificial Intelligence, vol. 31, 2001, pp. 7-40.

[127] I. M. Rekleitis, G. Dudek and E. E. Milios, *Multi-Robot Cooperative Localisation: A Study of Trade-offs Between Efficiency and Accuracy*, Proceedings of the IEEE/RSJ International Conference on Intelligent Robots and Systems (IROS), Lausanne, 2002, pp. 2690-2695.

[128] I. M. Rekleitis, G. Dudek and E. E. Milios, *Probabilistic Cooperative Localization and Mapping in Practice*, Proceedings of the IEEE International Conference in Robotics and Automation (ICRA), Taipei, 2003, pp. 1907-1912.

[129] H. Rezaee and F. Abdollahi, *Mobile Robots Cooperative Control and Obstacle Avoidance Using Potential Field*, Proceedings of the IEEE/ASME International Conference on Advanced Intelligent Mechatronics, Budapest, 2011, pp. 61-66.

[130] E. Rimon and D. E. Koditschek, *Exact robot navigation using artificial potential functions*, IEEE Transactions on Robotics and Automation, vol. 8, no. 5, 1992, pp. 501-518.

[131] S. I. Roumeliotis and G. A. Bekey, *Collective Localisation: A distributed Kalman filter approach to localisation of groups of mobile robots*, Proceedings of the IEEE International Conference on Robotics and Automation (ICRA), vol. 3, San Francisco, 2000, pp. 2958-2965.

[132] S. I. Roumeliotis and G. A. Bekey, *Distributed Multi-Robot Localization*, IEEE Transactions on Robotics and Automation, vol. 18, no. 5, 2002, pp. 781-795.

[133] S. I. Roumeliotis and I. M. Rekleitis, *Propagation of Uncertainty in Cooperative Multirobot Localization: Analysis and Experimental Results*, Autonomous Robots, vol. 17, no. 1, 2004, pp. 41-54.

[134] J. Saez-Pons, L. Alboul and J. Penders, *Multi-robot team formation control in the GUARDIANS project*, Industrial Robot: An International Journal, vol. 37, no. 4, 2010, pp. 372–383.

[135] E. Sahin, T. H. Labella, V. Trianni, J.-L. Deneubourg, P. Rasse, D. Floreano, L. Gambardella, F. Mondada, S. Nolfi and M. Dorigo, *SWARM-BOT: Pattern Formation in a Swarm Of Self-Assembling Mobile Robots*, Proceedings of the IEEE International Conference on Systems, Man and Cybernetics, vol. 4, Hammamet, 2002, pp. 145-150.

[136] J. Sanchez and R. Fierro, *Sliding mode control for robot formations*, Proceedings of the IEEE International Symposium on Intelligent Control, Houston, 2003, pp. 438-443.

[137] A. C. Sanderson, *A distributed algorithm for cooperative navigation among multiple mobile robots*, Advanced Robotics, vol. 12, no. 4, 1998, pp. 335-349.

[138] M. Saska, V. Vonasek and L. Prcaroneuccaronil, *Navigation and formation control employing complementary virtual leaders for complex maneuvers*, Proceedings of the 7th International Conference on Informatics in Control, Automation and Robotics, Funchal, 2010, pp. 141-146.

[139] F. E. Schneider, M. Moors, D. Wildermuth and A. Kräußling, *Relative position estimation in a group of robots*, Proceedings of the International Conference on Methods and Models in Automation and Robotics (MMAR), vol. 2, Międzyzdroje, 2003, pp. 751-756.

[140] F. E. Schneider and D. Wildermuth, *A potential field based approach to multi-robot formation navigation*, Proceedings of the 1st European Conference on Mobile Robotics (ECMR), Radziejowice, 2003, pp. 39-44.

[141] F. E. Schneider and D. Wildermuth, *Using an Extended Kalman Filter for Relative Localisation in a Moving Robot Formation*, Proceedings of the 4th International Workshop on Robot Motion and Control (RoMoCo'04), Puszczykowo, 2004, pp. 85-90.

[142] F. E. Schneider and D. Wildermuth, *Directed and Non-Directed Potential Field Approaches to Formation Navigation*, Proceedings of the 2nd IASTED International Conference on Automation, Control, and Applications (ACIT-ACA), Novosibirsk, 2005, pp. 338-343.

[143] F. E. Schneider and D. Wildermuth, *Experimental Comparison of a Directed and a Non-Directed Potential Field Approach to Formation Navigation*, Proceedings of the 6th IEEE International Symposium on Computational Intelligence in Robotics and Automation (CIRA), Espoo, 2005, pp. 21-26.

[144] F. E. Schneider and D. Wildermuth, *An Application of Relative Localisation for Multi-Robot Navigation*, Proceedings of the 2nd IASTED International Conference on Automation, Control, and Applications (ACIT-ACA), Novosibirsk, Russia, 20.-24. June 2005, pp. 344-349.

[145] F. E. Schneider, D. Wildermuth and A. Kräußling, *Discussion of Exemplary Metrics for Multi-Robot Systems for Formation Navigation*, International Journal of Advanced Robotic Systems, vol. 2, no. 4, 2005, pp. 345-353.

[146] F. E. Schneider, A. Kräußling and D. Wildermuth, *Tracking Methods for Relative Localisation*, Robot Motion and Control – Recent Developments, Lecture Notes in Control and Information Sciences 335, Springer, Berlin/Heidelberg, 2006, pp. 301-313.

[147] F. E. Schneider and D. Wildermuth, *Influences of the Robot Group Size on Cooperative Multi-Robot Localisation – Analysis and Experimental Validation*, Robotics and Autonomous Systems, doi: 10.1016/j.robot.2012.05.001, 2012.

[148] D. Schulz, W. Burgard, D. Fox and A. B Cremers, *Tracking Multiple Moving Targets with a Mobile Robot Using Particle Filters and Statistical Data Association*, Proceedings of the IEEE International Conference on Robotics and Automation (ICRA), vol. 2, Soul, 2001, pp. 1665-1670.

[149] T. J. Schwartz and M. Sharir, *On the "Piano Movers'" Problem I. The Case of a Two-Dimensional Rigid Polygonal Body Moving Amidst Polygonal Barriers*, Communications on Pure and Applied Mathematics, vol. 36, pp. 345–398, 1983.

[150] R. Solea, D. Cernega, A. Filipescu and A. Serbencu, *Formation control of multi-robots via sliding-mode technique*, Proceedings of the 7th International Conference on Informatics in Control, Automation and Robotics, Funchal, 2010, pp. 161-166.

[151] P. Song and V. Kumar, *A Potential Field Based Approach to Multi-Robot Manipulation*, Proceedings of the IEEE International Conference on Robotics and Automation (ICRA), Washington DC, 2002, pp. 870-876.

[152] J. Spletzer, A. K. Das, R. Fierro, C. Taylor, V. Kumar and J. P. Ostrowski, *Cooperative Localization and Control for Multi-Robot Manipulation*, Proceedings of the IEEE/RSJ International Conference on Intelligent Robots and Systems (IROS), vol. 2, Hawaii, 2001, pp. 631-636.

[153] K. Støy, *Using Situated Communication in Distributed Autonomous Mobile Robotics*, Proceedings of the 7th Scandinavian Conference on Artificial Intelligence, Odense, 2001, pp. 44-52.

[154] K. Sugihara and I. Suzuki, *Distributed Motion Coordination of Multiple Mobile Robots*, Proceedings of 5th IEEE International Symposium on Intelligent Control, Philadelphia, 1990, pp. 138-143.

[155] K. Sugihara and I. Suzuki, *Distributed algorithms for formation of geometric patterns with many mobile robots*; Journal of Robotic Systems, vol. 13, no. 3, 1996, pp. 127-139.

[156] I. Suzuki and M. Yamashita, *Agreement on a Common X-Y Coordinate System by a Group of Mobile Robots*, Proceedings of the Dagstuhl Seminar on Modelling and Planning for Sensor-Based Intelligent Robot Systems, Dagstuhl, September 1996, pp. 305-321.

[157] I. Suzuki and M. Yamashita, *Distributed Anonymous Mobile Robots Formation and Agreement Problems*, Proceedings of the 3rd International Colloquium on Structural Information and Communication Complexity, Siena, 1996, pp. 313-330.

[158] I. Suzuki and M. Yamashita, *Distributed anonymous mobile robot: Formation of geometric patterns*, SIAM Journal of Computing, vol. 28, no. 4, 1999, pp. 1347-1363.

[159] H. G. Tanner, A. Jadbabaie and G. J. Pappas, *Stable Flocking of Mobile Agents Part II: Dynamic Topology*, Proceedings of the 42nd IEEE Conference on Decision and Control, Maui, 2003, pp. 2016-2021.

[160] C. F. Thorpe, *Path Relaxation: Path Planning for a Mobile Robot*, Autonomous Mobile Robots Annual Report, Carnegie-Mellon University, The Robotics Institute, Mobile Robots Laboratory, 1985, pp. 39-42.

[161] S. Thrun, *A Probabilistic Online Mapping Algorithm for Teams of Mobile Robots*, International Journal of Robotics Research, vol. 20, no. 5, 2001, pp. 335-363.

[162] V.-H. Tran and S.-G. Lee, *A Stable Formation Control Using Approximation of Translational and Angular Accelerations*, International Journal of Advanced Robotic Systems, vol. 8, issue 1, 2011, pp. 65-75.

[163] N. Trawny and T. Barfoot, *Optimized Motion Strategies for Cooperative Localization of Mobile Robots*, Proceedings of the IEEE International Conference on Robotics and Automation (ICRA), vol. 1, New Orleans, 2004, pp. 1027-1032.

[164] A. E. Turgut, H. Çelikkanat, F. Gökçe, E. Sahin, *Self-organized flocking in mobile robot swarms*, Swarm Intelligence, vol. 2, no. 2, 2008, pp. 97-120.

[165] T. Ueyama, T. Fukuda and F. Arai, *Structure Configuration Using Genetic Algorithm For Cellular Robotic System*, Proceedings of the IEEE/RSJ International Conference on Intelligent Robots and Systems (IROS), vol. 3, Raleigh, 1992, pp. 1542-1549.

[166] I. Ulrich and I. Nourbakhsh, *Appearance-Based Place Recognition for Topological Localisation*, Proceedings of the IEEE International Conference on Robotics and Automation (ICRA), San Francisco, 2000, pp. 1023-1029.

[167] Y. Uny Cao, A. S. Fukunaga and A. B. Kahng, *Cooperative Mobile Robotics: Antecedents and Directions*, Autonomous Robots, vol. 4, no. 1, 1997, pp 7-23.

[168] P. Urcola, L. Riazuelo, M. T. Lázaro and L. Montano, *Cooperative navigation using environment compliant robot formations*, Proceedings of the IEEE/RSJ International Conference on Intelligent Robots and Systems (IROS), Nice, 2008, pp. 2789–2794.

[169] P. Vadakkepat, K. Chen Tan and W. Ming-Liang, *Evolutionary Artificial Potential Fields and Their Application in Real Time Robot Path Planning*, Proceedings of the IEEE Congress of Evolutionary Computation, San Diego, 2000, pp. 256-263.

[170] P. K. C. Wang, *Navigation Strategies for Multiple Autonomous Mobile Robots Moving in Formation*, Journal of Robotic Systems, vol. 8, no. 2, 1991, pp. 177-195.

[171] P. K. C. Wang, F. Y. Hadaegh and K. Lau, *Synchronized Formation Rotation and Attitude Control of Multiple Free-flying Spacecraft*, Guidance, Control and Dynamics, vol. 22, 1999, pp. 28-35.

[172] C.-C. Wang and C. F. Thorpe, *Simultaneous Localization and Mapping with Detection and Tracking of Moving Objects*, Proceedings of the IEEE International Conference on Robotics and Automation (ICRA), vol. 3, Washington, 2002, pp. 2918-2924.

[173] D. Wildermuth and F. E. Schneider, *Maintaining a Common Co-ordinate System for a Group of Robots based on Vision*, Robotics and Autonomous Systems, vol. 44, no. 3-4, 2003, pp. 209-217.

[174] H. Yamaguchi and T. Arai, *Distributed and Autonomous Control Method for Generating Shape of Multiple Mobile Robot Group*, Proceedings of International Conference on Intelligent Robots and Systems, Munich, 1994, pp. 800-807.

[175] H. Yamaguchi, *Adaptive formation control for distributed autonomous mobile robot groups*, Proceedings of the IEEE Conference on Robotics and Automation (ICRA), vol. 3, Albuquerque, NM 1997, pp. 2300-2305.

[176] H. Yamaguchi, T. Arai and G. Beni, *A distributed control scheme for multiple robotic vehicles to make group formations*, Robotics and Autonomous Systems, vol. 36, no. 4, 2001, pp. 125-147.

[177] F. Yang, F. Liu, S. Liu and C. Zhong, *Hybrid formation control of multiple mobile robots with obstacle avoidance*, Proceedings of the 8th World Congress on Intelligent Control and Automation, Jinan, 2010, pp. 1039–1044.

[178] F. Zhang, B. Grocholsky and V. Kumar, *Formations for Localization of Robot Networks*, Proceedings of the IEEE International Conference on Robotics and Automation (ICRA), vol. 4, New Orleans, 2004, pp. 3369-3374.

7 Eidesstattliche Versicherung

An Eides statt versichere ich, dass

1. die vorgelegte Arbeit – abgesehen von den ausdrücklich bezeichneten Hilfsmitteln – persönlich, selbständig und ohne Benutzung anderer als der angegebenen Hilfsmittel angefertigt wurde,
2. die aus anderen Quellen direkt oder indirekt übernommenen Daten und Konzepte unter Angabe der Quelle kenntlich gemacht sind,
3. die vorgelegte Arbeit oder ähnliche Arbeiten nicht bereits anderweitig als Dissertation eingereicht worden ist bzw. sind, sowie eine Erklärung über frühere Promotionsversuche und deren Resultate,
4. für die Erstellung der vorgelegten Arbeit und/oder die Gelegenheit zur Promotion keine fremde Hilfe, insbesondere keine entgeltliche Hilfe von Vermittlungs- bzw. Beratungsdiensten (Promotionsberatern / -vermittlern oder anderen Personen) in Anspruch genommen wurde.

Bonn, denn 20.10.2012

Frank E. Schneider